

## Potential application of hybrid forward osmosis – Membrane distillation (FO-MD) system for various water treatment processes

Afrah H. Kamel<sup>a</sup>, Raed A. Al-Juboori<sup>b</sup>, Muayad al-shaeli<sup>c</sup>, Bradley Ladewig<sup>c</sup>, Salah S. Ibrahim<sup>a</sup>, Qusay F. Alsalhy<sup>a,\*</sup>

<sup>a</sup> Membrane Technology Research Unit, Chemical Engineering Department, University of Technology-Iraq, Alsinaa Street 52, 10066-Baghdad, Iraq

<sup>b</sup> NYUAD Water Research Centre, New York University, Abu Dhabi Campus, P.O. Box 129188, Abu Dhabi, United Arab Emirates

<sup>c</sup> Paul Wurth Chair, Faculty of Science, Technology and Medicine, University of Luxembourg, 2, Avenue de l'Université, L-4365 Esch-sur-Alzette, Luxembourg

### ARTICLE INFO

#### Keywords:

Forward osmosis (FO)  
Membrane distillation (MD)  
Hybrid FO-MD systems  
Fouling  
Wetting  
Energy  
Pilot system

### ABSTRACT

Different membrane processes have been used to address water scarcity issues. Among them, membrane distillation (MD) is a promising technology due to its capacity to treat hypersaline water. Forward osmosis (FO) is another innovative technology that has the advantage of low operational energy. A hybrid system of these two technologies has proven to be an effective technique for the water treatment industry particularly for water reclamation and resource recovery. Understanding the fundamentals of this amalgamation and the challenges that brings with it is an important topic for the scientific and research community. This work presents a detailed review of the FO-MD systems enriched with the recent advances in this system. The opportunities and challenges for the individual technologies and the system overall were critically addressed. Successful pilot designs for the hybrid system were illustrated. Mathematical modeling for the water transfer in the hybrid system was also elaborated to identify the key points and boundaries of the processes. It is apparent that the inherent low energy conversion in MD and the need for draw solution regeneration are the prominent challenges of this system. Another important aspect to be highlighted is that the water transfer balance between MD and FO is the key requirement for a stable and successful operation. The use of alternative energy is possible but it is only feasible in specific cases such as the existence of seawater and wastewater facilities in a proximity or the case of produced water that contains geothermal heat. Implementing heat recovery in the MD stage, using functionalized particles as a source of osmolarity in the draw solution, and developing membrane materials with unique characteristics such as omniphobic and Janus MD membranes are effective strategies that have just recently shown to improve the systems economics and such strategies should be explored further.

### 1. Introduction

Water scarcity is a pressing global problem that affects numerous regions, threatening the availability of safe and clean water resources for communities and industries. As traditional water treatment methods struggle to meet the increasing demand, innovative technologies like hybrid FO-MD systems have emerged as a potential solution to address this challenge (Son et al., 2021a). FO-MD system combines the benefits of FO and MD to provide efficient, and versatile water purification solutions (Ibrar et al., 2019).

FO-MD system has gained immense attention recently due to their potency to efficiently treat a wide range of water sources, including seawater, brackish water, and wastewater (Suwaileh et al., 2019; Yen

et al., 2010). One of the primary advantages of FO-MD systems is their ability to operate at low pressures, which significantly reduces energy requirements as compared to other traditional pressure-driven membrane processes. FO-MD systems are highly efficient in removing organics, salts, and other pollutants, providing high-quality treated water suitable for different applications, including drinking water production, industrial processes, and agricultural irrigation (Ge et al., 2012). Another attractive trait of FO-MD systems is the capability to handle feedwater with high salinity or fouling potential. The FO process operates with a low hydraulic pressure, minimizing membrane fouling and reducing the requirement for frequent cleaning or replacement. The MD process operates at elevated temperatures, which can effectively disinfect water and remove organic compounds further improving water

\* Corresponding author.

E-mail address: [qusay.f.abdulhameed@uotechnology.edu.iq](mailto:qusay.f.abdulhameed@uotechnology.edu.iq) (Q.F. Alsalhy).

quality. FO-MD systems can also be integrated with different renewable energy sources such as solar or waste heat, making them an environmentally friendly option for water treatment. The utilization of waste heat can help lower operational costs and carbon emissions, contributing to sustainable water management practices (Yen et al., 2010; Ge et al., 2012; Bamaga et al., 2011; Cabrera-Castillo et al., 2021).

Several research studies have been published on using hybrid FO-MD systems for different types of water treatment. The progress in this research area since inception was captured through assessing the growth in the produced documents as shown in Fig. 1. The data in this figure were extracted from Scopus and Web of Science records by searching for the topic *Forward Osmosis-Membrane distillation hybrid system*. The obtained data were carefully screened to remove irrelevant records. There are several review studies that discussed FO-MD application in various industries. Each one of these studies had a special focus on a certain aspect. For example, Pei et al (Pei et al., 2021). focused on liquid food concentration, Ghaffour et al (Ghaffour et al., 2019). researched energy requirements of different MD hybrid systems and FO-MD was one of them, Naidu and co-workers (Naidu et al., 2020) paid attention to the potency of FO-MD systems for energy and resources recovery from waste streams, Singh et al. work (Singh et al., 2021) concerned only with the membranes' types and draw solution recovery technologies, and the scope of Ibrar et al (Ibrar et al., 2022). was only confined wastewater treatment applications. This study aims to provide a more recent and comprehensive review for FO-MD literature body where opportunities and challenges of applying this hybrid system for treating the most common water sources, seawater and wastewater are critically discussed. A special focus was given to the emerging novel materials used in draw solutions such as carbon quantum dots (CQDs) and the pilot-scale and innovative designs of MD and FO systems. The study started with a brief overview of FO and MD technologies individually, followed by discussing the opportunities and challenges. The applications of FO-MD systems and the theoretical boundaries of water transfer were also analyzed in this study. Finally, future research directions and prospects are proposed.

## 2. Forward osmosis (FO) process

### 2.1. Overview

The FO process is an engineered osmotic process in which a draw solution (DS) with high concentration is employed on one side of a semi-

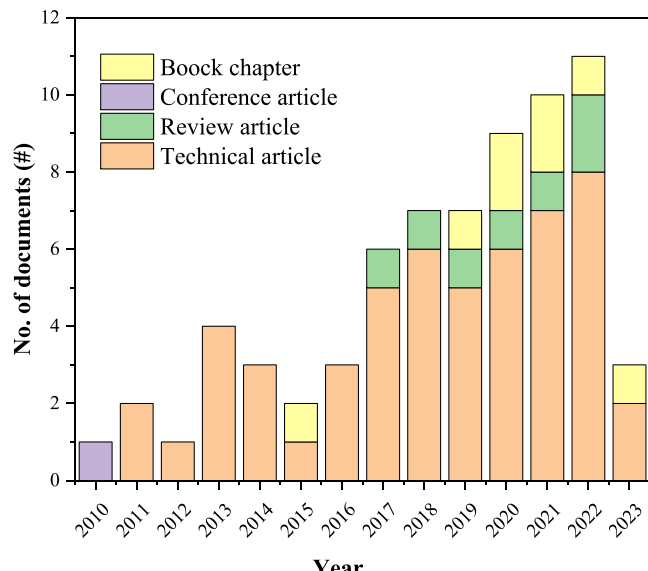


Fig. 1. Historical development of literature.

permeable membrane, and the water to be treated (feed solution (FS)) is fed to the other side of the membrane. Although FO is based on the osmosis principle, the word "forward osmosis" (FO) was likely coined to distinguish it from "reverse osmosis," which has been the title for the membrane desalination method for decades. Small molecules such as water flow through the semi-permeable membrane, mainly made of polymeric materials, whereas bigger molecules such as salts, sugars, starches, proteins, viruses, germs, and parasites are rejected (Xu et al., 2010). Although their driving forces are different, both RO and FO procedures use a semi-permeable membrane to successfully separate water from dissolved solutes. The primary difference between the two processes is that in the RO process, the driving force is provided by hydraulic pressure, whereas in the FO process, the driving force is created by the concentration difference. Sometimes, FO is mistakenly referred to as pressure retarded osmosis (PRO) process, but the two processes are different in their driving forces and applications. PRO was developed in the 1960 s as a potential power generation technique employing the salinity gradient since (Achilli et al., 2010; Yip and Eli-melech, 2012). The reason behind this confusion is that one of the operational modes for FO is termed PRO mode (described later).

In PRO process, the saline stream is mildly pressurized and the produced hydrostatic pressure due to the stream volume increase is utilized for electricity generation. PRO is thought to be a bridge between FO and RO, however, the net water flux remains in a range similar to that of FO (Sarp, 2019). Eq. 1 is the general formula for water transfer in FO, RO, and PRO (Cath et al., 2006), where  $J_w$  is water flux ( $\text{m}^3/\text{m}^2.\text{s}$ ),  $A$  is membrane's water permeability constant ( $\text{m}^3/\text{m}^2.\text{sPa}$ ),  $\Delta\pi$  is osmotic pressure (Pa),  $\sigma$  is reflection coefficient calculated by dividing the negative solute water phenomenology coefficient by pure water permeability (Hancock and Cath, 2009), and  $\Delta P$  is the applied hydraulic pressure (Pa). The product of this equation varies depending on the process applied, RO process,  $\Delta P > \Delta\pi$ , FO process,  $\Delta P = \text{zero}$ , and PRO process,  $\Delta\pi > \Delta P$ . The flux direction and the correlations between flux and applied and osmotic pressures in the three different processes, RO, FO, and PRO are illustrated in Fig. 2.

$$J_w = A(\sigma\Delta\pi - \Delta P) \quad (1)$$

Since the term osmotic pressure is important for FO process, it is useful to briefly cover its relevance to the discussion in this work. The pressure that would have to be supplied to a pure solvent to prevent it from flowing into a given solution by osmosis via a semipermeable barrier is known as the osmotic pressure of a solution. It is frequently used to express a solution's concentration. Osmotic pressure is a colligative property of a substance since it is proportional to the concentration of the solute and does not depend on the chemical makeup of the material (Tan and Ng, 2008). The osmotic pressure of a dilute solution can be estimated using the ideal gas law formula and the temperature and concentration of the solution (Yokozeki, 2006). The effective osmotic pressure is the portion of a solution's total osmotic pressure that influences the solvent's inclination to pass through a boundary, usually a semipermeable membrane (Mingming, 2012). The differential of osmotic pressure across the membrane( $\Delta\pi$ ), rather than the differential of hydraulic pressure, is used as the driving force in the FO process to transport water across the membrane (as in RO) (Cath et al., 2006). The partial pressure of the solute in the solution can be used to understand osmotic pressure. Osmotic pressures, like empirical gases, diverge from the ideal laws. Osmotic pressure can be calculated using van't Hoff equation (Wilson and Stewart, 2013), where  $\Phi$  is Osmotic pressure coefficient (-),  $I$  is Van't Hoff index (the number of dissociated ions per molecule (-)),  $C$  is solute concentration (mg/L),  $R$  is the universal gas constant, and  $T$  is the temperature in K.

$$\Delta\pi = \Phi i C R T \quad (2)$$

The membrane module design is an important step in constructing a reliable and efficient forward osmosis system. The FO module should provide a large surface area for mass transfer and offer durable

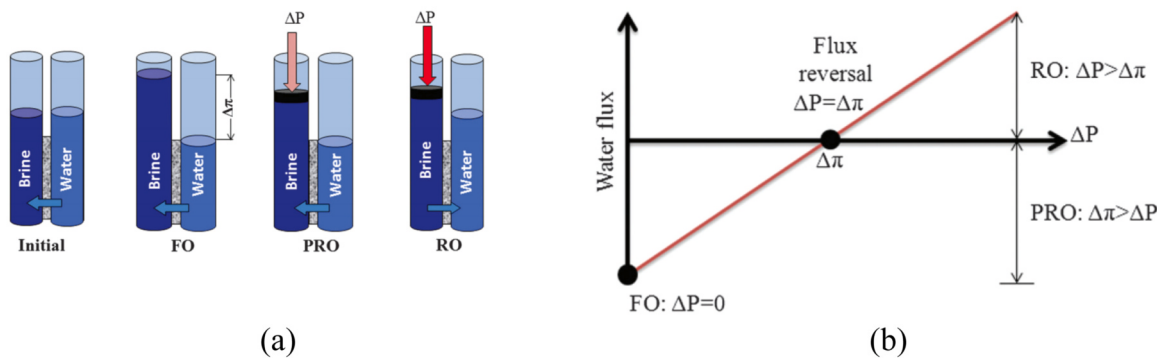


**Fig. 2.** Illustration for the differences between RO, FO and PRO in terms of (a) flux direction and (b) relationship between flux and osmotic and applied pressures adapted from (Lee et al., 1981) with copyright permission from Elsevier (License No. 5650791230656).

separation between the two streams, FS and DS. There are five configurations of FO modules that have been reported in the literature. These are plate and frame, tubular membrane, hollow fine fiber (HFF) membrane, spiral wound and hydration bags (Alghouti, 2016).

The type of materials used for synthesizing FO membrane is an important factor for the filtration process. Cattle, pig, and fish bladders; nitrocellulose (collodion); porcelain; and rubber were all used by early membrane researchers. Any thick, non-porous, and selectively permeable material could be used as a membrane for the FO process. In the 1970 s, all osmosis research (mostly PRO research) was conducted using RO membranes in tubular or flat sheet forms. In every case, the water flux was far lower than projected. RO membranes and membranes based on Polybenzimidazole (PBI) (Wang et al., 2010), aromatic polyamide (Thorsen and Holt, 2009), cellulose triacetate (CTA) (McCutcheon and Elimelech, 2007), and cellulose acetate (CA) (Su et al., 2010) were developed for FO processes and are commercially available. CA and polyamides are the most popular materials for making osmotic membranes because they can reject salts while allowing water to pass at a reasonable rate. The key requirements that should be present in an ideal membrane are a high-density active layer allows for a high salt rejection, high water permeability combined with membrane fouling resistance, low cost, mechanically sturdy, chemically stable, high-temperature resistance, and easy to clean (Qasim et al., 2015).

Membrane development techniques have a significant impact on membrane behavior and filtering effectiveness. Most researchers use traditional phase inversion to synthesize FO membranes, focusing on developing a dense selective layer on top of an asymmetric membrane (Klaysom et al., 2013). To maximize specific parameters, several research works have discussed innovative design methodologies and membrane production mechanisms. These include the following: functionalizing the membrane surface and/or embedding functionalized nanoparticles in the polymer, the membrane surface can be tailored to reduce fouling and increase water flows (Tiraferri et al., 2012),

stress-resistant reengineering of the support structure (Alsvik and Hägg, 2013), increasing mechanical strength by using electrospun nanofibres (Hoover et al., 2011), and for mechanical stability and high power density, innovative co-extrusion techniques can be used (Zhang et al., 2014).

The typical structure of FO membranes consists of a porous support layer (SL) that is laid underneath a less porous or smooth active layer (AL) as demonstrated in Fig. 3. The distribution of the pores vertically from active to support layer could be roughly uniform (symmetric membranes) or follows a widening pattern towards the support layer (asymmetric membrane). AL and SL both greatly influence forward osmosis performance. AL properties and structure governs the most important performance indicators namely water flux, salt rejection, and reverse solute flux (RSF) (Ibraheem et al., 2023). SL on the other hand regulates internal concentration polarization (ICP), osmotic gradient and as consequence water flux, and the mechanical strength. SL structural characteristics were also found to affect the fouling tendency of AL. Ramon and Hoek (Ramon and Hoek, 2013) showed through their theoretical modeling that a SL with higher water permeability results in more uniform water permeation and subsequently low fouling tendency as opposed to SL with low permeability through only localized spots (termed as hotspots). These findings were reported to agree with the experimental investigation for the effect of SL structure on AL fouling propensity (Lu et al., 2015). Hence, the structural and chemical properties of AL and SL are equally important key parameters that should be carefully considered when designing FO process.

In order to create an osmotic pressure difference during the FO process, lower FS and greater DS concentrations are required. The mode of FO orientations can also be altered simply by switching the side of FS or DS in the support or active layers. When FS and DS are placed on a membrane's active layer, they produce considerable disparities in ICP formation. As shown in Fig. 3, the active layer facing draw solution (AL-DS) and the active layer facing feed solution (AL-FS) are the two

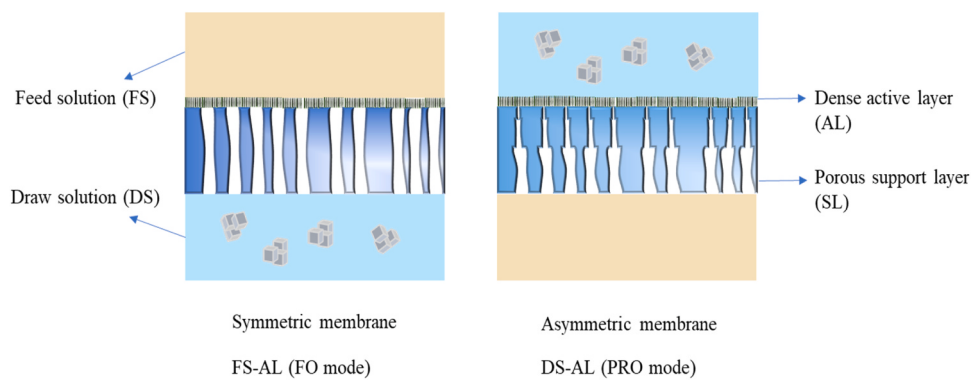


**Fig. 3.** FO process: membrane orientation and structural layout.

operating modes of the forward osmosis known as PRO and FO modes, respectively. In the AL-DS orientation, the salts from the DS can enter the AL and travel towards the support layer (Uragami, 2017). Compared to the salt content in the FS, continuous transfer of this salt leads to the accumulation of a larger concentration of salt content in the support layer region. Concentrative ICP is the word used to describe this state (Baker, 2012). When the active layer is exposed to the feed solution, the water from the FS permeates through to the support layer, diluting the salt concentration inside the support layer, and this is known as dilutive ICP (Baker, 2012). The osmotic pressure loss and concentration polarization (CP) in the FO mode are greater than that of PRO mode. However, FO still more commonly used compared to PRO mode due to likely the ease of fouling removal from the dense active layer as opposed to the porous support layer (Jafarinejad, 2021). FO mode may be preferable in applications such as wastewater treatment, membrane bioreactors, liquid food or protein concentration, and seawater desalination and brine concentration, where the feed solutions have higher fouling tendencies. When the feed solutions have lower fouling tendencies and/or low salinities (e.g., brackish water desalination), or when high concentration is not required, PRO mode is preferred (e.g., power generation) (Zhao and Zou, 2011a).

## 2.2. FO opportunities and challenges

The FO process has an extensive variety of applications, including desalination, direct fertigation, and osmotic power generation. However, only a few of these applications have currently been commercialized, such as water treatment, desalination, and water reclamation. FO technology can be applied in the above-mentioned processes and many more, such as power generation, enhanced oil recovery, produced water treatment, fluid concentration, protein concentration, thermal desalination feed water softening, and many other applications (Cath et al., 2006; McCutcheon et al., 2005; Phuntsho et al., 2013; Shaffer et al., 2015). FO process has many advantages such as low pressure and temperature requirements, low fouling propensity, minimal brine discharge, low energy consumption compared to other membrane technologies, high recovery rate, high fouling reversibility, and plausible rejection of a wide range of contaminants (Ibraheem et al., 2023; Nicoll, 2013; Song et al., 2022). Despite these attractive advantages of FO, the technology is hampered by several challenges that merits a detailed discussion. These challenges relate to the following aspects: CP, membrane fouling, reverse solute diffusion, and membrane resistance towards fouling and degradation (Al-Juboobi et al., 2022a).

### 2.2.1. Concentration polarization

Eq. 1 states that the water flux is proportional to the effective osmotic pressure differential across the membrane. Because the effective osmotic pressure differential is substantially lower than the bulk osmotic pressure differential, the water flux is much lower than projected theoretically. CP which occurs externally and internally is largely responsible for the significantly reduced water flux (Singh et al., 2023).

**2.2.1.1. External concentration polarization.** External CP (ECP) occurs on both the feed and permeate sides of the membrane, with concentrative ECP on the feed side and dilutive ECP on the permeate side. The feed solution flows against the active layer of the membrane in FO procedures. This creates a buildup of solute at the active layer, which causes a rise in the feed solution's osmotic pressure, resulting in the feed solution exerting more osmotic pressure. The draw solution on the permeate side of the membrane is diluted locally by the water passing through the membrane, which causes the draw solution's osmotic pressure to fall. ECP, both concentrative and dilutive, diminishes the system's effective osmotic driving force and consequently reduce water flux at the active layer (Suwaileh et al., 2022). The relationships between water flux and concentrative and dilutive ECP can

mathematically be expressed in Eqs. 3 and 4, respectively (McCutcheon and Elimelech, 2006). ECP is associated with other FO challenges such as RSF and fouling (discussed in subsections 2.2.2 and 2.2.3). RSF promotes ECP and fouling leading to the formation of cake mediated CP fouling (Suwaileh et al., 2022). ECP can be mitigated by increasing flow velocity and turbulence at the membrane surface and reducing the water flux (Al-Juboobi et al., 2022a). Although ECP plays a part in a considerably lower water flux than theoretically expected in FO processes, it has been reported to only have a minor role compared internal CP (ICP) which is believed to be the predominant contributor (Lutchmiah et al., 2014). It is important to note though that ECP has a noticeable impact on water flux when dealing with concentrated DSs with high water permeation at low cross flow velocities (Suwaileh et al., 2022).

$$\frac{\pi_{F,m}}{\pi_{F,b}} = \exp\left(\frac{J_w}{k_F}\right) \quad (3)$$

$$\frac{\pi_{D,m}}{\pi_{D,b}} = \exp\left(-\frac{J_w}{k_D}\right) \quad (4)$$

Where,  $\pi_{F,m}$ ,  $\pi_{F,b}$ ,  $\pi_{D,m}$ , and  $\pi_{D,b}$  are osmotic pressures at membrane surface from FS, in the feed bulk, at membrane surface from DS side, and in the bulk DS, respectively,  $J_w$  is water flux, and  $k_F$  and  $k_D$  are mass transfer coefficient at FS and DS, respectively.

**2.2.1.2. Internal concentration polarization (ICP).** Asymmetric membranes with a dense active layer on top of a thick porous support layer are now employed for FO. Depending on the direction of the membrane, this asymmetric structure is responsible for another membrane transport phenomena that can occur in addition to ECP. ICP refers to the salt build up that occur within the membrane's layers. ICP can be divided into two types: concentrative and dilutive. In PRO, the feed solution faces the porous support layer of the membrane resulting in ICP. Solute and water infiltrate through the porous support layer, forming a polarized layer (Cath et al., 2006). Concentrative ICP is similar to concentrative ECP in that it raises the feed solution's effective osmotic pressure, but it happens within the boundaries of the membrane layers. In the case of FO, the feed solution is directed at the dense active layer of the membrane, while the draw solution is directed at the porous support layer of the membrane. The draw solution within the porous support layer is diluted as water from the feed solution permeates the active layer of the membrane and enters the porous support layer (Cath et al., 2006). ICP is protected from any increases in flow velocity and turbulence at the membrane surface since it occurs within the membrane layers (Qasim et al., 2015).

The effect of ECP and ICP on FO process in its two operational modes and membranes structures is demonstrated in Fig. 4. The PRO mode is more prone to ICP than FO mode, however, due to the porosity of SL, the impact of ICP on the effective osmotic pressure gradient in PRO mode is lower than that of ECP in FO mode.

### 2.2.2. Fouling

Membrane fouling occurs when organic, inorganic materials, suspended and colloidal particles, or microorganisms accumulate, adsorb, or attach to a semipermeable membrane (Xie et al., 2017; Al-Juboobi and Yusaf, 2012). Table 1 shows examples of the different categories of fouling. Membrane fouling diminishes membrane performance, decreases lifespan and water flux, degrades permeate quality, increases energy usage, and reduces the overall process efficiency. It has a significant impact on the FO technology's economic feasibility (She et al., 2016; Zhang et al., 2016). The lack of recyclable and cost-effective DS, and the limited availability of information on membrane fouling are the three fundamental obstacles for FO technology (Chung et al., 2012). Although fouling of FO membranes is more reversible than fouling of RO membranes when FO membrane in FS-AL orientation, but removing fouling is still a challenge. It is important to clarify here the reasons that

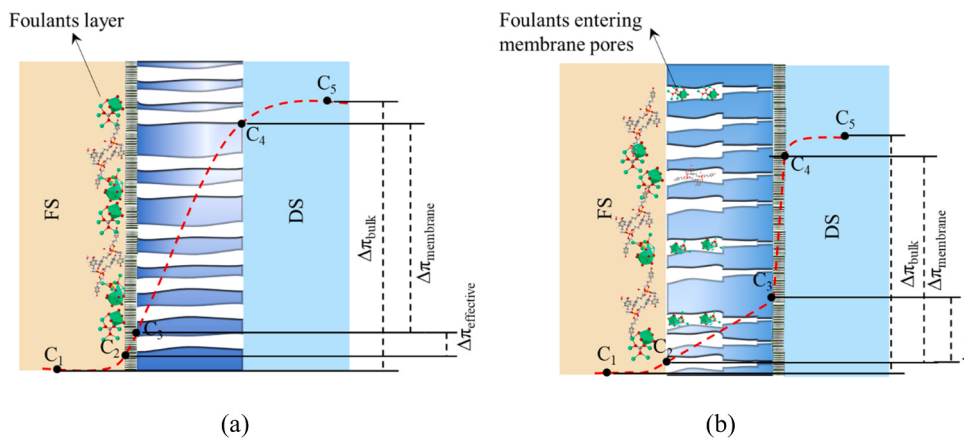


**Fig. 4.** Impact of CP on a) symmetric membrane (ECP) and b) asymmetric membrane (ICP).

**Table 1**

Different types of membrane fouling (Sreedhar et al., 2018).

Fouling type	Foulants	Mechanism	Reversibility and cleaning protocols	Ref.
Organic fouling	Natural organic compounds, polysaccharides, proteins	Chemical and hydrodynamic interactions	Almost completely reversible, osmotic backwashing	(Mototsa et al., 2014)
Inorganic fouling	CaSO <sub>4</sub> , CaCO <sub>3</sub> , SiO <sub>2</sub> , BaSO <sub>4</sub>	Crystallization	Partially reversible, hydraulic flushing	(Shirazi et al., 2010)
Colloidal fouling	Microbial deposition	Physiochemical, ligand-receptor and adhesive interactions	Recovery possible only by chemical cleaning with chlorine, high cross flux velocity, thick spacer	(Al-Juboori and Yusaf, 2012; Kwan et al., 2015)
Organic-inorganic fouling	Alginate and gypsum model foulants	Reverse salt diffusion causing cake formation	Decreased reversibility, Chemical cleaning protocols	(Liu and Mi, 2012)
Organic-colloidal fouling	Alginate and silica model foulants	—	Complicated fouling nature due to internal concentration polarization, not known	(Lee et al., 2005)

make FO fouling more reversible than that of RO. The high hydraulic pressure of RO along with the drag force produces highly compacted foulant layer as opposed to the loosely attached foulant layer in FO driven by drag force only (Xie et al., 2015).

In the AL-FS mode, the foulants in the FS are carried to the active layer surface of the membrane, resulting in a cake layer comparable to fouling of RO membranes, as shown in Fig. 4a. In AL-DS mode, fouling in the FO membrane is more complicated. Small contaminants enter the porous of SL due to convection forces and either get absorbed through the walls of the support layer's pores or retained by the active layer and accumulate on the active layer's back surface. More foulants get adhered to the entrapped foulants in the pores leading to pore-clogging. This is also termed as internal fouling. As more foulants accumulate, the fouling layer grows beyond the pores' depth. This type is referred to as mixed internal and external fouling. If the foulants are large molecules (e.g. organic matter) and cannot enter the porous support layer, they may only be gathered on the porous support layer's outer surface (external fouling) (She et al., 2016). Optimizing the hydrodynamic conditions of the feed stream (such as increasing the cross-flow rate, or applying pulsed flow) (Zhang et al., 2014), and using air scouring can be applied to remove external fouling from the membrane surface (Valladares Linares et al., 2012). These techniques can also be used for mitigating ECP. Internal fouling within the porous support layer acts as an unmixed layer. Hence, optimizing hydrodynamic conditions is not effective for this kind of fouling (Arkhangelsky et al., 2012). For alleviating ICP and internal fouling problems, tuning the structural parameters and surface chemistry of SL are applied (Al-Juboori et al., 2022a).

### 2.2.3. Reverse solute flux (RSF)

The reverse solute diffusion is governed by Fick's law (Eq. 5), where

B and ΔC are the solute permeability coefficient and the solute concentration difference, respectively (Stefani, 2014).

$$J_s = B \Delta C \quad (5)$$

The reverse solute diffusion is considered an inevitable challenge that negatively impacts FO. A new term named specific reverse solute flux ( $J_w/J_s$ ) is used to express the ratio between the forward water flux to the reverse draw solute flux across the semi-permeable membrane (Hancock and Cath, 2009). It is applied to evaluate the selectivity of the FO membrane, which is needed to understand the solute transport between the membrane layers. Philip et al (Philip et al., 2010) illustrated that RSF is not affected by the structure of the porous support layer and concentration of the draw solution. It is only affected by the selectivity feature of the thin active layer. Therefore, manufacturing FO membrane with high selectivity active layer is needed to minimize RSF. The hydration radius and the charge of the ion can also play a role in reducing the RSF. It has been observed that cations with divalent have less reverse diffusion rate than the monovalent ions. However, multivalent ions could cause high ICP (Phillip et al., 2010). Many studies have demonstrated that in FO mode, reverse solute diffusion is less pronounced than in PRO mode (Stefani, 2014; Akther et al., 2015; Chekli et al., 2018). The outcome of these studies also shows that the reverse solute diffusion increases proportionally by increasing the draw solution concentration in both modes (Stefani, 2014; Akther et al., 2015). The reverse solute diffusion phenomenon can be reduced by considering three approaches: seeking a competent draw solution, improving the selectivity of FO membranes, and choosing optimal operation parameters (Cai and Hu, 2016).

#### 2.2.4. Draw solutions

Draw solutions are a pivotal part of FO process, as they can be said to play a similar role to pumps in RO processes (Razmjou et al., 2013). The type of draw solution has a big impact on FO membranes and performance, thus choosing the right one is crucial (Mohammad et al., 2015). To drag water flux through the membrane, the draw solute must provide a higher osmotic pressure than the feed solute. The optimum draw solution should have a small size and charged ions, a low molecular weight, low viscosity, inexpensive, stable, non-toxic, membrane and system compatibility (Johnson et al., 2018). Some of the key characteristics that needs to be considered when selecting DS are summaries in Table 2. The evolution of the draw solution over time is depicted in Fig. 5. Volatile compound-based are the earliest draw solutions used, and different inorganic and organic materials have been used since then. As recent years have witnessed an impressive progress in nanotechnology field and this has influenced all Chemical Engineering processes and FO is nonexempt. FO process benefited from nanotechnology advancement in the synthesis of effective membranes and draw solutions. Many studies focused on analyzing the impact of different types of draw solutions on FO performance and other dedicated their work for surveying the outcomes of these studies in literature review reports. Few examples of these studies are quoted here that can be useful for keen readers in this area of FO process field (Lutchmiah et al., 2014; Sreedhar et al., 2018; Akther et al., 2015; Johnson et al., 2018; Chekli et al., 2016). A brief description of DS types along with their advantage and drawbacks are presented in the next few sub-sections.

**2.2.4.1. Volatile solutions.** In the 1960 s, volatile solutions like sulfur dioxide were used as a draw solute and could be recovered using a hot gas stripping operational state (Ray et al., 2018). These compounds are unsuitable for the FO process due to low water flux and a high diffusion rate, which results in reverse solute flux. It is also one of the nutrients that can speed up biofouling on the FO membrane's surface (Johnson et al., 2018).

**Table 2**

An overview of the characteristics of an ideal draw solution (Suwaileh et al., 2020; Chekli et al., 2012).

DS characteristics	Influence on the process
Molecular weight and viscosity	Draw solutions having a small molecular weight and low viscosity, and hence higher diffusion coefficient in aqueous solution is desirable for better process performance
Osmotic pressure	A draw solution osmotic pressure higher than that of the feed solution is desirable as it gives rise to high water fluxes across the membrane and thus higher process efficiency
RSF	A low reverse solution diffusion is advantageous since it raises the osmotic pressure in the draw solution and minimizes fouling
ICP	Draw solution should have minimal ICP, it decreases permeate flux significantly and also depends diffusivity, ion size and viscosity.
Temperature	High diffusivity, small molecule/ion size and lower viscosity of draw solution is desirable.
Other characteristics	Optimum temperature of draw and feed solution in keeping with the process is necessary to avoid abnormal values of permeability, solute diffusivity, water viscosity, thus minimizing reverse salt diffusivity
	In addition, specific characteristics of a draw solute may also influence the FO process performance. For example, a new class of DS can display unique properties. Such properties can be particle sizes or particle agglomeration due to special magnetic properties when using magnetic nanoparticles (MNPs). Some DS can also act as precursor to scaling and membrane fouling during reverse diffusion when DS containing $\text{SO}_4^{2-}$ and $\text{Mg}^{2+}$ are used, respectively

**2.2.4.2. Organic compounds.** Organic molecules, notably fructose and glucose solutions, have been investigated as DS particularly in saline water desalination (Yaeli, 1992). Surfactants with a steady and relatively high osmotic pressure at concentrations above the Critical Micelle Concentration are a fascinating group of organic draw solutes (Cai and Hu, 2016).

**2.2.4.3. Thermolytic solutions.** McCutcheon and Elimelech (McCutcheon and Elimelech, 2006) examined thermolytic solutions like ammonia carbonates as a viable DS for desalination applications. High flux was expected due to the DS's high osmotic pressure, but ICP harmed process performance, and high RSF and biofouling were reported due to the high diffusivity of ammonia, a potential nutrient for microbial growth (Johnson et al., 2018).

**2.2.4.4. Inorganic salts.** Simple inorganic salts such as  $\text{NaCl}$  are the most commonly utilized draw solutions.  $\text{MgCl}_2$ ,  $\text{Na}_2\text{SO}_4$ ,  $\text{CaCl}_2$ ,  $\text{Ca}(\text{NO}_3)_2$ ,  $\text{KCl}$ ,  $\text{MgSO}_4$ ,  $\text{KNO}_3$ ,  $\text{KSO}_4$ ,  $\text{NH}_4\text{HCO}_3$ ,  $(\text{NH}_4)_2\text{SO}_4$ , and others have all been investigated as draw solutions. Multivalent salts produce higher osmotic pressure than monovalent salts, however they have the tendency to promote biofouling through promoting ligand-receptor mechanism (ions-polysaccharide interactions) (Al-Juboori et al., 2022a). Ions with bigger hydration radius have higher rejection rate through membrane and consequently they cause less RSF (Achilli et al., 2010). Ions with big hydrated radii (larger than the membrane pore size) are rejected through size exclusion mechanisms leading to less RSF (Zou et al., 2019). It was found that the diffusion coefficient of common ions and cations such as  $\text{Na}^+$ ,  $\text{Mg}^{2+}$ ,  $\text{Cl}^-$  and  $\text{SO}_4^{2-}$  have a direct correlation with the hydrated radius of these species (Tajuddin et al., 2019). Hence, ions with big hydrated radii are preferred for preparing FO draw solution.

**2.2.4.5. Dendrimers.** The use of ethylenediamine core dendrimers with sodium succinamate terminal groups and pentaerythritol core dendrimers with sodium carboxylate terminal groups as a novel DS for dewatering RO concentrate was proposed by Adham et al (Adham et al., 2007). Dendrimers have nanostructures and are carefully created to carry molecules inside their voids or on the surface. They have high osmotic pressure and are easy to regenerate using ultrafiltration. In FO-MD system, Zhao et al (Zhao et al., 2014a), assessed poly (amidoamine) with COONA bonding as the draw solute for saltwater desalination. PAMAM-COONa with a larger molecular weight had lower osmotic pressure and water flux but a smaller reverse solute flux at the same solution concentration.

**2.2.4.6. Magnetic nanoparticles.** When big magnetic nanoparticles are suspended in DI water to form a draw solution, the solution becomes nonhomogeneous. As a result, unlike inorganic salt draw solutions, the osmotic pressure would be lower. The RSF, on the other hand, may not occur if the particle size is bigger than the membrane pores. It should be highlighted that while nanoparticle aggregation remains a serious concern, it may be easily re-concentrated and utilized in the FO process. To avoid aggregation, Na and coworkers (Na et al., 2014) used a co-precipitation approach to create novel hydrophilic citrate coated magnetic nanoparticles (cit-MNP1 and cit-MNP2) that were dispersed in water to generate a draw solution. A hydrophilic citrate coating was added to the surface to prevent aggregation. Citrate's carboxylic groups were able to bond to Fe ions, resulting in their inclusion on the surface of  $\text{Fe}_3\text{O}_4$  nanoparticles. The water flux of cit-MNP2 was remarkable compared to other coatings, although membrane fouling was a problem in the FO operation. On the other hand, contact between the membrane's cellulose material and magnetic nanoparticles resulted in a significant reduction in water flux. This is because the ultrasonic approach cannot prevent nanoparticle aggregation. The performance of the nanoparticles DS was shown to be influenced by the pore size

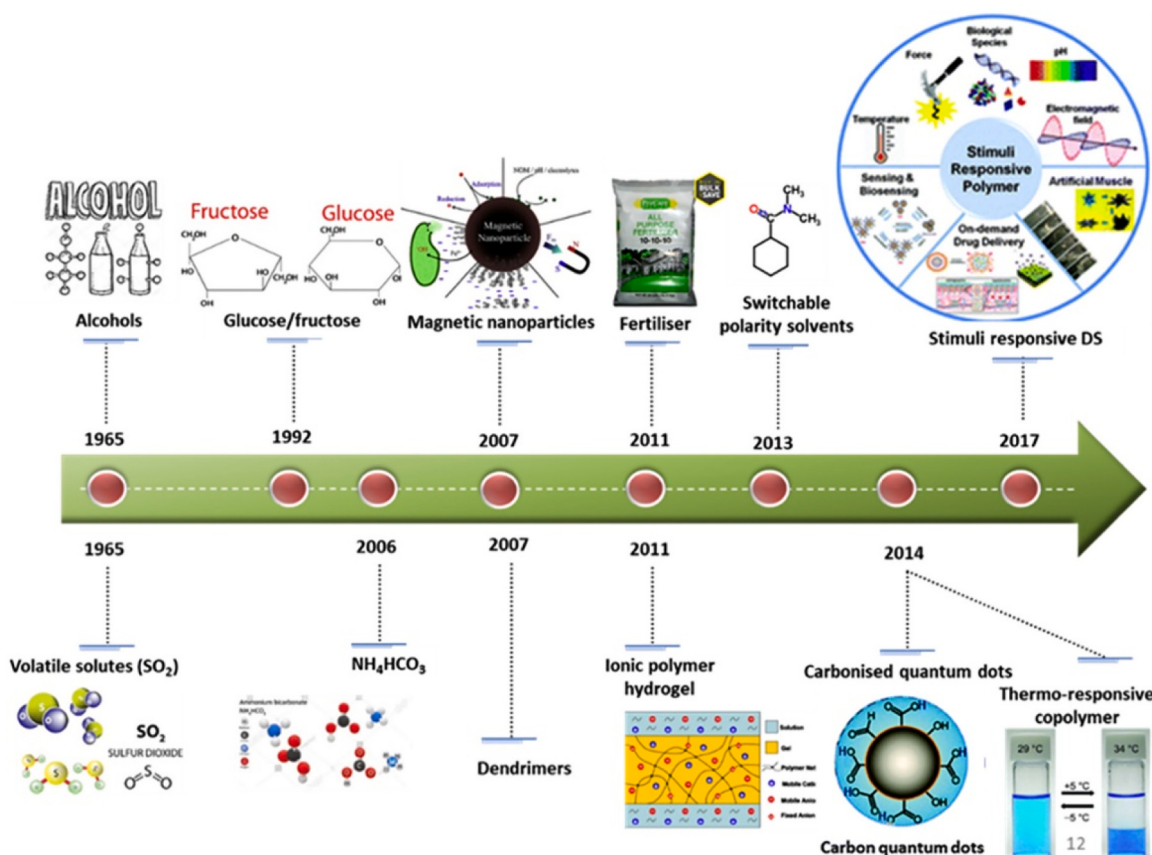


Fig. 5. Draw solution options development with time. Copied from (Suwaileh et al., 2020) with copyright permission from Elsevier (License No. 5650800669010).

distribution and hydrophilicity of the CTA membrane.

**2.2.4.7. Hydrogels.** The hydrogels' monomer composition, network structure, and hydration are all important features that can be utilized for making an effective DS. The potential of hydrogels as a DS was initially investigated by Li et al (Li et al., 2013). Hydrogels, which are crosslinked hydrophilic polymers with water entrapped within the network, can create a large amount of water flux in a FO application. Unfortunately, the hydrogel's water recovery is insufficient. A key stumbling block was the disparity in swelling and de-swelling speeds of the thermally responsive hydrogels. Cai et al (Cai et al., 2015) developed novel hydrogels based on thermally sensitive polyionic liquids, with a water flux that was more than quadrupled above that of PNIPAM-based semi-IPN hydrogels.

**2.2.4.8. Inorganic fertilizers.** When the FO is regarded as a stand-alone process, and diluted DS can be utilized directly for fertigation, inorganic fertilizers are an interesting option as a DS for seawater and wastewater extraction. For flow and RSF measurements, Phuntsho et al (Phuntsho et al., 2011) tested nine inorganic fertilizers in FO application. Because urea has the highest RSF of all fertilizers, it has been proposed to be avoided in blended fertilizers. The best fertilizers were ranked in the following order  $\text{NH}_4\text{NO}_3 > \text{KCl} > \text{NH}_4\text{Cl}$ .

**2.2.4.9. Switchable polarity solvents (SPS).** Stone et al (Stone et al., 2013) were the first to use SPS as DS based on tertiary amine compounds. The solubility of amine molecules varies with carbon dioxide content ( $\text{CO}_2$ ), and the hydrophobic amine turns hydrophilic and ionizes when it reacts with  $\text{CO}_2$ , resulting in a draw solution with an extremely high osmotic pressure. Regeneration can be accomplished using low-grade waste heat or nitrogen purging, in which  $\text{CO}_2$  is removed, and

the amine is restored to its hydrophobic non-ionic neutral form, allowing phase separation from water. However, unlike ammonium carbamate, SPS is not thermolytic, and another difficulty could be their compatibility with FO membranes, as tiny molecular amines swell and destroy the membrane rejection layer, reducing selectivity.

**2.2.4.10. Thermo-responsive copolymer and stimulus-responsive nanoparticles.** A range of stimuli-response hydrogels has recently been proposed as DS in FO. This unique type of hydrogel-driven FO technique that uses solar energy to regenerate the DS has been gaining high attention. Because of the structure's natural shrinkage, light or thermoresponsive hydrogels can release fresh water when exposed to sunshine. For example, light or thermoresponsive hydrogels can absorb enough water at the maximum volume phase transition temperature and dewater at temperatures higher than the volume phase transition temperature (Long et al., 2018). It is reasonable to conclude that the properties of these draw solutions had a significant impact on membrane performance. The particle size and size distribution of a hydrogel, for example, can reduce the amount of water that passes through the membrane. When utilizing a higher particle diameter-based draw solution, the membrane endeavor to create increased water flux. On the other hand, some draw solutions had small particle diameters, which allowed tiny molecules to pass through the bigger membrane pores, leading to a high RSF (Hartanto et al., 2015). Because the copolymer draw solution had a high molecular weight, big particle size, and viscosity, the membrane would yield the least amount of water flux at the expense of the energy required to pump the extremely viscous draw solute and the additional pressure-driven regeneration mechanism. Apart from the previous difficulties, producing drinking water and recycling the diluted draw solution may result in high energy consumption and running costs, which is still a challenge for all draw systems. As a result of the mutual interference of network structure, the

behavior of the thermo-responsive draw solute tends to deteriorate. The enlarged network could increase the pressure. However, data on anticipated energy usage and operational costs for each thermo-responsive polymer is currently lacking.

**2.2.4.11. Carbon Quantum Dots (CQDs)-emerging promising draw solution.** Carbon-based quantum dots (CQDs, C-dots, or CDs) are a new class of carbon nanomaterials with diameters below 10 nm and an abundance of functional groups (Zhang et al., 2018). They were originally obtained in 2004 via the preparative electrophoresis purification of single-walled carbon nanotubes (Xu et al., 2004). As a new nano-carbon member, carbon-based quantum dots have slowly become a rising star due to its benign, abundant, and inexpensive nature, great water dispensability and ease of synthesis, and functionalization (Baker and Baker, 2010; Fowley et al., 2013). Much progress has been made in the last decade (Baker and Baker, 2010). CQDs can contain various functional groups on the surfaces, such as amino, hydroxyl, carboxyl, carbonyl, and other oxygenous groups, depending on the precursors and reaction parameters, making CQDs very water-soluble and biocompatible (Sarkar et al., 2016; Guo et al., 2013). Using these strengths, CQDs have been used to improve pure water permeability and antifouling properties of membranes (Zhao and Chung, 2018). As a result of their quantum confinement effect and optical stability qualities, CQDs have a moderate photoluminescent signal, strong fluorescence activity, and durability (Shi et al., 2019), prominent biocompatibility, colorful photoluminescence, low cost, and toxicity (Zhang and Yu, 2016), excellent hydrophilicity, environmental friendliness and high chemical inertness (Fowley et al., 2013; Lim et al., 2015).

CQDs have been made from several natural carbon sources, such as citric acid, in prior studies (Lim et al., 2018; Wang et al., 2019a), graphitic micro-particles, denatured milk (Athika et al., 2019), zein biopolymer (Azizi et al., 2019), sodium hydroxide (Lei et al., 2019), dried leaf (Joshi et al., 2018), broccoli (Arumugam and Kim, 2018), food wastes (Fan et al., 2020), ammonium citrate (Singh et al., 2019), ginkgo leaf (Jiang et al., 2019), grass (Sabet and Mahdavi, 2019), humic acid (Cheng et al., 2019), ascorbic acid (Wang et al., 2019a) and gelatin (Parthiban et al., 2018). Only a few studies have reported using waste biomass to produce CQDs in the past (Shi et al., 2019). Giving the projected increase of biomass waste production as population grows and the attractive traits of CQDs, utilizing this waste for synthesizing the latter is an important research area. Citric acid, which contains carbonyl, carboxyl, and hydroxyl groups, is one of the most popular raw materials used in the manufacture of CQDs, according to previous researches (Piri et al., 2019). This basic material can be substituted with sustainable materials with a comparable chemical structure. Plant wastes, fruit fibers, leftover coffee or tea powders, and palm oil industrial wastes, for example, all have high carbon content and might be a potential alternative. The chemical structure, quantum size, and photoluminescent properties of CQDs are dependent on the chemical structure of the raw materials as well as the fabrication methods used (Yu et al., 2018). Excitation-dependent fluorescence emission can be produced through the formation of oxygen-containing functional groups in CQD structures. CQDs' physicochemical features can also be tweaked by varying precursor concentrations, reaction time, solution pH, and reaction temperature (Kalaiyarasan and Joseph, 2019).

Since the discovery of CQDs, a large variety of techniques for the preparation of CQDs have been developed. Generally, synthesis methods of CQDs can be classified into two groups: top-down and bottom-up methods. The top-down approach breaks down larger carbon structures via chemical oxidation, discharge, electrochemical oxidation, and ultrasonic methods (Lim et al., 2015). However, a drawback of this approach includes the requirement of expensive materials, harsh reaction conditions, and long reaction time (Wang and Hu, 2014). The bottom-up approach refers to converting smaller carbon structures into QDs of the desired size. This bottom-up approach includes the

application of a number of techniques such as of hydrothermal treatment, ultrasonic treatment, thermal decomposition, pyrolysis, carbonization, microwave synthesis, and solvothermal method to synthesize QDs (Sharma and Das, 2019). There are three issues to consider when preparing CQDs (Wang and Hu, 2014): i) during carbonization, carbonaceous aggregation can occur, which can be avoided utilizing electrochemical synthesis, restricted pyrolysis, or solution chemistry techniques, ii) size control and uniformity are critical for uniform characteristics and mechanistic studies and can be improved via post-treatment techniques such as gel electrophoresis, centrifugation, and dialysis, and iii) surface qualities that are important for solubility and certain applications that can be tweaked during preparation or post-treatment.

The application of CQDs as a draw solution for FO process is an emerging field that still require further studying to unravel the true potential and challenges associated with such an application. So far, the outcomes of the few studies investigated CQDs use in FO process have shown promising results. Guo et al (Guo et al., 2014). synthesized CQDs from citric acid and functionalized it with Na. The produced CQDs-Na had osmotic pressure of 53.6 atm at a concentration of 0.5 g/ml. The CQDs-Na produced a stable water flux of about 30 L/m<sup>2</sup>.h which was double that of NaCl (0.2 M) with negligible RSF. A recent study prepared CQDs from tulsi leaves and used it along with 50% glycerol (CQDs-G) as antibacterial DS for FO process with synthetic wastewater (Doshi and Mungray, 2020). It was found that CQDs-G achieved water flux 25% higher than that with 1 M NaCl Ds with RSF four times lower. Other studies explored the possibility of integrating CQDs into FO membrane structure to improve its characteristics such as permeability, RSF and fouling resistance (Deng et al., 2021; Mahat et al., 2020). For more detailed coverage of the recent advancement in CQDs application in FO system, readers are referred to a recent literature review work (Dutta et al., 2023). Table 3 presents different classes of DS along with some examples and merits and shortcomings of these classes.

## 2.2.5. Relationships between FO process challenges

The five key challenges in FO are not isolated but closely related to each other. Fig. 6 illustrates the relationships between ICP, RSF, membrane fouling, membrane characteristics, and the draw solute properties in FO. It can be seen that the membrane support layer should be as porous as possible to reduce ICP and that the active membrane layer should be highly selective to decrease the reverse solute diffusion. The reduced reverse solute diffusion can help to reduce membrane fouling even further. Small ion/molecule can reduce ICP for the draw solute (Zhao and Zou, 2011a), but it can also increase reverse solute diffusion and membrane fouling. As a result, the requirements for favorable draw solutes become even more important. In general, significant membrane fouling can be caused by high reverse solute transport and vice versa (Lay et al., 2010). ICP and membrane fouling may also have a negative impact on water flux in FO (Tang et al., 2010). At the same time, membrane fouling, ICP, and reverse solute diffusion are all influenced by membrane parameters and draw solute qualities.

## 3. Membrane distillation

### 3.1. Overview

One of the relatively newer technologies still in its research and development stage is MD, patented by Bodell in 1963 (Ravi et al., 2020). MD is a membrane-based non-isothermal process that utilizes a suitable hydrophobic microporous membrane, primarily used to desalinate seawater. The operation of MD makes use of the temperature difference (thermal gradient) created across the membrane. On one side of the membrane, known as the feed side, the separation of salt from water is achieved by heating the feed solution (e.g., seawater) at temperatures below the boiling point of the solution. On the other side, known as the permeate side, a cooler solution is run directly or indirectly in contact

**Table 3**  
Different types of draw solutes for forward osmosis.

Draw solute	Examples	Advantages and disadvantages
Inorganic salts [Achilli et al., 2010; Li et al., 2017]	KHCO <sub>3</sub> , MgCl <sub>2</sub> , NaCl, Ca(NO <sub>3</sub> ) <sub>2</sub> , (NH <sub>4</sub> ) <sub>2</sub> SO <sub>4</sub>	Helpful in primary studies, can be used to understand parameters affecting performance of FO, energy consuming regeneration, their application is limited.
Organic compounds [Ge and Chung, 2015; Cai et al., 2016]	organic acids sodium salts, hydroacid complexes zwitterions,	Higher water permeation than polymers, lower reverse flux, energy consuming regeneration, their application is limited.
Polymers (Gwak et al., 2015)	Polyethylene glycol, polyacrylic acid, dextran, copolymers	Low water flux, low reverse flux, high viscosity, non-responsive, their application is limited.
Magnetic nanoparticle (Na et al., 2014)	Coated iron oxide (Fe <sub>3</sub> O <sub>4</sub> )	Low to reasonable water flux, facile recovery by magnetic field, low reverse flux, agglomeration problem, very special applications.
Thermo-responsive Hydrogels (Razmjou et al., 2013; Cai et al., 2015)	Semi-IPNs, polyionic liquids, copolymers with PSA, PNIPAm.	Exceptional auto-regeneration characteristics, NO reverse flux, likelihood of semi-continuous FO process, low water permeation yet great progress in new responsive hydrogels based on polyionic liquids.
Metathesis precipitable salts (Alnaizy et al., 2013)	CuSO <sub>4</sub> /MgSO <sub>4</sub> + Ba(OH) <sub>2</sub> + H <sub>2</sub> SO <sub>4</sub> , Al <sub>2</sub> (SO <sub>4</sub> ) <sub>3</sub> + CaO	On academic studying, chemicals and acid/base are required in recovery process, tiresome recovering steps, worries of toxicity, no viable application is available for now.
Volatiles or dissolved gases [Ray et al., 2018; Johnson et al., 2018].	CO <sub>2</sub> , NH <sub>3</sub> , SO <sub>2</sub> , dimethyl ether	High possible osmotic pressure, DS is prepared under pressure, potential operational problems, very high reverse flux possibility, toxicity problem.
NH <sub>3</sub> -CO <sub>2</sub> combination (Li et al., 2015)	Carbonate and carbamate, ammonium bicarbonate.	High osmotic pressure, very widely investigated, imperfect elimination of NH <sub>3</sub> , inappropriate for drinking purposes, high reverse flux, recovery requiring both liquid-to-gas and gas-to-liquid transitions, scaling.
Solvents with switchable polarity (Stone et al., 2013)	PDMAEMA-CO <sub>2</sub> , tertiary amines-CO <sub>2</sub> ,	CO <sub>2</sub> used for protonation, liquid-liquid phase separation during recovery, possibility of harm to membranes, liquid-solid phase separation, no harm to membrane and low reverse flux for PDMAEMA, more studies needed for application.
Thermally responsive organic compounds (Noh et al., 2012)	PEI, PPG, ionic liquids, glycol ether	Most investigated on LCST type molecules, high water permeation possibility; thermally responsive ionic liquids are better than the rest, possibility of great power cost saving, more studies are needed on pilot scale.
Ionic species functionalized carbon quantum dots [Guo et al., 2014]	Na-CQDs	Carbon quantum dots (CQDs) with diameters less than 10 nm, low toxicity, excellent hydrophilicity, environmental friendliness, low cost, excellent water dispensability, and ease of syntheses and functionalization. The generated CQDs can contain various functional groups on their surfaces, such as amino, hydroxyl, carboxyl, carbonyl, and other oxygenous groups, very water-soluble and biocompatible.

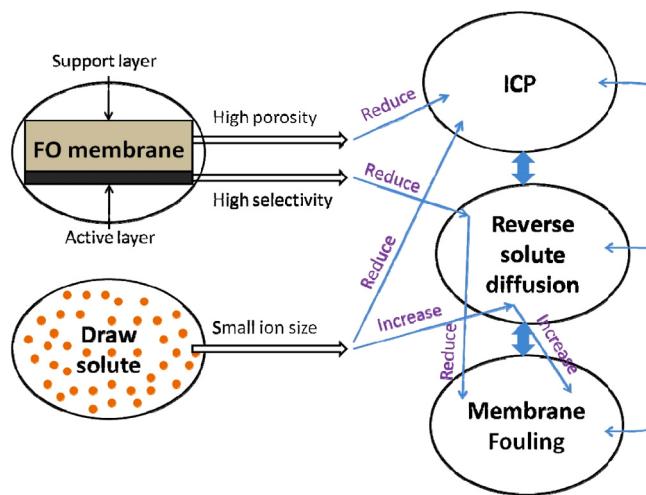


**Fig. 6.** Relationships between important elements and challenges of FO process. Copied from (Zhao et al., 2012) with copyright permission from Elsevier (License No. 5650801187089).

with the membrane. The water vapor evaporates from the membrane-liquid interface at the feed side, leaving the salt behind as the retentate in the feed solution. The presence and absence of vapor on the feed and permeate sides create a vapor pressure gradient. The water vapor thus moves across the membrane through the pores. The water vapor then condenses at the cooler permeate side as permeate flux (fresh water). Along with the mass (water vapor) transfer, heat transfer occurs simultaneously across the membrane (Ravi et al., 2020; Deshmukh et al., 2018). The water vapor transfer across the membrane can theoretically be described by Eqs. 6–8 (Al-Juboori et al., 2022b), where  $J_w$  is the water flux ( $\text{kg}/\text{m}^2\cdot\text{s}$ ),  $B_w$  water vapor permeability through the membrane,  $p^0$  is the water vapor pressure on hot feed side subscripted with  $w_h$  and cold permeate side subscripted with  $w_c$ ,  $a_w$  is water activity,  $T$  is the temperature ( $^\circ\text{C}$ ),  $X_s$  is the solute molar fraction, and  $\alpha$  and  $\beta$  are parameters their values depend on the type of the solute.

$$J_w = B_w(p_{wh}^0 a_{wh} - p_{wc}^0 a_{wc}) \quad (6)$$

$$p_w^0(T) = e^{(23.1964 - \frac{3816.44}{T - 46.13})} \quad (7)$$

$$a_w = (1 - X_s) \exp(\alpha X_s^2 + \beta X_s^3) \quad (8)$$

There are four configuration of MD process, direct contact (DCMD), air gap (AGMD), vacuum (VMD) and sweep gas (SGMD) as illustrated in Fig. 7. In DCMD, the membrane is in direct contact with liquid phase. It is a basic arrangement commonly used in the food sector for desalination and concentrations of aqueous solutions. When compared to other MD types, heat loss by conduction in DCMD is greater. As a result, commercial applications do not employ this configuration (Wang and Chung, 2015). In AGMD, an air gap is introduced between the membrane and the condensation surface. The permeate gas vapor condenses on the cold surface inside the module. Because it functions on a small temperature difference, the flow obtained is often minimal, necessitating a larger membrane surface area due to higher mass transfer resistances. Because heat conduction loses less in AGMD, it has been chosen an energy-efficient module. In the AGMD design, the latent heat can be recovered during the condensation of the vapor on the cooling plate (Wang and Chung, 2015; Pangarkar et al., 2016). The vacuum is applied to the permeate side in VMD module to lower the vapor pressure and thus increase the driving force. Because the condensation occurs outside the membrane module, this design requires external condensation. Compared to other MD designs, VMD can generate the highest driving force, resulting in a greater permeation flux and superior thermal energy conversion when a high-efficiency external condenser is

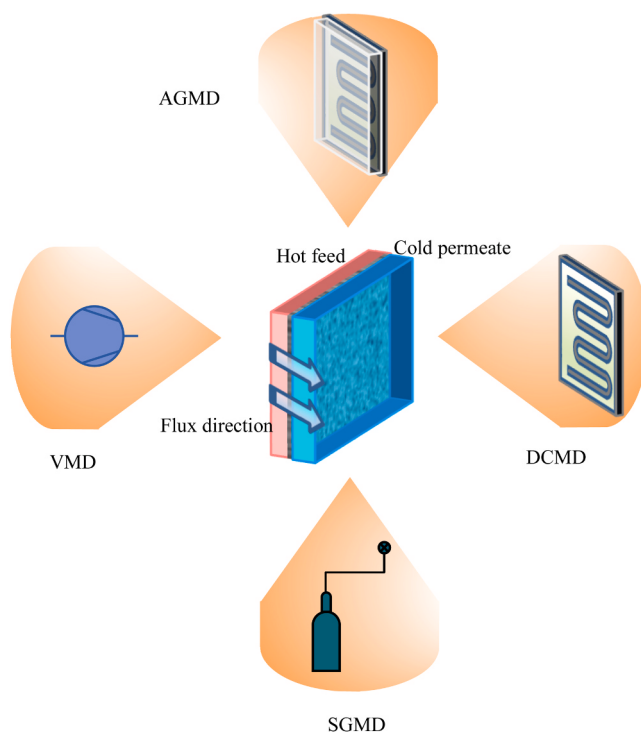


**Fig. 7.** Membrane distillation configurations.

employed. As a result, VMD is an appealing module in various applications including RO brine concentration, heavy metal removal, alcohol purification, and so on. The VMD was commonly used to remove volatile components from aqueous solutions. The key benefit of this design is that conductive heat loss is minimal (Wang and Chung, 2015; Pangarkar et al., 2016). An inert gas stream is employed to sweep the vapor at the permeate side in SGMD. Similar to VMD, an external condenser is required for obtaining the liquid permeate. The downside of this configuration is the little volume of permeate diffuses in the vast volume of the sweep gas, necessitating the employment of a large condenser. Therefore, there are only few investigations in the literature that explored this process due to this constraint (Wang and Chung, 2015; Pangarkar et al., 2016). Table 4 summarizes the advantages, disadvantages and the potential application areas of MD configurations.

Although Eqs. 6–8 apply to all MD process in general, mass and heat transfer mechanisms vary from one configuration to other. The water vapor transfer in MD happens in three stages from feed to membrane boundary layer, through the membrane pores and from permeate side to the condensation element. The first stage is similar in all MD configurations where mass transfer is governed by the nature of the flow regime in the feed side. The mass transfer coefficient in the feed side can be computed by the empirical relationships of the flow dimensionless numbers (Al-Juboori et al., 2021). The second and the third stages of vapor transfer varies depending on the configuration type. In AGMD, DCMD (excluding deaerated), and SGMD, the water vapor flow mechanism is determined by the value of Knudsen number ( $K_n$ ) (Johnson and Nguyen, 2017). If  $K_n < 0.01$ , the dominant mechanism is molecular diffusion. Knudsen diffusion mechanism becomes prominent when  $K_n > 10$ . Between these two values, the transfer mechanism is explained by molecular-Knudsen diffusion. For VMD and deaerated DCMD, The vapor transfer through the membrane pores can be described by Poiseuille flow mechanism (Fane et al., 1987). For DCMD and VMD, there is no resistance to the transfer of the water, it either gets sucked by vacuum or condense directly on the cold plate. The vapor transfer in the permeate side of AGMD is dictated by molecular diffusion mechanism (Johnson and Nguyen, 2017). For SGMD, the vapor transfer in the permeate side is influenced by the flow characteristics of the gas, and mass transfer

**Table 4**

Fundamental advantages, disadvantages, and applications area of MD configurations (Kullab, 2011; Abu-Zeid et al., 2015).

Configuration of MD	Advantage	Disadvantage	Application Area
DCMD	<ul style="list-style-type: none"> <li>• High permeate flux.</li> <li>• Simple design and operation.</li> <li>• The possibility to recover the internal heat.</li> </ul>	<ul style="list-style-type: none"> <li>• Thermal efficiency is low.</li> <li>• High influence of thermal and concentration polarizations.</li> <li>• The possibility to permeate pollution is high.</li> </ul>	<ul style="list-style-type: none"> <li>• Desalination.</li> <li>• Nuclear industry</li> <li>• Food industry</li> <li>• Pharmaceutical textile as well as chemical industries.</li> </ul>
AGMD	<ul style="list-style-type: none"> <li>• Thermal efficiency is high.</li> <li>• Conduction heat loss is low.</li> <li>• The possibility to recover the internal heat.</li> </ul>	<ul style="list-style-type: none"> <li>• The air gap resistance to water vapor transport causes low permeate flux</li> <li>• Large footprint</li> </ul>	<ul style="list-style-type: none"> <li>• Desalination.</li> <li>• Food industry.</li> <li>• Chemical industry</li> </ul>
SGMD	<ul style="list-style-type: none"> <li>• High mass transfer rate</li> <li>• Low conductive heat loss</li> </ul>	<ul style="list-style-type: none"> <li>• Relatively difficult to recover heat</li> <li>• Dealing with sweep gas relatively complex</li> <li>• Large outer condenser is required</li> </ul>	<ul style="list-style-type: none"> <li>• Desalination</li> <li>• Chemical industry</li> </ul>
VMD	<ul style="list-style-type: none"> <li>• Flux permeation is high</li> <li>• Less heat loss via conduction</li> <li>• The boundary layer of thermal and concentration that can be formed on permeate side is small</li> </ul>	<ul style="list-style-type: none"> <li>• The chance of pore wetting is high</li> <li>• Relatively difficult to recover heat</li> </ul>	<ul style="list-style-type: none"> <li>• Desalination.</li> <li>• Food industry.</li> <li>• Chemical industry</li> <li>• Textile industry</li> </ul>

coefficient can be estimated using the empirical flow relationships alluded to earlier. The heat transfer across MD module follows the same three stages as the mass transfer. Information about thermal properties of the membrane and water along with the dimensions are usually utilized for theoretical estimation of the heat entering and existing the MD system. Empirical correlations are commonly used for estimating heat transfer resistance and the boundary layer temperature of the different zones (Johnson and Nguyen, 2017).

### 3.2. MD pilot-scale design systems

MD is a non-isothermal process, and hence the design should provide not only acceptable flow conditions, low-pressure drop, and high packing density, but also a good heat recovery function and thermal stability (El-Bourawi et al., 2006). In large-scale applications, membrane distillation system can be built in different module design such as plate-and-frame, spiral-wound, hollow fibers and multi effect vacuum configuration. The plate-and-frame is the simplest and the first design for pilot-scale MD system that was developed by the Swedish company Scarab AB. The first developed model was an AGMD in the form of stacked cassettes with a membrane surface area of  $2.3 \text{ m}^2$  and achieved a gain output ratio (GOR) of 0.72 (Kullab, 2011). Two pilot plants of this system were installed in Sweden: one in a thermal cogeneration plant with a capacity of  $1\text{--}2 \text{ m}^3/\text{day}$  and the second one for wastewater treatment with GOR of less than 1 (Kullab, 2011). After this,

TNO patented an MD system run with cross flow which led to the development of Memstill system (operation principle is illustrated in Fig. 8a). The main challenges with plate-and-frame design is the presence of dead zones, leakages and poor heat recovery (Guillén-Burrieza et al., 2012). The spiral-wound design was first proposed by Gore et al (Gore et al., 1985). and Fraunhofer Institute for Solar Energy Systems developed the principle further and built several solar desalination systems based on permeate gas MD (PGMD) (Kullab, 2011). The schematic illustration of this system is shown in Fig. 8b. The spiral wound has better heat recovery capacity than plate-and-frame and hence better GOR. However, the trade-off between permeate flux and GRO is the main challenge that makes operating this system a bit complicated (Winter et al., 2011). Hollow fiber (HF) systems were developed as solution for obtaining high membrane surface area and to overcome the difficulty in removing scale and foulants from membrane surface (Kullab, 2011). An example of HF-VMD system is provided in Fig. 8c. KmX cooperation was one of the leading companies in developing HFMD systems. They constructed HF-VMD system with capacities of 10–1000 m<sup>3</sup>/day (Kullab, 2011). Econity was the other company that was specialized in building HFMD systems, and one of their systems was installed in the largest seawater desalination pilot plant in South Korea with a capacity of 400 m<sup>3</sup>/day (Lee et al., 2019). Several attempts were reported by industry and research entities for developing internal heat recovery system in HF, but it was proven to be as complicated as that in spiral wound (Kullab, 2011). Vacuum multi effect MD (V-MEMD) system was coined by Heinzl and commercialized by memsys (Heinzel et al., 2012). V-MEMD works on a similar principle to multi effect distillation as the latent heat of condensation is utilized to further evaporate the feed solution in the following stages. A schematic diagram of V-MEMD system is depicted in Fig. 8d. There are two main frames in each effect, membrane frame and foil frame that are separated by polypropylene spacer that serves as permeate channel (Chen et al., 2020). Although heat recovery improves energy efficiency of V-MEMD, it negatively impacts its productivity. It was reported that as the number of effects increases, the GOR increases moderately (Kullab, 2011). V-MEMD has a promising scalability potential as installations of plate and frame system of this design were reported to be as high as 100 m<sup>3</sup>/day (Thomas et al., 2017).

### 3.3. Membrane materials

Polymeric materials are widely used for the preparation of membranes. In general, they can be categorized into three types which are glassy polymers, ionic polymers, and rubbery polymers (Gao, 2016). In the application of MD being using exclusively hydrophobic membranes, these membranes are manufactured from non-polar polymers naturally feature excellent hydrophobic characteristics, good chemical resistance, and high thermal stability, for example, polypropylene (PP), polytetrafluoroethylene (PTFE), and polyvinylidene fluoride (PVDF) (Winter, 2014). Generally, the membrane used in the MD system should have good resistance for harsh chemicals such as acids or bases, high thermal stability, impose little resistance for mass transfer, low tortuosity, and possess minimal thermal conductivity to reduce heat loss by conduction through the membrane layer (Alkhudhiri et al., 2012). Camacho et al (Camacho et al., 2013). listed the following criteria for a good MD membrane candidate: the membrane should be porous and not be moistened by the aqueous solutions, the capillary condensation should not occur inside the membrane pores, water vapor should only be transported across the pores, and the membrane should not change the vapor-liquid equilibrium of the various components in the process liquids.

The two most prevalent membrane materials are PTFE and PVDF, which are applied in membrane distillation. However, the PTFE membrane outperforms the PVDF membrane in terms of permeate flux amount, salts rejection ratio, highest hydrophobic characteristics, good thermal stability, and chemical resistance (Pangarkar et al., 2016).

Supported membranes have been used in the implementation of MD, considering that the supporting layer should not exert a significant resistance to mass transport (Sanmartino et al., 2016). The main important features in MD membrane are to be hydrophobic with minimal resistance to vapor transfer. To achieve these characteristics researchers have been testing different synthesis strategies and exploring bolstering the conventional polymeric structure (commonly PVDF and PTFE) with different additives such as carbon nanotubes, graphene, lithium chloride, titanium dioxide, silicon dioxide, fluorinated substances, polyvinylpyrrolidone and others (Hussain et al., 2022). There is another trend in MD membrane materials research that aims to manufacturing omniphobic membranes that can reject a wide range of contaminants with various surface tensions and reduce the risk of wetting. Although omniphobic MD membranes have a great potential for reducing wetting events and expand the MD applications to include treating wastewater and produced water, their manufacturing is still expensive and requires using environmentally harmful chemicals such as fluorinated solvents (Ni et al., 2021). There also exist the research area that concerns with developing Janus MD membranes. The latter is defined as a membrane that has two sides with distinctive water affinity properties, one hydrophobic/superhydrophobic and one hydrophilic/superoleophobic (Galiano et al., 2023). There are many examples in the literature about different novel materials that have been used in synthesizing MD membranes that are hard to be adequately captured here, however, a few examples will be given to highlight importance of continuing the paths of exploring this area. For instance, a recent study reported potency of cyclic olefin polymers for manufacturing MD membranes with stable high water flux and salt rejection of 15 L/m<sup>2</sup>.h and 99.99% using synthetic solution of 30 g/L NaCl (Sabzekar et al., 2021). Another study was motivated by the rising interest in promoting circular economy and environmental protection by synthesizing composite MD membrane from recycled polyethylene plastic and alumina (Hanen et al., 2023).

### 3.4. MD opportunities and challenges

MD process possesses many advantages such as operation lower pressure compared to pressure-driven membranes, the capacity for separating materials that are thermal sensitive like food products, 100% theoretical rejection of ions, macromolecules, and colloids, large separation factor of non-volatile solutes, capacity to handle high salinity feed solutions, ability to treat solutions with high corrosivity, and the possibility to utilize every form of low-grade waste heat (Alkhudhiri et al., 2012; Alcheikhhamdon et al., 2015). Despite the plausible advantages of MD process, it still faces some challenges such as low permeate flux in comparison with pressure-driven membrane processes, the trapped air within the membrane pores leads to a further mass transfer resistance, limiting the MD permeate flux especially in AGMD and DCMD, and membrane fouling, scaling, and pore wetting (Alkhudhiri et al., 2012; Kayvani Fard et al., 2016). The latter are the most arduous challenges.

#### 3.4.1. MD Fouling

Fouling is defined as the adhesion of unwanted material on solid surfaces with an associated detriment of function (Warsinger et al., 2015). MD like other membrane processes is susceptible to the different types of foulants highlighted in Table 1. However, the severity of fouling in MD is less than that of pressure driven membrane due to the absence of the strong hydraulic forces that pushes foulants towards the membrane surface (Al-Juboobi and Yusaf, 2012; Alkhudhiri et al., 2012). As explained in Section 2.2.2. that foulants accumulation onto the membrane surface can occur on different depth, it could fill the pores for small foulants (pore blocking), or builds up on the blocked or empty pores for large foulants (cake formation) (Al-Juboobi et al., 2021). Membrane fouling as a phenomenon can be described by the chemical and physical interactions between foulants and membrane surface. These interactions are explained by the

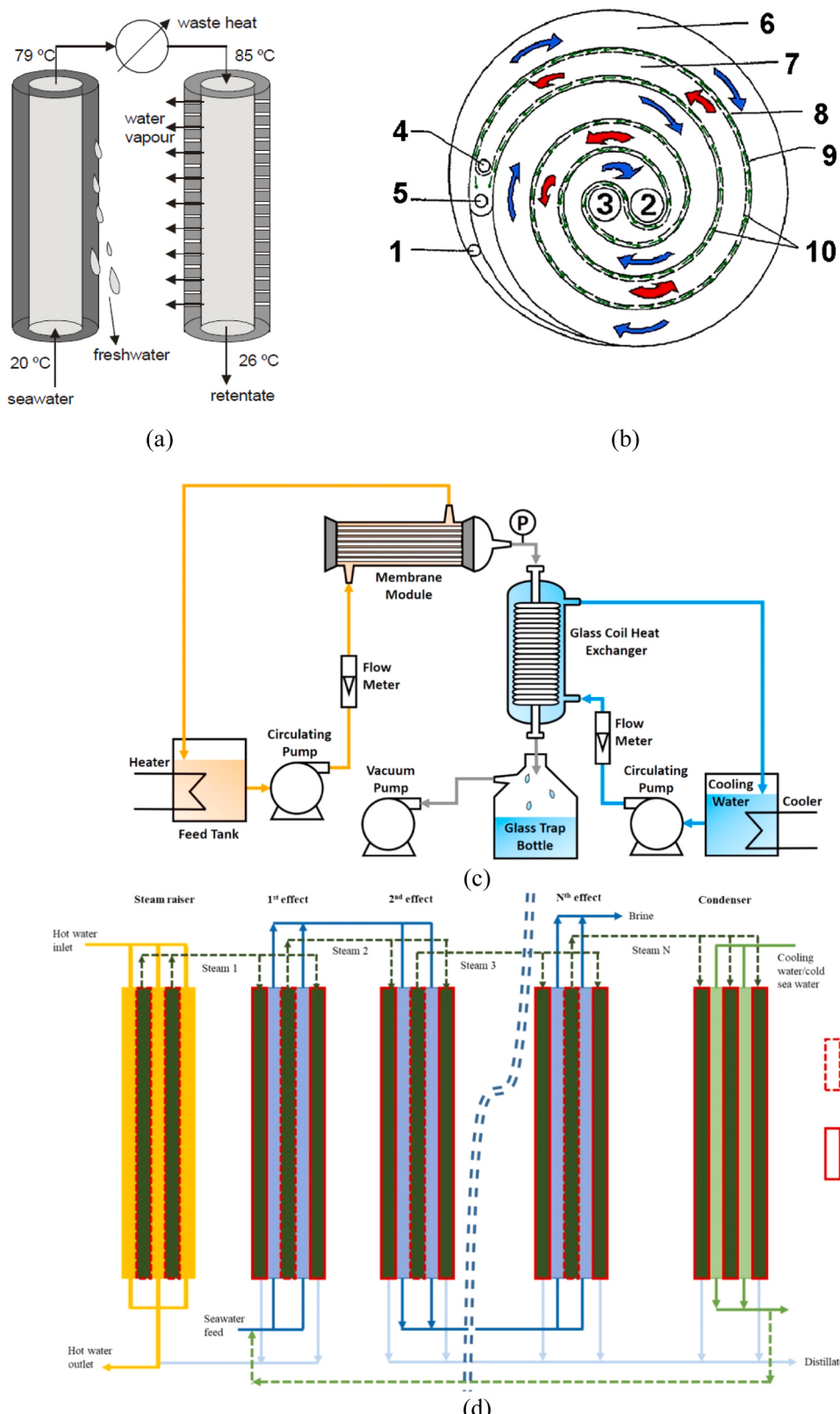


**Fig. 8.** 5650810073193), (b) Schematic of the spiral wound module concept: (1) condenser inlet, (2) condenser outlet, (3) evaporator inlet, (4) evaporator outlet, (5) distillate outlet, (6) condenser channel, (7) evaporator channel, (8) condenser foil, (9) distillate channel and (10) hydrophobic membrane. 5650810906931).  
 (a) Examples of MD pilot-scale system design: a) Memstill system, copied from (Meindersma et al., 2006) with copyright permission from Elsevier (License No. (b) Copied from (Winter et al., 2011) with copyright permission from Elsevier (License No. (c) 5650810641149), and d) V-MEMD, copied from (Chen et al., 2020) with copyright permission from Elsevier (License No. (d) 5650810434090), (e) HF-VMD, copied from (Chen et al., 2018) with copyright permission from Elsevier (License No.

Derjaguin–Landau–Verwey–Overbeek (DLVO) and the extended-DLVO theories (Al-Juboori and Yusaf, 2012). The responsible forces for these interactions are Van der Waals and the electrical double layer. The accumulated fouling layer can add mass and heat transfer resistances that decrease the water flux (Yang et al., 2022). The foulants deposition onto membrane pores can also lead to feed solution entrapment into the pores leading to partial membrane wetting (Alkhudhiri et al., 2012). Scaling is an important issue in MD process given that its use for high salinity feed solution. Magnesium and calcium are the most abundant ions in seawater. The precipitation of calcium carbonate which is one of the major culprits when it comes to membrane scaling increases with increasing temperature (Figueira et al., 2023).

In order to effectively combat fouling and scaling problem a good understanding of feed solution characteristics, operation conditions and membrane surface properties are necessary. Information about salts concentration, solubility, diffusivity, and ionic strength in feed solution, membrane characteristics such as porosity, pore size distribution, charge and hydrophobicity, and operating flow rate and temperature are important to be scrutinized to devise an effective solution for the fouling problems. The common strategies for controlling fouling in MD and other membrane processes are applying pre-treatment such as precipitation of high concentration salts, chemical cleaning, synthesizing self-cleaning membranes, developing vibrating spacers, and tuning membrane surface properties to reduce its fouling propensity (Al-Juboori and Yusaf, 2012; Alkhudhiri et al., 2012; Lalia et al., 2015).

#### 3.4.2. MD wetting

Membrane wetting is defined as the permeation of water into membrane micropores (Yang et al., 2022). This phenomenon leads to the reduction in the vapor flux across the membrane and may also deteriorate the quality of the produced water. Membrane wetting occurs due to the accumulation of inorganic and amphiphilic foulants and/or membrane degradation (Gryta, 2019). Another possible reason for wetting is the applied hydraulic pressure exceeding the liquid entry pressure of the membrane (Warsinger et al., 2015). As explained in the previous section, foulants could also facilitate liquid entrapment inside membrane pores. In cases where there is sudden drop in operating

temperature due to system shutdown or malfunction, this leads to reduction in saturation vapor pressure which in turn cause condensation inside the membrane pores (Rezaei et al., 2018).

There are three types of wetting depending on its severity as illustrated in Fig. 9. As demonstrated in this figure, the non-wetted membrane has the largest contact angle with the liquid and the highest amount of vapor. In the surface wetted membrane, the amount of vapor pass through the membrane decreases, but there is no liquid transfer from the feed side to the permeate side. For partially wetted membrane, the vapor transfer in the membrane pores reduces significantly, and liquid passage across the pore is experienced. The most severe case of wetting is the completely wetted membrane where vapor transfer ceases due to the pores being filled with liquid. The quality of the produced water is only affected in the last two cases. Wetting cannot be rectified without shutting down the process. Lowering operating pressure below the liquid entry pressure does not guarantee the cessation of wetting and similarly chemical cleaning may result in internal scaling (Rezaei et al., 2018; Gryta, 2017). The only safe way for restoring membrane hydrophobicity is offline chemical cleaning followed drying.

#### 3.4.3. Temperature and concentration polarization

The primary reason of the low flux production is the polarization phenomenon which consists of the temperature polarization (TP) and CP (Zhang et al., 2023a). TP occurs when a temperature gradient deteriorates along the length of the MD membrane. TP is frequently linked to inadequate heat transfer and results in a decrease in both the vapor pressure difference and the energy efficiency of MD systems (Camacho et al., 2013). CP on the other hand takes place within MD when solutes, ions, or impurities found in the feed solution accumulate near the membrane's surface as water vapor traverses through. This situation gives rise to a boundary layer characterized by higher solute concentrations adjacent to the membrane. This layer generates a 'reverse' diffusive force for freshwater on the permeate side, thereby impeding the transfer of vapor from the feed to the permeate (Yun et al., 2006). The impact of CP on membrane performance is illustrated in Fig. 3 which applies to MD membrane.

Numerous research studies have explored the impact of TP on the

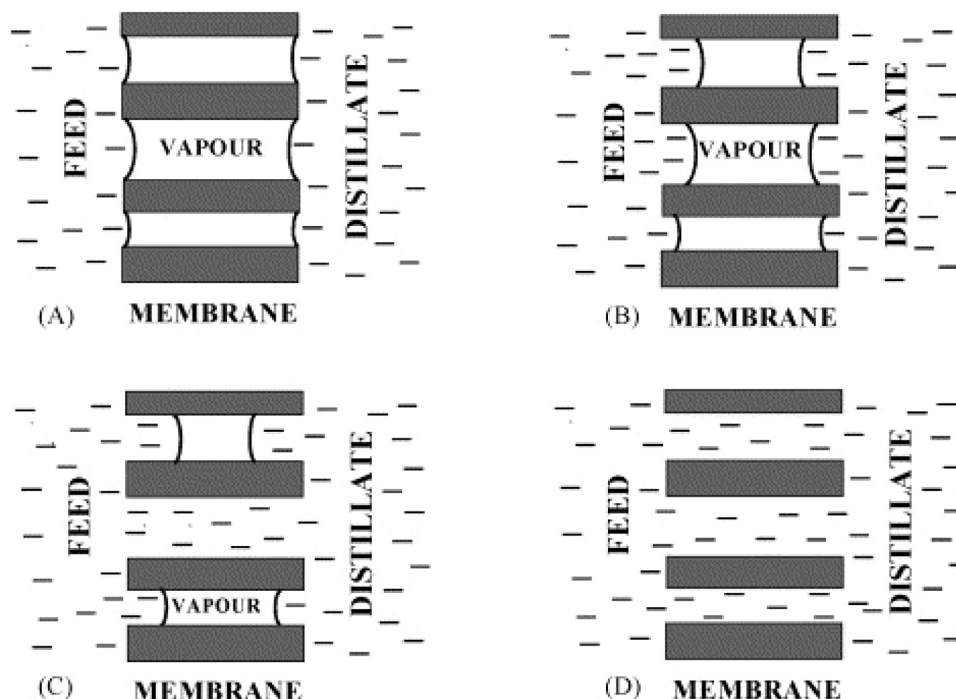


Fig. 9. MD wetting types. Copied from (Gryta, 2007) with copyright permission from Elsevier (License No. 5650811122645).

permeation flux in MD. TP could result in flux decline of up to 50–80% (Abu-Zeid et al., 2015). TP problem is more pronounced in long membrane modules as they have a greater conductive heat loss through the membrane, resulting in lower average distillate flux (Anvari et al., 2020). This limitation hampers the large-scale development of MD. The accumulation of a thermal boundary layer caused by TP significantly diminishes MD's thermal efficiency. To maintain a high permeate flux, the most effective methods involve increasing either the feed flow rate or the feed temperature, both of which lead to higher energy consumption (Ullah et al., 2018). Similarly, CP has a significant impact on MD performance. It results in considerable mass transfer resistance. Although it is generally believed that CP does not significantly affect permeation flux since its impact on feed vapor pressure is minor, CP can accelerate salt crystallization on the membrane surface as the feed concentration approaches saturation and this impedes mass transfer (Lokare and Vidic, 2019). It has been noted that the salt concentration at the membrane surface can be up to 30% higher than in the bulk concentration as the feed solution approaches saturation (Lokare et al., 2017a). Another notable effect of CP on MD processes is membrane scaling due to the deposition of non-volatile molecules on the membrane surface (Olatunji and Camacho, 2018). It was reported that flux reduction due to CP effects varies from 10% to 52% under different operating conditions, and when the solution approaches saturation, there is a sudden 90% decline in flux (Lokare and Vidic, 2019; Bouchrit et al., 2015). To mitigate TP and Cp, various strategies are employed, such as utilizing multi-stage or cascade configurations that utilize permeate heat to preheat the feed solution, integrating other heat recovery systems for optimized energy use, developing membranes and spacers that improve mass and heat transfer across membranes (e.g. vibrating spacers, self-heating membranes (Al-Juboobi et al., 2021); Ahmed et al., 2022).

### 3.4.4. Inherent low energy conversion efficiency

The ability of using solar and low-grade energy in MD process is commonly viewed as a positive trade, but there are still challenges that hinder this application and render it less attractive than RO technology. MD belongs to the family of thermal desalination technologies that includes also multi-stage flash (MSF), mechanical vapor compression (MVC), and multi-effect distillation (MED). Thermal desalination technologies including MD purify the water by applying thermal energy exceeding the latent heat of vaporization ( $\Delta H_{vap}$ ) of water (2400 kJ/kg  $\approx$  667 kWh/m<sup>3</sup>) (Sharqawy et al., 2010). This large amount of energy is significantly higher than the separation specific Gibbs energy of 1.06 kWh/m<sup>3</sup> for water recovery of 50% from saline water with salinity of 35000 mg/L (Elimelech and Phillip, 2011). When assessing the efficiency of thermal desalination techniques, GOR is used. GOR is defined as the ratio of  $\Delta H_{vap}$  to the total thermal energy input into the system (Jalilah, 2019). The least efficient thermal treatment system would have a GOR of 1 where there is no heat recovery and this number could increase to one to two magnitude of orders for efficient systems equipped with recovery techniques. In general, MD systems have higher GOR compared to MED and MSF for small systems (<1000 m<sup>3</sup>/day) (Deshmukh et al., 2018). For larger systems, the latter technologies have a higher GOR. The thermodynamic reversibility is another factor that affirms the possibility of energy recovery in processes. Thermodynamic reversibility in MD process is not possible. Due to the difference in the salinity of feed and permeate solution, feed solution must always be at a temperature slightly higher than the permeate solution to ensure zero driving force (Deshmukh et al., 2018).

Different approaches have been used to reduce the energy consumption of the MD systems. One of these approaches is integrating solar energy with MD system. Huang et al (Huang et al., 2018). have immobilized graphene-based material in hydrophobic PTFE membrane surface for water desalination via photothermal membrane distillation (PMD). An ultrathin graphene-based film fabricated by a scalable process, serves as efficient solar absorbers (absorption efficiency of rGO/pDA-rGO > 80%), ultrafast water permeable channels, and high

salt resistance network. Their findings showed that as compared with the virgin PTFE, the water vapor flux of the modified membrane was improved by 78.6%. Since the feed water was heated by the solar power, and with the immobilization of graphene material, the system has shown excellent energy consumption compared to other MD processes. At the same time, the graphene-based PTFE membranes has demonstrated ultrahigh salt rejection.

Another approach is using low-grade waste heat. This approach has attracted considerable attention among researchers as the heat can be transferred within the industry process. Many industries produce huge amount of heat waste in different forms such as textile industry, food processing industry, petrochemical industry and marine transportation industry (Su et al., 2021). Integration of MD with industrial waste heat showed very attractive results. For example, Dow et al (Dow et al., 2016). used the waste heat from a gas fired power station to heat the wastewater and then combined with a DCMD system to recover freshwater. Their findings demonstrated that the water recovery rate of 92.8% was achieved with a water permeation flux of 2–5 L/m<sup>2</sup>.h. The authors also found that the water production of 8000 m<sup>3</sup>/day could be obtained for a continuous operating 500 MW rated power station. Another study, Lokare et al (Lokare et al., 2017b). utilised the waste heat waste that is produced from the natural gas compressor station to concentrate the industrial wastewater to 30 wt% salinity.

Apart from the industrial scale applications, the incorporation of waste heat with MD system also expands to special scenarios such as the freshwater supply for the passengers on cruise ships where the freshwater storage is very valuable. Bahar and Ng (Bahar and Ng, 2020) developed a multi-stage AGMD desalination system with the waste heat recovery from a marine engine for on-board ships. It has been concluded that a Specific Energy Consumption (SEC) 1.58–2.63 kW h/m<sup>3</sup> with the feed temperature at a range between 40 and 60 °C for a freshwater demand between 1 and 15 m<sup>3</sup>/day. Thus, using a waste heat for MD system could be very helpful as compared to other traditional desalination processes in terms of energy consumption. In another study, Criscuoli et al (Criscuoli et al., 2008). stated that the lab-scale DCMD and VMD systems have shown the lowest energy consumption of 3.55 kW h/m<sup>3</sup> and 1.1 kW h/m<sup>3</sup>, respectively. Although these values were achieved when deionized water (DI) was used as the feed stream in MD modules. This study proved that the VMD module has a better energy performance than the DMCD module. Park et al (Park et al., 2020). compared the SEC of thermally driven and electrically driven crystallization process in a hybrid FO/RO/crystallization process, which has shown that at the lowest case, the SEC were 14.684 kW h/m<sup>3</sup> thermally and 1.355 kW h/m<sup>3</sup> electrically, respectively.

The utilization of solar and low-grade energy is not free from challenges. For instance, the use of simple solar thermal collector require a large physical footprint that could translates into a large capital cost (Karanikola et al., 2014). While there are laudable efforts being spent on fabricating materials for efficient conversion of solar energy into heat in solar collectors, such materials are still costly (Wang et al., 2019b). The diurnal and seasonal intermittency of solar energy is another challenge. Based on the United State of America case, the biggest share of industrial waste heat is generated from power plants (Deshmukh et al., 2018). About 95% of the waste heat is at a temperature of 42 °C (Gingerich and Mauter, 2015), which is unsuitable for efficient MD process. Geothermal exploitation is also hampered by the high drilling cost of and the constraints associated with well's location (Deshmukh et al., 2018). Geothermal energy might be easily accessible for some industries such as oil and gas where MD could be utilized to treat produced water.

The GOR of MD process can be improved by fine tuning membrane structure and system design. A theoretical investigation of membrane parameters impact on performance indicated that increasing membrane porosity and pore size and reducing thickness, tortuosity and thermal conductivity can increase permeability coefficient and the efficiency of thermal energy transfer (Deshmukh et al., 2018). However, a special care should be paid to porosity and pore size as excessive increase of

these parameters could compromise the structural integrity of the membrane during operation and increase its susceptibility to wetting (Boo et al., 2016). To overcome these possible implications of increasing membrane porosity and pore size while maintain high permeability coefficient, Deshmukh et al (Deshmukh et al., 2018), suggested fabricating a sandwiched porous membrane between two dense layers. The improvement in system design particularly recovery of latent heat and reduction of heat losses could also improve the efficiency of the MD systems. Another possible way to improve GOR of MD systems is reducing the pressure in membrane pores which present the main resistance for vapor transfer. It was stated that such a reduction can be achieved by deaerating the feed and permeate streams, which can be costly (Deshmukh et al., 2018).

#### 4. MD-FO hybrid system

##### 4.1. Fundamentals of the integrated system

In order to make the most out of the synergy between MD and FO system, it is important to understand the theoretical background of the combined process and how one affects the performance of the other. As it was discussed in Section 2.1 that the driving force for water transfer in FO membrane is difference in the osmotic pressure between the feed and draw solution sides. However, Eq. 1 is very generic and it does not show the factors that influence the driving force. These factors include RSF, ECP and ICP. Lee et al (Lee et al., 1981), laid the foundation for the mathematical expression that incorporates these factors by developing formulas that describe water and salt transfer in PRO system. The formulas derived by Lee and co-workers was then modified for FO system in PRO mode by Loeb et al (Loeb et al., 1997). The latter formula was then further developed by McCutcheon and Elimelech (McCutcheon and Elimelech, 2006) for FO system runs on FO mode that took into consideration the effect of concentrative and dilutive CPs, but assumes zero salt permeability (in other word, neglecting RSF) as shown in Eq. 9, where  $\pi_{D,b}$  and  $\pi_{I,b}$  are the bulk osmotic pressure in draw solution and feed sides, respectively (can be calculated applying Eq. 2),  $k$  is the mass transfer coefficient that can be calculated from empirical relationships of the flow dimensionless numbers and  $K$  is solute resistivity for diffusion that can be computed from Eq. 10, where  $D$  is the diffusion coefficient of the solute, and  $t$ ,  $\tau$  and  $\varepsilon$  are membrane's thickness, tortuosity and porosity, respectively. Eq. 9 was developed further Yip et al (Yip et al., 2011), to produce Eq. 11 (Ibrar et al., 2022) that includes the impact of RSF on water flow in addition to the effect of CP. So far, these formulas have considered concentrative and dilutive CP as well as RSF effects on water flux, but the impact of ECP on the support layer was not accounted for and this is what Nagy (Nagy, 2014) addressed as formulated in Eq. 12 (Ibrar et al., 2022), where  $B$  is the salt permeability,  $S$  is the structural parameter of the membrane ( $= \tau\tau/\varepsilon$ ) and  $D_D$  is the diffusion coefficient of DS. The closest model for simulating real FO process is the one reported by She et al (She et al., 2016), that takes into account the impact of fouling on mass transfer processes in FO with FS-AL orientation as expressed in Eq. 13, where  $F_{cep}$  is concentration polarization factor for concentrative external concentration polarization which can be calculated using Eq. 14 ( $k_{cep} = D/\text{active layer thickness } (t_{AL})$ ),  $J$  with subscript w,f and s,f is the water and salt flux in the fouling test,  $\beta$  is Van't Hoff coefficient,  $F_{dcp}$  is concentration polarization factor for dilutive concentration polarization that can be determined using Eq. 15 ( $k_{dcp} = D/S + t_{SL}$ ),  $R_g$  is the universal gas constant, and  $R_m$  and  $R_f$  are the hydraulic resistance of membrane and foulant layer that can be measured experimentally.

$$J_w = A \left[ \pi_{D,b} \exp \left( -\frac{J_w}{k} \right) - \pi_{F,b} \exp (J_w K) \right] \quad (9)$$

$$K = \frac{t\tau}{D\varepsilon} \quad (10)$$

$$J_w = A \left[ \frac{\pi_{D,b} \exp(-J_w K) - \pi_{F,b} \exp \left( \frac{J_w}{k} \right)}{1 + B / J_w \left[ \exp \left( \frac{J_w}{k} \right) - \exp(-J_w K) \right]} \right] \quad (11)$$

$$J_w = A \left[ \frac{\pi_{D,b} \exp \left[ -J_w \left( \frac{1}{k_D} + \frac{S}{D_D} \right) \right] - \pi_{F,b} \exp \left( \frac{J_w}{k_F} \right)}{1 + B / J_w \left[ \exp \left( \frac{J_w}{k_F} \right) - \exp \left( -J_w \left( \frac{1}{k_D} + \frac{S}{D_D} \right) \right) \right]} \right] \quad (12)$$

$$J_w = A \left[ \frac{(\pi_{D,b} - \pi_{F,b}) - F_{cep,F} \left( \pi_{F,b} + \frac{J_{sf}}{J_{wf}} \beta R_g T \right) - F_{dcp,f} \left( \pi_{D,b} + \frac{J_{sf}}{J_{wf}} \beta R_g T \right)}{\mu (R_m - R_f)} \right] \quad (13)$$

$$F_{cep} = \exp \left( \frac{J_w}{k_{cep}} \right) - 1 \quad (14)$$

$$F_{dcp} = 1 - \exp \left( -\frac{J_w}{k_{dcp}} \right) \quad (15)$$

For simplicity, the water vapor flow in MD is analogized as an electrical current that is impeded by three intrinsic resistances (inverse of mass/heat transfer coefficients) of feed, membrane and permeate. From the feed side, temperature and concentration polarization along with fouling are the driver for this resistance. In the membrane section, the air filling the pores and the low conductivity of membrane is what resists the heat and mass transfer. TP is the only reason behind the resistance against mass and heat transfer in the permeate side. When it comes to modelling mass transfer in the hybrid MD-FO system, the authors are only aware of the study conducted by Zohrabian et al (Zohrabian et al., 2020), that performed such exercise. Their model is based on mass balance for FO system combined with direct contact DM that runs in counter current mode. They started off with the assumption that no losses occur in the system and the change in flow of the MD feed along the length of the feed channel is equivalent to the flux collected on the permeate side (Eq. 16). This equation can be simplified by dividing both sides by the area of the effective area of MD membrane (Eq. 17), where  $Q_{MD,d}$ ,  $u_{MD}$  and  $x_{MD}$  are the MD flow rate, feed velocity and feed channel length, respectively,  $N_{MD}$ ,  $w_{MD}$ ,  $h_{MD}$  and  $\rho$  are the permeate mass flux, width and length of MD membrane and density of water, respectively. Eq. 17 can also be applied for the permeate side. Based on the same principle, they also formulated an expression for the change on the concentration of the MD feed solution as shown in Eq. 18, where  $C_{MD,d}$  is the solute concentration along the membrane length.

$$\frac{dQ_{MD,d}}{dx_{MD}} = -\frac{N_{MD}w_{MD}}{\rho} \quad (16)$$

$$\frac{du_{MD,d}}{dx_{MD}} = -\frac{N_{MD}}{\rho h_{MD}} \quad (17)$$

$$\frac{dC_{MD,d}}{dx_{MD}} = -\frac{N_{MD}C_{MD,d}}{\rho u_{MD,d}h_{MD}} \quad (18)$$

Zohrabian et al (Zohrabian et al., 2020), also performed a series of mass balance on the feed, draw and permeate tanks to capture the dynamic change in water volume and solute concentration as presented in Eqs. 19–22, where  $V_f$  is the volume of the FO feed,  $Q_{FO,fin}$  and  $Q_{FO,fout}$  are flow rate of entering and exiting the FO feed tank, respectively,  $C_f$  is the solute concentration of FO feed,  $C_{FO,fin}$  is the solute concentration of FO feed at the entry line of the feed tank,  $Q_{FO,din}$  and  $Q_{FO,dout}$  are the FO draw flow rate entering and exiting the draw solution tank, respectively,  $V_f$  is the volume of the draw solution, and  $Q_{d,din}$  and  $Q_{d,dout}$  are the MD flow rate entering and exiting the draw tank, respectively. The initial mass permeate flux MD and the change in the flux were derived based on

dusty gas model as presented in Eqs. 23 and 24, respectively, where  $\delta$  is the MD membrane thickness,  $P_T$  is total pressure,  $Kn$  is Knudsen number,  $D_{w,a}^{PT}$  is the diffusion coefficient of molecular diffusion,  $T_m$  is the average membrane temperature  $D_{Kw}$  is the diffusion coefficient,  $y_{a,pm}$  and  $y_{a,dm}$  are air molar fraction on permeate and feed (draw) solution sides,  $J_{DMO}$

is the initial MD volumetric flux ( $N_{MD}/\rho$ ),  $a_0$  initial membrane open pore area,  $m_s$ ,  $\rho_{MD,d}$  and  $\rho_s$  are the draw solute mass fraction and densities of the draw solution and draw solute, respectively.  $H_{MD,d}$ ,  $d_s$ ,  $\eta$  and  $c_m$  are the draw solution channel hydraulic diameter, draw solution channel diameter, friction coefficient and coefficient of deposited mass,

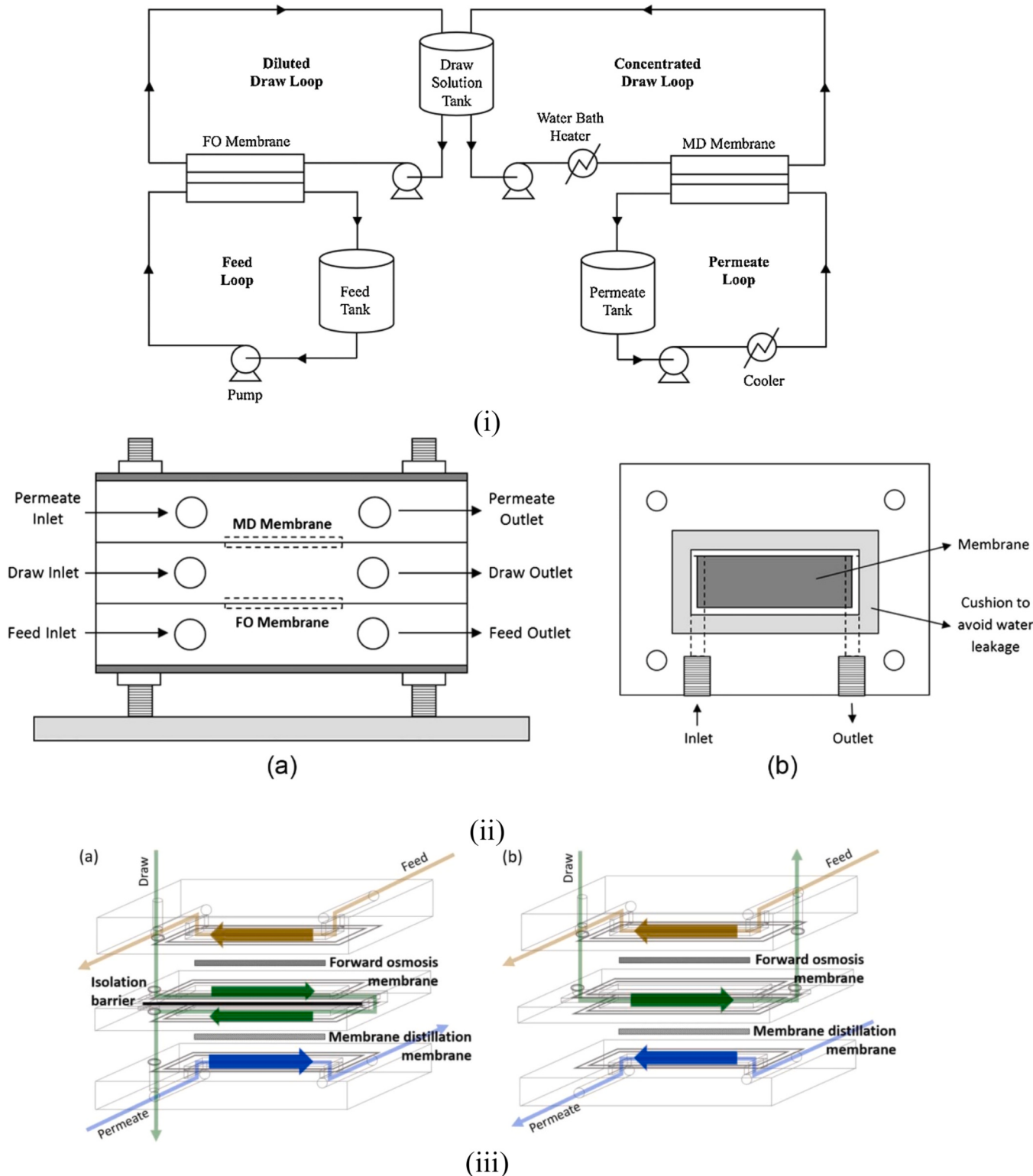


**Fig. 10.** FO-MD system configurations: i) Typical design, copied from (Zohrabian et al., 2020) with copyright permission from Elsevier (License No. 5650811500312), ii) compact cell with shared draw solution compartment, copied from (Son et al., 2021b) with copyright permission from Elsevier (License No. 5650820736432), and iii) compact cell with isolation barrier, copied from (Husnain et al., 2015) with copyright permission from Elsevier(License No. 5650820430686)

respectively.  $C_L$ ,  $C_T$ , and  $C_A$  are lubrication constant, stress coefficient, and system dependent constant.  $C_1$  and  $C_2$  are the integration constants of Eq. 22 derivation. In order to solve Eqs. 21 and 22, the values of membrane-water interface temperature on feed and permeate sides should be calculated first, and the formulas for these varies depending on the configuration of MD (Johnson and Nguyen, 2017). Eqs. 19–24 are useful for comparison with experimental data as they are derived based on global mass balance of feed, draw and permeate compartments of FO-MD system which incorporates the dynamic change in the resistance of CP, TP and fouling layer. The water transfer balance (WTB) is the key criteria in FO-MD system and  $J_w$  (Eq. 13) should always be equal or slightly lower than  $J_{MD}$  (Eq. 24) to maintain high osmotic pressure. It was reported that such a condition can be met at a temperature range of  $62.5 \pm 0.5^\circ\text{C} - 72.5 \pm 0.5^\circ\text{C}$  (Ibrar et al., 2022).

$$\frac{dV_f}{dt} = Q_{FO,fin} - Q_{FO,fout} \quad (19)$$

$$\frac{dC_f}{dt} = \frac{1}{V_f} [C_{FO,fin}Q_{FO,fin} - C_fQ_{FO,fin}] \quad (20)$$

$$\frac{dV_d}{dt} = Q_{FO,din} + Q_{MD,din} - Q_{FO,dout} - Q_{MD,dout} \quad (21)$$

$$\frac{dC_d}{dt} = \frac{1}{V_d} [C_{FO,din}Q_{FO,din} - C_{MD,in}Q_{MD,din} - C_dQ_{FO,dout} - C_dQ_{MD,dout}] \quad (22)$$

$$N_{MD} = \frac{(\varepsilon_{MD}/\tau_{MD})P_T(1+Kn)D_{w,a}^{P_T}}{\delta_{MD}R_g T_m} \ln \left[ \frac{D_{Kw}y_{a,pm} + (1+Kn)D_{w,a}^{P_T}}{D_{Kw}y_{a,dm} + (1+Kn)D_{w,a}^{P_T}} \right] \quad (23)$$

$$J_{MD} = \frac{J_{MD0}}{a_0} \exp - \frac{3\rho_{MD,d}m_s c_m Q_{MD,d}}{2\rho_s d_s H_{MD,d} C_T^2 a_0} \left[ C_{LE} e^{\frac{C_T}{\eta} \left( C_1 + \frac{t}{C_L} \right)} + \eta C_T C_A t \right] - C_2 \quad (24)$$

#### 4.2. FO-MD common designs

There are three designs for FO-MD system that have been reported in the literature as illustrated in Fig. 10. The first one (Fig. 10 i) where FO and MD share the draw solution tank is the most common design. The second design was proposed as compact a system for the hybrid FO-MD (Husnain et al., 2015) (Fig. 10 ii). However, the high temperature of MD feed in the compact design might negatively affect the polymeric FO membrane (Ibrar et al., 2022). Hence, Son et al (Son et al., 2021b), suggested the implementation of isolation barrier in the compact FO-MD system to reduce the risk of temperature impact on FO membrane structural integrity (Fig. 10 iii). The advantages and disadvantages of these systems are summarized in (Ibrar et al., 2022). In any of these designs, cooling would be required to reduce temperature of the draw solution especially at elevated temperature that are recommended for achieving efficient WTB unless a thermotolerant membranes are used in the FO system. Such membranes are not existent in the market except for Porifera FO membrane although the there was no reported data on long-term tests for these membranes (Ibrar et al., 2022). There are some lab-scale attempts for synthesizing FO membranes that can work in this temperature range (Wei et al., 2005), but scaling up was not considered and it is hard to anticipate its feasibility. In addition to membrane thermal tolerance, the rising temperature of DS could impact the overall performance of FO-MD system. Based on van't Hoff equation, the osmotic pressure of the draw solution is directly related to the temperature which in turn increase osmotic pressure gradient leading to higher water flux. The flux could also be increased due to the improved water diffusion, and lowered water viscosity with increasing the temperature (Shin and Kim, 2018). However, such temperature rise can also increase RSF due to increased solution diffusion. The temperature rise may also reduce membrane rejection (Shin and Kim, 2018). High temperature could also increase CP and membrane scaling due to the increasing

water flux leading to the rise in the solute concentration at the membrane surface (Zhao and Zou, 2011b). The scale of temperature effect on FO performance connected to MD as a DS recovery process may vary depending on the type of DS. Almoalimi et al (Almoalimi et al., 2022), observed that glucose performed better than NaCl as a DS at a temperature of  $50^\circ\text{C}$  using ammonium solution a feed. Increasing the temperature of MD increase water flux for both DSs, but the improvement of the flux with glucose was almost double that of NaCl. RSF also increased as the temperature was risen and it was worse with NaCl compared to glucose (two folds higher). Most importantly, glucose resulted in complete rejection of ammonium ions while NaCl failed to achieve the same.

### 5. FO-MD applications in water treatment

#### 5.1. Seawater treatment

FO-MD system have emerged as promising technologies for various water treatment applications, including seawater desalination. However, when considered individually, both technologies have limitations when applied on a large scale (Giagnorio et al., 2021; Awad et al., 2019; Soukane et al., 2021; Viader et al., 2021). Desalination researchers have explored the FO-MD hybrid system, which can respond to and tackle the growing challenge of global clean water shortages (Kwon et al., 2016; Parveen, 2018). The hybrid FO-MD system's equipment is simple to set up and configure, and energy consumption may be kept to a minimum (Chekli et al., 2016; Nasr and Sewilam, 2015). Also, the capacity of MD for handling high salinity water gives it the competitive edge over pressure-driven membrane processes. For various purposes, numerous studies on the FO process have been undertaken utilizing various draw solutions and various types of draw solution recovery. The focus of this work is on the hybrid FO-MD system.

There are many studies that explored the use of FO-MD for seawater desalination. Few examples of these studies are discussed at length here and the outcomes of other are summarized in Table 5. Ahmed et al (Ahmed et al., 2023), designed and implemented a pilot-scale FO-MD system for the for the desalination of the Arabian Gulf seawater (AGS) using a solution of NaCl (70000 mg/L) as a DS. Under the optimized operating conditions, the FO-AGMD system achieved an average water recovery rate of 33% at an MD operating temperature of  $85^\circ\text{C}$ . The water flux remained stable, ranging between 6.3 and  $7.3 \text{ L/m}^2.\text{h}$  for the FO and 3.75 and  $4 \text{ L/m}^2.\text{h}$  for the MD. The primary power consumption of the FO-AGMD system was attributed to the heating and cooling processes, which were used to heat the feed water to approximately  $85^\circ\text{C}$  and cool the permeate to around  $10^\circ\text{C}$  in the MD section. This power consumption varied within the range of 10–12 kW/h. Zohrabian and co-authors conducted a modeling study to evaluate the technical feasibility of FO-MD process for water treatment (Zohrabian et al., 2020). This investigation involved testing different DSs including polydiallyldimethyl ammonium chloride (PDAC), tetraethylammonium bromide (TEAB), and NaCl. Their study revealed that fouling was more pronounced in the FO component compared to the MD part of the system. However, through modeling, they successfully identified optimal feed temperature and crossflow velocity for the MD process to achieve high water recovery in the hybrid system. Ultimately, their research recommended the use of the FO-MD process as a promising technology for water treatment when operated under optimized conditions. Al-Furaiji and collaborators assessed the potential of the hybrid FO-MD process for highly saline-produced water treatment (Al-Furaiji et al., 2019). They investigated the evaluation of four different DSs, namely monovalent NaCl, KCl, lithium chloride (LiCl), and MgCl<sub>2</sub>. The 10 M concentrated LiCl solution exhibited the highest osmotic pressure at 1600 atm, resulting in the highest flux in the FO process. However, this solution produced the lowest flux in the MD component due to its low vapor pressure. Conversely, NaCl and KCl showed high MD flux but lower performance in the FO section. A 4.8 M MgCl<sub>2</sub> demonstrated comparable fluxes in both the MD and FO parts of the hybrid system.

**Table 5**

FO-MD hybrid system for seawater desalination examples from previous studies.

Feed Solution	Draw Solution	FO Membrane	MD Membrane	Membrane Orientations	Conditions	Performance	Ref.
DI water + seawater	(1,2,3-Trimethylimidazolium iodide) and (1, 1,2, 2-Tetramethyl-3, 3 - methylenedimidazolium diiodide solution)	Commercial CTA flat sheet FO membrane	Durapore 0.45 m HVHP	FO and PRO	For FO system: flow velocities FS and DS: 0.25 L/min, counter-current flow membrane area = $1.6 \times 10^{-3} \text{ m}^2$ temperature: $23 \pm 0.5^\circ\text{C}$ for FO-MD membrane area for FO and MD: $3.2 \times 10^{-3} \text{ m}^2$ DS type: 4-type (0.5 M) Membrane area FO and MD: $3.2 \times 10^{-3} \text{ m}^2$ Tin FS: 38.5 Tin DS: 49.7 Tin distillate: 18.7 Flow FS and DS: 0.13 m/sec Flow distillate: 0.013 m/sec	FS: DI water Water flux: 10–23 L/m <sup>2</sup> .h ) PRO mode) and 5–12 L/m <sup>2</sup> .h ) FO mode in FO unit (0–5 M of DS) with less than 5 g/m <sup>2</sup> h of reverse solute flux in both modes and 8 L/m <sup>2</sup> .h in MD (0.5 M) DS. FS: seawater Water flux = 6 L/m <sup>2</sup> .h for (PRO)	(Yen et al., 2010)
DI water, seawater (0.6 M NaCl)	Poly(sodium styrene-4-sulfonate-co-n-isopropylacrylamide) (PSSS-PNIPAM)	TFC FO membrane commercial Flat sheet	PVDF membrane commercial HF	PRO	Concurrent, flow velocity FS and DS: 25 cm/s effective membrane area FO: $1 \times 2 \text{ cm}^2$ , membrane area MD: $22.4 \text{ cm}^2$ , Temp MD: 50°C Temp permeate: $10^\circ\text{C}$ flow velocity MD: 20 cm/s membrane FO: $1 \text{ cm} \times 2 \text{ cm}$ flow velocity of 25 cm/s MD membrane: $22.4 \text{ cm}^2$ Concurrently $T_{\text{MD feed in}} = 45^\circ\text{C}$ , $T_{\text{MD permeate}} = 10^\circ\text{C}$	Water flux FO: 3.5 L/m <sup>2</sup> .h Water flux MD: 2.5 L/m <sup>2</sup> .h DS: 33.3 wt% 15 SN (PSSS-PNIPAM) Reverse salt flux: 2 g/mH	(Zhao et al., 2014b)
DI water, NaCl solution	Na-CQDs solution	Commercial TFC FO Membrane (flat sheet)	PVDF (HF)	PRO		Water flux: 29.8 L/m <sup>2</sup> .h (DI as FS, 0.4 gm/ml Na-CQDs as DS) and Water flux: 10.4 L/m <sup>2</sup> .h (actual sea water as FS, 0.4 gm/ml Na-CQDs as DS) Water flux: 7.3 L/m <sup>2</sup> .h (0.6 M NaCl as FS, 0.4 gm/ml Na-CQDs as DS) and 3.4–4 L/m <sup>2</sup> .h in MD unit ( $45^\circ\text{C}$ ) for first five cycles.	(Guo et al., 2014)
DI water and 3.5 wt% NaCl and seawater (Singapore coast)	poly(amidoamine) terminated with sodium carboxylate groups (PAMAM-COONa) (33.3 wt%) [2.5-generation (2.5 G) PAMAM-COONa]	TFC FO membrane commercial Flat sheet	PVDF membrane fabrication HF	PRO	effective membrane area FO: $1 \times 2 \text{ cm}^2$ , membrane area MD: $28 \text{ cm}^2$ Temp MD: 50°C Temp permeate: $10^\circ\text{C}$	Water flux (PRO mode): 29.7 and 9 L/m <sup>2</sup> .h for FS of DI water and seawater Reverse salt flux: 10 g/mH water fluxes under (PRO mode): 30, 9, and 7.5 L/m <sup>2</sup> .h with DI water, seawater from Singapore coast, and simulated seawater as the feed solutions, respectively. (water flux FO mode: 12 L/m <sup>2</sup> .h for (33.3 wt%) [2.5-generation (2.5 G) PAMAM-COONa])	(Zhao et al., 2014a)
DI water and NaCl Solution (0.6 M)	NaCl, KCl, and MgCl <sub>2</sub>	CTA FO membrane commercial Flat sheet	PVDF membrane commercial HF	FO	effective membrane area FO: $30.42 \text{ cm}^2$ , membrane MD HF area: $0.034 \text{ m}^2$ flow rate: 1LPM Temp MD: $25\text{--}60^\circ\text{C}$	Water flux MD: 3.3 L/m <sup>2</sup> .h Water flux FO $1.48 \times 10^{-6}$ – $2.5 \times 10^{-6}$ m/s flux at FS = 0.6 M NaCl and conc. DS: 2–4 M temp FO ( $25\text{--}60^\circ\text{C}$ ) at a conc. DS: 0.6–4 M Water flux MD: $7.2 \times 10^{-6}$ – $4.5 \times 10^{-6}$ m/s, FS: seawater (MD at $60^\circ\text{C}$ )	(Kwon et al., 2016)
DI water and NaCl Solution (3.5 wt%)	Na <sub>5</sub> Fe-CA	TFC FO membrane fabrication	PVDF membrane fabrication	FO	effective membrane area FO: $10 \text{ cm}^2$ , membrane MD HF: diameter of 3/8 in. and a length of 20 cm, FO process counter-current flow, MD process co-current flow, flow rates of all FO and	Water flux FO/MD = $14\text{--}19.2/32 \text{ L/m}^2\text{.h}$ at FS: DI water temp FO ( $25\text{--}60^\circ\text{C}$ ) at Conc. DS: 1.5 M Water flux FO/MD = $3.9\text{--}6/32 \text{ L/m}^2\text{.h}$ at FS: seawater (MD at $60^\circ\text{C}$ )	(Wang et al., 2015)

(continued on next page)

**Table 5 (continued)**

Feed Solution	Draw Solution	FO Membrane	MD Membrane	Membrane Orientations	Conditions	Performance	Ref.
DI water, seawater	(poly(isobutylene-alt-maleic anhydride) with NaOH [PIAM-Na])	CTA FO membrane commercial Flat sheet	PTFE membrane commercial flat sheet	FO and PRO	MD: 100 ml/ min cross-flow velocity FS and DS: 8.5 cm/s, temp (FS and DS) PRO:25°C, Temp feed MD:60°C Temp permeate:20°C	Conc. DS: 0.3–0.4 g/ml Water flux PRO: 32 L/m <sup>2</sup> .h at conc.: 0.375 g/ml and Temp. 60°C Water flux FO:11 L/m <sup>2</sup> .h and 18 L/m <sup>2</sup> .h at temp (25 and 60 °C, respectively Reverse salt flux: 0.196 gMH at 60 °C Water flux FO: 4 L/m <sup>2</sup> .h and 6 L/m <sup>2</sup> .h at temp (25 and 60) °C, respectively Water flux MD: 40–30 L/m <sup>2</sup> .h form conc 0.3–4 g/ml and Temp 50 °C	(Kumar et al., 2016)
DI water, synthetic brackish water, seawater	Al <sub>2</sub> (SO <sub>4</sub> ) <sub>3</sub> :MgCl <sub>2</sub> [0.5 M MgCl <sub>2</sub> + 0.05 M Al <sub>2</sub> (SO <sub>4</sub> ) <sub>3</sub> ]	CTA FO membrane commercial Flat sheet	PTFE membrane commercial flat sheet	FO and PRO	Temp FS and DS:25°C effective membrane area FO: 41.40 cm <sup>2</sup> , membrane area MD: 100 cm <sup>2</sup> cross-flow velocity FS and permeate MD:0.083 m/s. Temp MD:55°C Temp permeate:25°C Flow rate:0.5LPM	Water flux: 4.01–4.79 L/m <sup>2</sup> .h in the FO mode and 7.30–8.92 L/m <sup>2</sup> .h in PRO mode, pH: 6.5, water flux and reverse solute flux of 0.5 M MgCl <sub>2</sub> + 0.05 M Al <sub>2</sub> (SO <sub>4</sub> ) <sub>3</sub> were 8.92 L/m <sup>2</sup> .h and 0.94 gMH, respectively, in PRO mode. Water flux PRO: 15.09 L/m <sup>2</sup> .h in mode and 8.18 L/m <sup>2</sup> .h in FO mode as [ 1 M MgCl <sub>2</sub> + 0.05 M Al <sub>2</sub> (SO <sub>4</sub> ) <sub>3</sub> ] (specific reverse solute flux: 0.096 g/L in PRO and specific reverse solute flux: 0.151 g/L in FO. DI water FS (water flux: 15.12 L/m <sup>2</sup> .h in PRO mode and water flux: 8.09 L/m <sup>2</sup> h in FO mode), brackish water FS (water flux: 9.40 L/m <sup>2</sup> h in PRO mode and water flux: 5.03 L/m <sup>2</sup> .h in FO mode), and sea water FS (water flux: 3.95 L/m <sup>2</sup> .h in PRO mode and water flux: 2.11 L/m <sup>2</sup> .h in FO mode), water flux MD: 4.95 – 5.7 L/m <sup>2</sup> .h form pore size (0.1–1) μm and R%: 99.93–99.06	(Nguyen et al., 2018)
DI water, synthetic brackish water, seawater	EDTA–2Na and Na <sub>3</sub> PO <sub>4</sub>	CTA FO membrane commercial Flat sheet	PTFE membrane commercial flat sheet	FO	Flow rate FS and DS: 0.5 L/min Temp FS and DS = 25°C effective membrane area FO: 41.40 cm <sup>2</sup> , membrane area MD: 100 cm <sup>2</sup> Flow rate FS and distillate: 1.5 L/min, Temp MD:55°C Temp permeate:25°C	[0.3 M EDTA–2Na and 0.55 M Na <sub>3</sub> PO <sub>4</sub> ] water flux FO= 9.17 L/m <sup>2</sup> .h Water flux: 6.12 L/m <sup>2</sup> .h with FS brackish water and 3.10 L/m <sup>2</sup> .h with FS: seawater, R MD:99.99% Specific reverse solute flux: 0.053 g/L, Jw: 6.12 L/m <sup>2</sup> .h FS brackish water, Jw: 3.1 L/m <sup>2</sup> .h FS seawater, Jw MD: 8.51 L/m <sup>2</sup> .h FS: DI water and seawater Water flux K-CQDs: 10.94–13.924 L/m <sup>2</sup> .h, water flux: 3.779–5.371 L/m <sup>2</sup> .h at conc.: 0.3–0.56 g/ml respectively. Water flux Na-CQDs = [10.343–11.935] L/m <sup>2</sup> .h and water flux = [1.591–2.784] L/m <sup>2</sup> .h respectively. Water flux K-CQDs= 6.166 L/m <sup>2</sup> .h and Water flux Na-CQDs= 3.779 L/m <sup>2</sup> .h	(Nguyen et al., 2020)
DI water and seawater (NaCl Solution (3.5 wt%) and raw Arabian Gulf water	K-CQDs Na-CQDs	CTA FO membrane commercial Flat sheet	PTFE membrane commercial flat sheet	FO	Flow rate FS and DS: 0.5 L/min Temp FS and DS = 29°C effective membrane area FO: 33.516 cm <sup>2</sup> , membrane area MD: 14.44 cm <sup>2</sup> Flow rate FS and distillate: 0.5 L/min and 0.3 L/min Temp MD: (50, 60) °C Temp permeate:20°C	Water flux K-CQDs: 10.94–13.924 L/m <sup>2</sup> .h, water flux: 3.779–5.371 L/m <sup>2</sup> .h at conc.: 0.3–0.56 g/ml respectively. Water flux Na-CQDs = [10.343–11.935] L/m <sup>2</sup> .h and water flux = [1.591–2.784] L/m <sup>2</sup> .h respectively. Water flux K-CQDs= 6.166 L/m <sup>2</sup> .h and Water flux Na-CQDs= 3.779 L/m <sup>2</sup> .h	(Kamel, 2022)

(continued on next page)

**Table 5 (continued)**

Feed Solution	Draw Solution	FO Membrane	MD Membrane	Membrane Orientations	Conditions	Performance	Ref.
Arabian Gulf seawater	70,000 ppm NaCl	Spiral wound Thin film composite with polyamide coating	Spiral wound AGMD	FO	Operation capacity: 50 m <sup>3</sup> /day FO membrane area: 3 m <sup>2</sup> MD membrane area: 5.6 m <sup>2</sup> FO feed and draw flow rates: 600 L/h and 400 L/h, respectively. FO feed temperature: 25 °C. MD feed and permeate temperatures: 85 °C and 10 °C, respectively.	at FS: RAG water at conc. 0.5 g/ml reverse solute flux K-CQDs = [0.016–0.025] g/Mh, reverse solute flux Na-CQDs = [0.041–0.062] g/Mh, Js/Jw K-CQDs = [0.0015–0.0018] Specific reverse solute flux: Na-CQDs = [0.0040–0.0052] at conc.[0.3–0.5]g/ml Water flux MD at 50°C for diluted K-CQDs when FS of FO is DI water, seawater and RAG water = 11.426–7.722 L/m <sup>2</sup> .h, 9.107–5.332 L/m <sup>2</sup> .h, and 5.886 L/m <sup>2</sup> .h respectively. At 60°C Water flux: 14.889–11.184 L/m <sup>2</sup> .h, 12.604–8.795 L/m <sup>2</sup> .h, and 9.349LMH, respectively. Water flux MD at 50°C for diluted Na-CQDs when FS of FO is DI water, seawater and RAG water: 10.561–7.168 L/m <sup>2</sup> .h, 8.31–4.813 L/m <sup>2</sup> .h, and 5.609 L/m <sup>2</sup> .h respectively. At 60°C Water flux: 14.716–11.323 L/m <sup>2</sup> .h, 12.465–8.968 L/m <sup>2</sup> .h, and 9.765 L/m <sup>2</sup> .h, respectively. Rejection for all: 100% Water recovery: 33% RSF: ~ 100 g/m <sup>2</sup> .h FO flux: 6–8 L/m <sup>2</sup> .h Heating and cooling power consumption: 10–12 kW/h	(Ahmed et al., 2023)

Overall, this study illustrated the potential of the FO-MD process for treating hypersaline. FO-MD can be used to concentrate the reject brine from RO plants. FO can reduce the volume of brine, and MD can recover additional freshwater, minimizing environmental impacts and enhancing resource recovery. FO-MD is also suitable for desalting brackish water sources, providing a sustainable and energy-efficient approach to freshwater production in regions with limited freshwater resources. Duong et al (Duong et al., 2015). investigated a system that combines FO with DCMD for desalinating seawater. Their findings indicated that by recycling the brine back into the feed tank, they could achieve an optimal water recovery rate ranging from 20% to 60%. This approach significantly reduced the specific energy consumption by half while also observing minimal fouling issues. Moreover, when they increased the feed temperature to 50 °C and reduced the flow rate, the thermal efficiency of the DCMD system showed a remarkable improvement. The use of a warmer feed solution enhanced the transport of the high salinity feed, resulting in higher water recovery rates.

A summary of the experimental conditions and the outcome of the studies investigated FO-MD hybrid system for synthetic and natural seawater is presented in Table 5. The main motivation of these studies was to increase water recovery and ameliorate the system operation by testing different membrane materials, draw solution types and working conditions. For example, four compounds of 2-methylimidazole were tested as draw solution (2 neutral and 2 charged) and it was found that

charged methylimidazole produced higher flux and lower RSF compared to the neutral ones (Yen et al., 2010). Reducing the temperature between feed and distillate in MD was found to reduce the separation rate, but improves the selectivity in the draw solution (Koo et al., 2013). Vetting the data presented in Table 1 also shows that PRO mode seems to be more effective compared to FO in terms of flux production. Guo et al (Guo et al., 2014). achieved one of the highest reported flux for FO using COD-Na<sup>+</sup> (29.8 L/m<sup>2</sup>.h), which was about 55% higher than that of 2 M NaCl.

## 5.2. Wastewater

Other applications of the FO-MD system include wastewater treatment such as dye wastewater and mining wastewater, water recovery from oily wastewater, nutrient recovery from urine and digested sludge and others. FO-MD systems have been used for treating industrial wastewater including water generated from the textile industries and metal and mining processing. The FO-MD system can effectively treat wastewater from textile industries, which often contain dyes, chemicals, and high salinity. FO can separate water from contaminants, while MD can help recover valuable chemicals or dyes from the concentrated draw solution. Thus, integration of FO-MD has displayed significant potential in the textile industry for reclaiming water and recovering valuable chemicals. Li et al (Li et al., 2020). evaluated the application of FO-MD

for simulated textile industry wastewater using three different modes of operations, A where DS was replenished manually, B where DS was diluted until the target concentration factor (CF) achieved, and C where DS was regenerated using MD process. They used three different membranes for FO process namely poly(triazole- co-oxadiazole- co-hydrazine) (PTAODH-1.0, where 1.0 represents the molar ratio of 4-aminobenzoic acid to the repeating unit of PODH during the synthesis), commercial thin-film composite FO membrane (CSM-TFC), and commercial cellulose triacetate (HTI-CTA). They found that applying mode C using PTAODH-1.0 membrane achieved dyes CF of 10 with a total specific cost of 0.34 USD/L.

The FO-MD system was also applied for water reclamation in advanced municipal wastewater treatment plants. Ricci et al (Ricci et al., 2019) introduced a submerged hybrid FO-MD module and critically assess its performance in domestic wastewater treatment. The submerged hybrid module was compared to the side-stream configuration. Lower water fluxes were found for hybrid module due to more significant polarization. Although the hybrid system exhibits reduced flux rates, it consumes less energy when compared to the side-stream configuration because there is no need to transport the feed solution to an external compartment. Furthermore, the hybrid system demonstrated exceptional rejection rates for Total Organic Carbon (TOC), Total Nitrogen (TN), Ammonium (NH<sub>4</sub>), and Trace Organic Compounds (TrOCs), achieving 94.9%, 93.8%, 99.8%, and over 97.5% rejection, respectively.

Landfill leachate is a type of wastewater that is often highly contaminated with organic and inorganic compounds. The FO-MD system can concentrate and treat landfill leachate, minimizing the volume of waste while reclaiming water. Zhou et al (Zhou et al., 2017) combined FO and MD process to treat high salinity hazardous waste landfill leachate. Their findings indicated that the most effective flow rates for FS, DS, and DS concentration in the FO stage were 0.87 L/min, 0.31 L/min, and 4.82 M, respectively. In the MD stage, the best inlet solution temperatures were  $72.5 \pm 0.5$  °C and  $62.5 \pm 0.5$  °C when the salt concentrations in the FS were 25,000 mg/L and 60,000 mg/L (expressed as NaCl equivalents). The system consistently achieved salt rejection rates (monovalent and divalent salts) exceeding 96%, while the rejection rates for TOC and TN remained above 98%. Notably, NH<sub>4+</sub>-N, Hg, As, and Sb were eliminated completely from the wastewater. In this study, the operating conditions of FO were optimized using response surface methodology (RSM) by optimizing water flux, enhancing pollutant removal efficiency, and minimizing RSF. The integrated FO-MD system surpassed the individual FO or MD processes in effectively removing contaminants from high-salinity wastewater.

In the oil and gas sector, FO-MD technology can be employed to treat produced water, which contains oil, salts, and other contaminants. Oily water contains a complex mixture of organic substance (mainly dissolved and dispersed oil compounds) and inorganic substance (high concentrations of mineral salts, total dissolved solids TDS up to ten of thousands ppm). Oily water is also characterized with high temperature (i.e., thermal energy) and high salinity (i.e., osmotic energy) besides its water and oil resources. Thus, FO can separate water from the oil phase, and MD can further purify the water for reuse or safe discharge. Lu et al (Lu et al., 2018) developed an integrated system consists of UF-FO-MD for the dual purposes of the treatment and energy utilization of oily water. The results showed that UF efficiently removed suspended solids and larger oil droplets, while FO and MD processes removed dissolved contaminants and finer oil particles resulting in treated water suitable for various applications, including various industrial processes or it could safely be discharge.

FO-MD has also been used in combination with other membrane systems for treating wastewater. For instance, Al Mahri and co-researchers developed a model for an electro-osmotic membrane bioreactor (eOMBR) to assess the hybrid FO-MD process for wastewater treatment (Al Mahri et al., 2020). In this setup, FO was carried out using desalination brine as a DS and wastewater as an FS. The diluted brine

from the FO process was recycled in an MD process configured with DCMD. Their model was designed based on specific parameters and conditions, and it allowed them to evaluate essential aspects of the process, including reverse salt leakage, water flux, and internal concentration polarization of the membrane. The study found that the FO-MD process could produce water with an estimated energy consumption of 13.20 kWh/m<sup>3</sup> and a cost of \$1.90/m<sup>3</sup>. Once again, this study confirmed the efficiency of the FO-MD process for potential applications in both wastewater treatment and brine concentration.

The FO-MD system has recently been examined in the context of treating flue gas desulfurization wastewater (Anderson et al., 2021). This integrated system has demonstrated its capability to recover water and capture low-grade heat efficiently. The experimentation involved a temperature range of 43–65 °C and the use of different draw solutes, including sodium NaCl, CaCl<sub>2</sub>, and poly(acrylic acid)-sodium salt (PAA-Na). When employing 3.4 M draw solute concentrations (comprising of NaCl and CaCl<sub>2</sub>), the system achieved an impressive total water recovery rate of 89%. Furthermore, it obtained water flux rates of up to 37 L/m<sup>2</sup>·h for FO and 25 L/m<sup>2</sup>·h for MD.

FO-MD can be applied to treat agricultural runoff, which may contain pesticides, fertilizers, and other contaminants that could have detrimental effects on natural water bodies. It can help recover freshwater for irrigation while reducing the environmental impact of agricultural practices. FO-MD systems can recover valuable nutrients such as phosphorus and nitrogen from agricultural runoff, which can be repurposed as fertilizers. This nutrient recovery not only reduces water pollution but also minimizes the need for chemical fertilizers, contributing to sustainable agriculture (Al-Juboori et al., 2022a). FO-MD was proven to be an effective system for recovering water from real dairy wastewater (Song et al., 2018). This study showed that a flux of clean water of up to 18 L/m<sup>2</sup>·h at 45 °C using cellulose triacetate membrane.

**Table 6** presents the recent research studies of using FO-MD to treat various wastewaters. It is worth noting that the quality of the product water and the FO-MD performance differs from one process to the other, depending on the source and composition of the treated wastewater. The interest in applying FO-MD for wastewater treatment is not only related to water reclamation, but also recovery valuable resources such as nitrogen and phosphorous which are used as a fertilizer for the soil. The challenges here are to obtain high quality water and recovered products. The membrane rejection capacity is the most important factor in FO-MD application for wastewater treatment as there are challenging contaminants such as trace organic compounds and heavy metals that are present in this feed water.

## 6. Energy and economics discussions

The most important elements for assessing any treatment process are energy and cost requirements, value of the product, simplicity of operation and maintenance and environmental impact. These factors should be taken into account when assessing the feasibility of FO-MD for seawater and wastewater treatments. For seawater, the competitive technology is reverse osmosis. The advantage of FO-MD for seawater desalination is ability to handle high salinity feed compared to RO. However, RO is a well-established mature technology with an ongoing improvement that makes it more economically attractive for treatment plant operators. For example the FO membrane cost was reported to be as high as ten times of that for RO membrane (Ibrar et al., 2022). The lifespan of MD given it is a thermally driven membrane is expected to be lower than that of other membrane processes. Additionally, the pumping energy required for RO process (Eq. 25) is lower than the thermal energy required for MD alone (equation 26, where Cp is the specific heat capacity of water, 4.18 kJ/kg.K and ΔT is the temperature increase required in MD process). However, the potential niche for FO-MD system is in the treatment of desalination brine. This area is likely to attract attention in the near future with the increasing tightening of environmental regulations regarding waste discharge. What could also help in

**Table 6**

Recent research studies of using FO-MD hybrid system for different types of wastewater.

Application	Feed Solution	Draw Solution	FO and MD membrane type	Performance	References
Synthetic dye Wastewater	50 ppm of acid orange 8 solution	Polyelectrolytes (PAA-Na)	FO: CA HF membrane MD: PVDF HF	Water transfer rate: 0.18 L/h in both side (AL-DS mode PRO, 0.48 g/ml PAA-Na solution as DS at 66 °C) and MD unit. Water flux: Up to 40 L/m <sup>2</sup> .h (at 80 °C with 0.6 g/ml DS and acid orange 8 as feed) Reverse salt flux (RSF): Up to 0.14 g/m <sup>2</sup> .h.	(Ge et al., 2012)
Dye wastewater	wastewater containing an acid dye	A poly(acrylic acid) sodium(PAA-Na (0.6 M)	FO: CA MD:PVDF	Flux:15–25 L/m <sup>2</sup> .h, RSF= 0.09–0.15 g/m <sup>2</sup> .h. A complete rejection was detected for PAA-Na by FO and MD	(Ge et al., 2012)
Industrial wastewater	flue gas desulfurization (FGD) wastewater	NaCl (3 M)	FO: PA TFC MD: TF-200 PTFE active layer supported by polypropylene (PP)	Flux = 3–20 L/m <sup>2</sup> .h, RSF=N/A, Severe membrane fouling, including CaSO <sub>4</sub> scaling, was detected in FO. MD could re-concentrate the diluted DS up to 50% recovery rate with no significant flux decline	(Lee et al., 2018)
Textile wastewater	model textile wastewater (1 g/L)	Na <sub>2</sub> SO <sub>4</sub> (1.5 M)	FO: CTA (HTI) and TFC MD: PTFE membrane	Water flux= 18.6 ± 0.4 L/m <sup>2</sup> .h, RSF= 5.1–8 g/m <sup>2</sup> .h	(Li et al., 2020)
Wastewater reclamation	DI water, Synthetic wastewater	MgCl <sub>2</sub> solution	FO: cellulose acetate propionate (CAP)-cellulose acetate (CA) HF MD: PVDF HF	Water flux: 19.9 L/m <sup>2</sup> .h in FO 0.5 M MgCl <sub>2</sub> as DS and DI water as FS at 343 K and 16.3 L/m <sup>2</sup> .h in MD unit. Water flux: 13–13.7 L/m <sup>2</sup> .h with 0.5 M MgCl <sub>2</sub> and synthetic wastewater (i.e. heavy metal ions) as feed Minimal reverse draw solute	(Su et al., 2013)
Sewer mining water reclamation	Mining raw Sewage	NaCl solution (1.5 M)	FO: Commercial CTA flat sheet membrane MD: Thin PTFE active layer on PP supporting layer.	Water Flux: 8 L/m <sup>2</sup> .h in both FO (1.5 M NaCl as DS at 40°C) and MD unit (draw and distillate temperatures of 40°C and 20 °C respectively).	(Xie et al., 2013)
Water recovery from oily wastewater	Oily wastewater	NaCl solution	FO: TFC-CTA, HF membrane MD: PVDF HF	Water flux: 20–32.5 L/m <sup>2</sup> .h in FO (2 M NaCl as DS at 60 °C) and oily wastewater (i.e. 4000 ppm petroleum) as feed; Up to 40 L/m <sup>2</sup> .h at 60 °C and DI water as feed. Reverse salt flux: Up to 7.3 g/m <sup>2</sup> .h (DI water as feed). and 5.8 LMH in MD unit	(Zhang et al., 2014)
Phosphorus and clean water recovery from digested sludge	Digested sludge) TOC 647 mg/L, solids1800 mg/L(	MgCl <sub>2</sub> solution (1.5 M)	FO: Commercial CTA flat sheet membrane MD: PTFE	Water flux: 9 L/m <sup>2</sup> .h in both FO (1.5 M MgCl <sub>2</sub> as DS at 40 °C) and MD unit (draw and distillate temperatures of 40°C and 20 °C respectively)	(Xie et al., 2014)
Water reclamation from gas drilling	shale gas drilling flow-back fluid (SGDF)	NaCl, KCl and MgCl <sub>2</sub>	FO: Commercial CTA flat sheet membrane MD: CF <sub>4</sub> -plasma-modified PVDF	Water flux: Up to 23 L/m <sup>2</sup> .h with 3.0 M KCl as DS at 25 °C and pre-treated shale-gas drilling flow-back fluid as feed. Acceptable reverse salt flux	(Li et al., 2014)
Secondary effluent from Wastewater plant	Wastewater , DI water	NaCl solution (0.25–2 M)	FO: Commercial CTA flat sheet membrane MD: Asymmetric PP	Both FO and MD membrane flux remains constant at 14.4 L/m <sup>2</sup> .h during 1200 min operation (DI water (20 °C), 1 M NaCl solution (50 °C), and DI water (20 °C) were used as FS, DS and permeate solutions, respectively).	(Husnain et al., 2015)
Water and nutrient recovery from urine	Human Urine	NaCl solution	FO: Commercial CTA flat sheet membrane MD: PTFE membrane	Average water transfer rate (first 8 h): 0.008 L/h in FO (1 M NaCl as DS at 39 °C in AL-FS mode) and 0.015 L/h (2.5 M NaCl solution as DS at 53 °C) in MD unit	(Liu et al., 2016)
Oil and gas wastewater	Synthetic and real fracking wastewater	Organic solution: (potassium acetate, potassium formate, sodium glycolate, and sodium propionate)	FO: A flat sheet of TFC membrane MD: PVDF membrane	For DS: organic solutions Jw: 10.50–13.26 L/m <sup>2</sup> .h and 19.05–24.05 L/m <sup>2</sup> .h for synthetic fracking and real fracking wastewater respectively	(Islam et al., 2019a)
Dairy wastewater	real dairy wastewater (DWW) recycling	NaCl (1 M)	FO: cellulose triacetate-embedded polyester screen support CTA-ES and aquaporin inside (AQP) MD: PTFE	FO flux:10–18 L/m <sup>2</sup> .h; MD flux ~ 18 L/m <sup>2</sup> .h, RSB= 2–5 g/m <sup>2</sup> .h. A fouled CTA-ES membrane could be restored 90% of the flux after membrane cleaning	(Song et al., 2018)

(continued on next page)

**Table 6 (continued)**

Application	Feed Solution	Draw Solution	FO and MD membrane type	Performance	References
Water reclamation from leachate	Landfill leachate	1 M NaCl	FO: Commercial TFC modified with polyamidoamine (PAMAM)/ polydopamine (PDA) and carboxylated cellulose nanocrystal (CCN) MD: PTFE/PET membrane	Water flux: 30.6 L/m <sup>2</sup> .h with a RSF of 6.9 g/m <sup>2</sup> h (gMH). Lower flux decline compared to unmodified TFC ( $\leq 43.7\%$ vs $\leq 59.45\%$ ). Higher flux recovery compared to unmodified TFC ( $\geq 94.2\%$ vs $\geq 79.0\%$ )	(Zhang et al., 2023b)
Water reclamation from wastewater	Synthetic high-salinity organic wastewater	Polyacrylic acid sodium (PAAS), sodium polystyrene sulfonate (PSS) and polyethylene glycol (PEG)	FO: polyacrylonitrile (PAN) membrane coagulated with DI water (PAN1) and with NaOH (PAN2) MD: PVDF membrane	Water flux for PAN1 and PAN2 with PAAS: 16.43–25.51 L/m <sup>2</sup> .h, with PSS 12.11–18.78 L/m <sup>2</sup> .h, and 3.04–5.05 L/m <sup>2</sup> .h with PEG. PAN2 had higher J <sub>w</sub> than PAN1. RSF is ~2.5 gMH for PAAS, ~5–7.5 gMH, and 32–40 gMH for PAAS, PSS, and PEG, respectively.	(Cao and Zhu, 2023)
Produced water(Oily wastewater)	Synthetic oily water (100–5 ppm) and real oily water	oily water FO: MD	Cellulose triacetate Polytetrafluoroethylene UF: TiO <sub>2</sub> /ZrO <sub>2</sub> mixture	FO flux: 0.65 L/m <sup>2</sup> .h, UF: Flux = 39.8, 110, 304 and 1357 L/m <sup>2</sup> .h, Rejection = 150 kDa membrane and 0.14 μm membrane had oil recovery rate of 83.9% and 63.5%, FO-MD: at 50 mg/L, flux declined by 0.6% (from 5 to 2.6 L/m <sup>2</sup> .h)	(Lu et al., 2018)
Highly saline fracking wastewater	fracking wastewater	NaCl and NaP	FO: polyamide (PA) MD: PVDF(mean pore size 0.22 μm, porosity 75%) MF: nylon 6/SiO <sub>2</sub> composite nanofiber mat coated by polyvinyl acetate	Water flux FO: 4.5 L/m <sup>2</sup> .h /bar MF flux for Psf: 2728 L/m <sup>2</sup> .h /bar and for nanocomposite = 4814 L L/m <sup>2</sup> .h /bar MF as a pre-treatment process removed ~52% of TOC and ~98.5% of turbidity. High average water fluxes (19.98 L/m <sup>2</sup> .h for NaCl and 30.97 L/m <sup>2</sup> .h for sodium propionate draw. 98.5% of initial water flux can be restored with the fabricated nanocomposite membrane. Membrane distillation (demonstrated solute rejection ~ 99.99%)	(Islam et al., 2019b)
Fracturingproduced water (PW)	PW1 from Fayetteville Shale and PW2 from Marcellus Shale	NaCl (2 M)	FO: Flat sheet cellulose triacetate (CTA) membranes MDL Ethylene chlorotrifluoroethylene (ECTFE) copolymer, provided by 3 M (Maplewood, MN) and polytetrafluoroethylene (PTFE), provided by Pall Corporation (Port Washington, NY).	Electrocoagulation (EC) removed total organic carbon and total suspended solids by up to 78% and 96%, respectively. Using of 2.0 M NaCl in DI water as DS resulted in 76% water recovery from PW1 (TDS=11.2 g/L) and 30% water recovery from PW2 (TDS=57.2 g/L). Increasing the DS concentration to 5.0 M significantly increased the water recovery for PW2, while this increase for PW1 was less than 10%. Integrated EC-FO-MD stable over a long-term run, collecting ~7 L permeate	(Sardari et al., 2019)
Landfill Leachate	waste landfill leachate	NaCl solution FO:	FO: Thin film composite membrane MD: polytetrafluoroethylene-polyvinylidene fluoride composite (PTFE-PVDF) active layer and polyethylene terephthalate (PET) support layer	Rejection rates of salt by FO-MD were higher than 96% with high salinity FS. Rejection rates of toxic ions were higher than 98% by FO-MD. NH <sub>4</sub> <sup>+</sup> -N, Hg, As and Sb were completely removed.	(Zhou et al., 2017)
Synthetic wastewater	As(III) solution (1000 ppm)	Oxalic acid complex (Na-Cr-OA, 1 M)	FO: TFC-PES MD: PVDF	Flux: 18–20 L/m <sup>2</sup> .h; RSF: 0.2–0.5 g/m <sup>2</sup> .h. An outstanding As(III) rejection with 30–3000 μg/L As(III) in the permeate was accomplished when As(III) feed solutions conc varied from $5 \times 10^4$ – $1 \times 10^6$ μg/L. As (III) removal with a water recovery up to 21.6% (FO mode) and 48.3% (PRO mode) were also achieved in 2 h	(Ge et al., 2016)
Concentration of protein solution	bovine serum albumin (BSA) solution	NaCl (0.5 M)	FO: PBI NF hollow fiber membrane MD: PVDF-PTFE	Water flux: 2.5–6 L/m <sup>2</sup> .h; RSF: 6–18 g/m <sup>2</sup> .h. the integrated system is stable in continuous operation when the dehydration rate across the FO membrane is the same as the water vapor rate across the MD membrane	(Wang et al., 2011)

(continued on next page)

**Table 6 (continued)**

Application	Feed Solution	Draw Solution	FO and MD membrane type	Performance	References
Domestic wastewater	real domestic wastewater treatment	NaCl (0.6 M)	FO: CTA MD: PVDF	Water flux: 18–20 L/m <sup>2</sup> .h, removal efficiency is more than 90%. Fouling in FO is caused by organic substances like polysaccharides and proteins, whilst in MD, fouling is caused by inorganic salts and was not as severe as that of the FO membrane. Higher stability after 120 hr operation	(Li et al., 2018)
High salinity oily wastewater		NaCl (5 M), KCl (4 M), LiCl (4.8 & 10 M) and Mg C <sub>2</sub> (4–4.8) M	FO: TFC MD:PP	In FO: LiCl showed higher fluxNaCl and KCl showed a different behavior of a high MD flux and low or negative FO flux. In MD: LiCl (10 M) showed lower flux due to the lower vapour pressure. MgCl <sub>2</sub> at 4.8 M demonstrated comparable fluxes for both FO and MD	(Al-Furaiji et al., 2019)
Mass recovery from diary wastewater	dairy wastewater	NaCl (2 M)	FO:CTA MD: PVDF and PP	Flux: 10–12 L/m <sup>2</sup> .h and RSF: 2–8 g/m <sup>2</sup> .h. Return of 12–13 million \$ corresponding to annual net profit of 800,000 \$.	(Aydiner et al., 2014)
Tetracycline Wastewater	simulate antibiotic wastewater (tetracycline)	NaCl (2 M)	FO: TFC polyacrylonitrile (PAN) nanofiber support MD: PVDF	A high water flux of 57 L/m <sup>2</sup> .h was obtained against 2 M NaCl solution. TC rejection was over 99.9% and wastewater can be reclaimed in a FO-MD process. 15–22% water recovery was achieved after 7 hr operation in the FO-MD hybrid process.	(Pan et al., 2017)
Produced water	Desalter Effluent (DE) Wash Water (WW) Three Phase Separator (3PS), Reverse Osmosis (RO) Reject Water oil separator (WOSEP) Outlet	water oil separator stream (WO)	FO:TFC MD:PTFE	In FO: Flux= 8.30 L/m <sup>2</sup> .h and 26.78 when WO was used. CP and colloidal CaSiO <sub>3</sub> layer on membrane support caused FO flux declineIn MD: Flux= 14.41 L/m <sup>2</sup> .h when WO was used For FO-MD system, Flux= 5.62–11.12 L/m <sup>2</sup> .	(Nawaz et al., 2021)

improving the attractiveness of FO-MD application in seawater treatment is considering metals recovery especially when coupling the system with a precipitation process (León-Venegas et al., 2023). The other possible scenario where FO-MD is envisaged to be feasible is the availability of waste or natural heat that can be utilized for MD process albeit it is location and process dependent as mentioned earlier.

$$E_{pumping} = \frac{Q\Delta P}{\eta} \quad (25)$$

$$E_{heating} = QC_p\Delta T \quad (24)$$

As for wastewater treatment application, FO-MD probably has better chances for large or full-scale implementation compared to sweater treatment applications. The reason behind this is the multi benefits that can be realized with such a system. FO-MD can be combined with an aerobic membrane bioreactor (AnMBR) to improve biogas production that can be harnessed for electricity and heat generation (Ansari et al., 2017), which in turn can be utilized for FO and MD operation (Fig. 11 a). In addition to biogas production, ammonia is produced in the AnMBR, which can be recovered by other process to produce fertilizers (Al-Juboori et al., 2022b). Other application for FO-MD in wastewater is combining it with membrane contactor to produce high purity concentrated ammonium salts that could be used as fertilizers or raw materials for other industries (Fig. 11 b) (Al-Juboori et al., 2022a). The other advantage that can be reaped from FO-MD system implementation in wastewater treatment plant is the removal of nitrogen that can reduce the energy required for aeration in the activated sludge process which accounts approximately for 1% of the world energy consumption (Al-Juboori et al., 2022a).

## 7. Conclusion and future directions

Hybrid FO-MD systems have proven to be a highly efficient and versatile solution for different water treatment processes. The low operational pressure of FO-MD system and the capability of treating challenging feedwater are the main attractive traits of the system. FO-MD systems excel in removing organics, salts, and pollutants from various water sources, including seawater, brackish water, wastewater, and industrial effluents. Their high-water recovery rates ensure optimal utilization of available water resources, reducing wastage and addressing water scarcity challenges. The two important aspects that determine the feasibility of the FO-MD system is the selection of the draw solution and sourcing out the energy required for heating the water for MD process. The recent research advancement led to the emergence of innovative draw solutions that have high osmotic pressure and easy to regenerate with the minimal rise of concentration polarization such as CQDs. The intrinsic high energy associate with thermally driven water transfer in MD is another challenge that is yet to be overcome. New pilot system designs such as V-MEMD have resulted in plausible thermal energy recovery, but still the electrical power may render the FO-MD system unfeasible option for seawater and wastewater treatment. Hence, the use of solar or waste energy is still inevitable to improve the attractiveness of the process. However, the sustainability of these resources is site specific. The most important factor that secures an efficient integration of FO and MD is the WTB. The flux of FO and MD should be equal. The FO-MD system is likely to reach large scale application in wastewater industry due to the multi benefits that could be earnt such as energy generation, water and nutrients recovery, and energy saving for nitrogen removal.

Future research should focus on system design where the negative impact of elevated temperature of MD process on FO membrane and

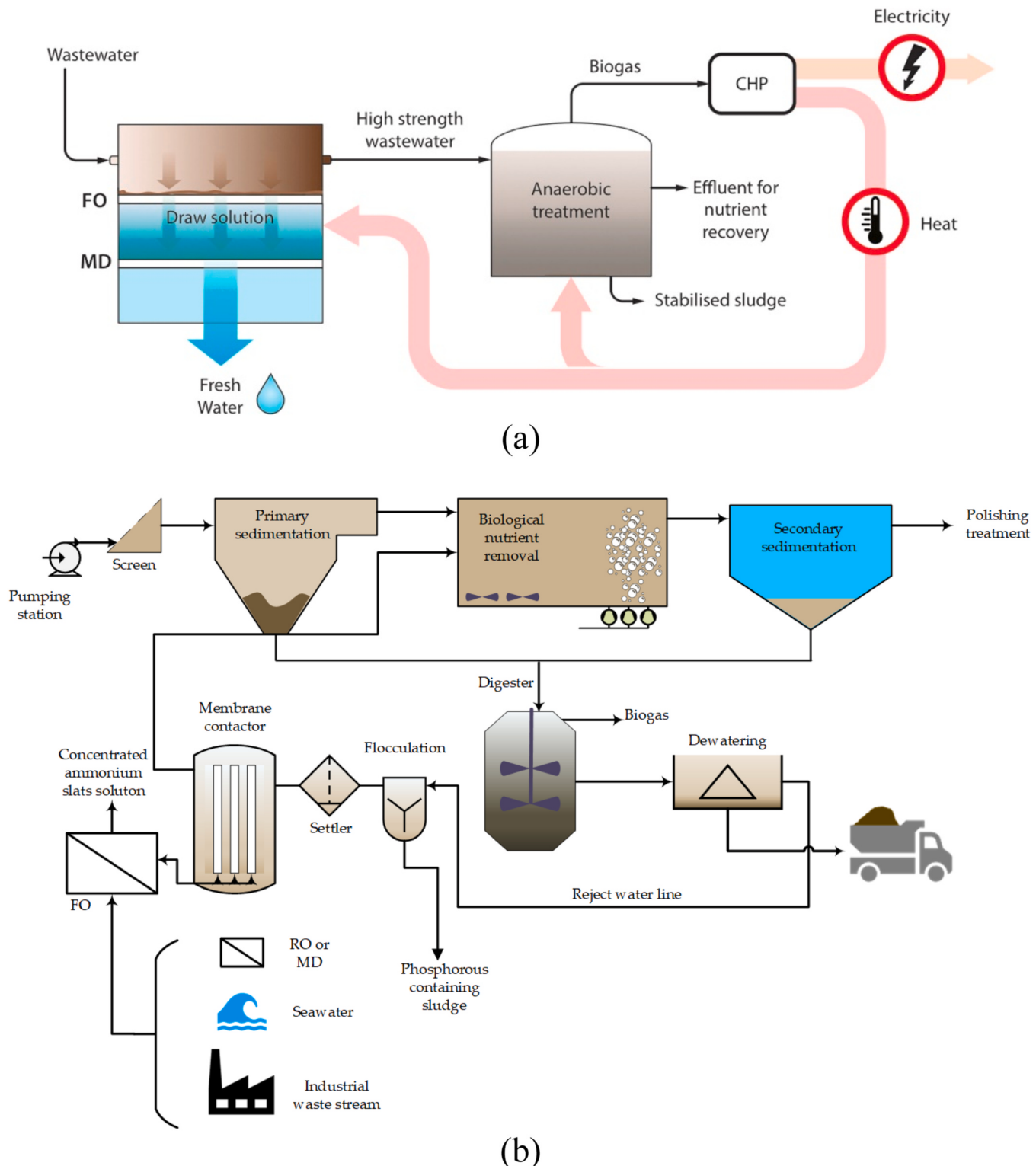


**Fig. 11.** Applications of FO-MD hybrid system for wastewater treatment and resource recovery: (a) FO-MD-AnMBR, copied from (Ansari et al., 2017) with copyright permission from Elsevier (License No. 5650821040246) and (b) FO-MD-membrane contactor copied from (Al-Juboori et al., 2022a), an open access article distributed under the terms and conditions of the Creative Commons Attribution License (CC BY).

scaling issues is minimized. More research into membrane materials with a focus on wetting and fouling resistance while maintaining mechanical, chemical and thermal stability is required. Continuing the efforts for finding optimal draw solution is also necessary. Particle based draw solutions with electrical or magnetic properties seem to be a promising class of materials that merits further investigations. Modified

polymeric composite materials with active chemical groups and embedded nanoparticles are another potential candidate for preparing efficient draw solutions.

## Declaration of Competing Interest

The authors declare that they have no known competing financial interests or personal relationships that could have appeared to influence the work reported in this paper.

## References

- Abu-Zeid, M.A.E.-R., Zhang, Y., Dong, H., Zhang, L., Chen, H.-L., Hou, L., 2015. A comprehensive review of vacuum membrane distillation technique. *Desalination* 356, 1–14.
- Achilli, A., Cath, T.Y., Childress, A.E., 2010. Selection of inorganic-based draw solutions for forward osmosis applications. *J. Membr. Sci.* 364 (1–2), 233–241.
- Adham, S., Oppenheimer, J., Liu, L., Kumar, M., 2007. Dewatering Reverse Osmosis Concentrate from Water Reuse Applications Using Forward Osmosis. *Water Reuse Foundation Alexandria*.
- Ahmed, F.E., Lalia, B.S., Hashaikheh, R., Hilal, N., 2022. Intermittent direct joule heating of membrane surface for seawater desalination by air gap membrane distillation. *J. Membr. Sci.* 648, 120390.
- Ahmed, M., Alambi, R.K., Bhadrachari, G., Al-Muqahwi, S., Thomas, J.P., 2023. Design and optimization of a unique pilot scale forward osmosis integrated membrane distillation system for seawater desalination. *J. Environ. Chem. Eng.* 11 (3), 109949.
- Akther, N., Sodiq, A., Giwa, A., Daer, S., Arafat, H.A., Hasan, S.W., 2015. Recent advancements in forward osmosis desalination: a review. *Chem. Eng. J.* 281, 502–522.
- Al Mahri, B.B.A., Balogun, H.A., Yusuf, A., Giwa, A., 2020. Electro-osmotic thermal process model for performance enhancement of forward osmosis integrated with membrane distillation, 238. *Separation and Purification Technology*, 116494.
- Alcheikhhamdon, A.A., Darwish, N.A., Hilal, N., 2015. Statistical analysis of air-gap membrane desalination experimental data: Hypothesis testing. *Desalination* 362, 117–125.
- Al-Furaiji, M., Benes, N., Nijmeijer, A., McCutcheon, J.R., 2019. Use of a forward osmosis-membrane distillation integrated process in the treatment of high-salinity oily wastewater. *Ind. Eng. Chem. Res.* 58 (2), 956–962.
- Alghouti, M.S., 2016. Assessing Forward Osmosis As Potential Alternative Seawater Desalination Technology, in: *Civil Water Resources Engineering*. Gaza.
- Al-Juboori, R.A., Yusaf, T., 2012. Biofouling in RO system: mechanisms, monitoring and controlling. *Desalination* 302, 1–23.
- Al-Juboori, R.A., Naji, O., Bowtell, L., Alpatova, A., Soukane, S., Ghaffour, N., 2021. Power effect of ultrasonically vibrated spacers in air gap membrane distillation: Theoretical and experimental investigations. *Sep. Purif. Technol.* 262, 118319.
- Al-Juboori, R.A., Al-Shaali, M., Aani, S.A., Johnson, D., Hilal, N., 2022a. Membrane technologies for nitrogen recovery from waste streams: scientometrics and technical analysis. *Membranes* 13 (1), 15.
- Al-Juboori, R.A., Kaljunen, J.U., Righetto, I., Mikola, A., 2022b. Membrane contactor onsite piloting for nutrient recovery from mesophilic digester reject water: the effect of process conditions and pre-treatment options. *Sep. Purif. Technol.*, 122250.
- Alkhudhiri, A., Darwish, N., Hilal, N., 2012. Membrane distillation: a comprehensive review. *Desalination* 287, 2–18.
- Almoalimi, K., Liu, Y.-Q., Booth, A., Heo, S., 2022. Temperature effects of MD on municipal wastewater treatment in an integrated forward osmosis and membrane distillation process. *Processes* 10 (2), 355.
- Alsvik, I.L., Hägg, M.-B., 2013. Pressure retarded osmosis and forward osmosis membranes: materials and methods. *Polymers* 5 (1), 303–327.
- Anderson, W.V., Cheng, C.-M., Butalia, T.S., Weavers, L.K., 2021. Forward osmosis-membrane distillation process for zero liquid discharge of flue gas desulfurization wastewater. *Energy Fuels* 35 (6), 5130–5140.
- Ansari, A.J., Hai, F.I., Price, W.E., Drewes, J.E., Nghiem, L.D., 2017. Forward osmosis as a platform for resource recovery from municipal wastewater-A critical assessment of the literature. *J. Membr. Sci.* 529, 195–206.
- Anvari, A., Azimi Yanchesheh, A., Kekre, K.M., Ronen, A., 2020. State-of-the-art methods for overcoming temperature polarization in membrane distillation process: a review. *J. Membr. Sci.* 616, 118413.
- Arkhangelsky, E., Wicaksana, F., Chou, S., Al-Rabiah, A.A., Al-Zahrani, S.M., Wang, R., 2012. Effects of scaling and cleaning on the performance of forward osmosis hollow fiber membranes. *J. Membr. Sci.* 415–416, 101–108.
- Arumugam, N., Kim, J., 2018. Synthesis of carbon quantum dots from Broccoli and their ability to detect silver ions. *Mater. Lett.* 219, 37–40.
- Athika, M., Prasath, A., Duraisamy, E., Sankar Devi, V., Selva Sharma, A., Elumalai, P., 2019. Carbon-quantum dots derived from denatured milk for efficient chromium-ion sensing and supercapacitor applications. *Mater. Lett.* 241, 156–159.
- Awad, A.M., Jalab, R., Minier-Matar, J., Adham, S., Nasser, M.S., Judd, S.J., 2019. The status of forward osmosis technology implementation. *Desalination* 461, 10–21.
- Aydiner, C., Sen, U., Topcu, S., Ekinci, D., Altinay, A.D., Koseoglu-Imer, D.Y., Keskinler, B., 2014. Techno-economic viability of innovative membrane systems in water and mass recovery from dairy wastewater. *J. Membr. Sci.* 458, 66–75.
- Azizi, B., Farhadi, K., Samadi, N., 2019. Functionalized carbon dots from zein biopolymer as a sensitive and selective fluorescent probe for determination of sumatriptan. *Microchem. J.* 146, 965–973.
- Bahar, R., Ng, K.C., 2020. Fresh water production by membrane distillation (MD) using marine engine's waste heat. *Sustain. Energy Technol. Assess.* 42, 100860.
- Baker, R.W., 2012. Membrane technology and applications. John Wiley & Sons.
- Baker, S.N., Baker, G.A., 2010. Luminescent carbon nanodots: emergent nanolights. *Angew. Chem. Int. Ed.* 49 (38), 6726–6744.
- Bamaga, O.A., Yokochi, A., Zabara, B., Babaqi, A.S., 2011. Hybrid FO/RO desalination system: preliminary assessment of osmotic energy recovery and designs of new FO membrane module configurations. *Desalination* 268 (1), 163–169.
- Boo, C., Lee, J., Elimelech, M., 2016. Omniphobic polyvinylidene fluoride (PVDF) membrane for desalination of shale gas produced water by membrane distillation. *Environ. Sci. Technol.* 50 (22), 12275–12282.
- Bouchrit, R., Boubakri, A., Hafiane, A., Bouguecha, S.A.-T., 2015. Direct contact membrane distillation: Capability to treat hyper-saline solution. *Desalination* 376, 117–129.
- Cabrera-Castillo, E.H., Castillo, I., Ciudad, G., Jeison, D., Ortega-Bravo, J.C., 2021. FO-MD setup analysis for acid mine drainage treatment in Chile: An experimental-theoretical economic assessment compared with FO-RO and single RO. *Desalination* 514, 115164.
- Cai, Y., Hu, X.M., 2016. A critical review on draw solutes development for forward osmosis. *Desalination* 391, 16–29.
- Cai, Y., Wang, R., Krantz, W.B., Fane, A.G., 2015. Exploration of using thermally responsive polyionic liquid hydrogels as draw agents in forward osmosis. *Rsc Adv.* 5 (118), 97143–97150.
- Camacho, L.M., Dumée, L., Zhang, J., Li, J.-d., Duke, M., Gomez, J., Gray, S., 2013. Advances in membrane distillation for water desalination and purification applications. *Water* 5 (1), 94–196.
- Cao, Z., Zhu, T., 2023. The applications of porous FO membranes and polyelectrolyte draw solution in the high-salinity organic wastewater treatment with a hybrid forward osmosis-membrane distillation system. *J. Appl. Polym. Sci.* 140 (1), e53266.
- Cath, T.Y., Childress, A.E., Elimelech, M., 2006. Forward osmosis: principles, applications, and recent developments. *J. Membr. Sci.* 281 (1), 70–87.
- Chekli, L., Phuntsho, S., Shon, H.K., Vigneswaran, S., Kandasamy, J., Chanan, A., 2012. A review of draw solutes in forward osmosis process and their use in modern applications. *Desalin. Water Treat.* 43 (1–3), 167–184.
- Chekli, L., Phuntsho, S., Kim, J.E., Kim, J., Choi, J.Y., Choi, J.-S., Kim, S., Kim, J.H., Hong, S., Sohn, J., Shon, H.K., 2016. A comprehensive review of hybrid forward osmosis systems: Performance, applications and future prospects. *J. Membr. Sci.* 497, 430–449.
- Chekli, L., Pathak, N., Kim, Y., Phuntsho, S., Li, S., Ghaffour, N., Leiknes, T., Shon, H.K., 2018. Combining high performance fertiliser with surfactants to reduce the reverse solute flux in the fertiliser drawn forward osmosis process. *J. Environ. Manag.* 226, 217–225.
- Chen, Q., Muhammad, B., Akhtar, F.H., Ybyraiymkul, D., Muhammad, W.S., Li, Y., Ng, K.C., 2020. Thermo-economic analysis and optimization of a vacuum multi-effect membrane distillation system. *Desalination* 483, 114413.
- Chen, Y.-R., Chen, L.-H., Chen, C.-H., Ko, C.-C., Huang, A., Li, C.-L., Chuang, C.-J., Tung, K.-L., 2018. Hydrophobic alumina hollow fiber membranes for sucrose concentration by vacuum membrane distillation. *J. Membr. Sci.* 555, 250–257.
- Cheng, J., Xu, Y., Zhou, D., Liu, K., Geng, N., Lu, J., Liu, Y., Liu, J., 2019. Novel carbon quantum dots can serve as an excellent adjuvant for the gp85 protein vaccine against avian leukosis virus subgroup J in chickens. *Poul. Sci.* 98 (11), 5315–5320.
- Chung, T.-S., Zhang, S., Wang, K.Y., Su, J., Ling, M.M., 2012. Forward osmosis processes: Yesterday, today and tomorrow. *Desalination* 287, 78–81.
- Criscuoli, A., Carnevale, M.C., Drioli, E., 2008. Evaluation of energy requirements in membrane distillation. *Chem. Eng. Process.: Process. Intensif.* 47 (7), 1098–1105.
- Deng, Y.H., Chen, J.H., Yang, Q., Zhuo, Y.Z., 2021. Carbon quantum dots (CQDs) and polyethyleneimine (PEI) layer-by-layer (LBL) self-assembly PEK-C-based membranes with high forward osmosis performance. *Chem. Eng. Res. Des.* 170, 423–433.
- Deshmukh, A., Boo, C., Karanikola, V., Lin, S., Straub, A.P., Tong, T., Warsinger, D.M., Elimelech, M., 2018. Membrane distillation at the water-energy nexus: limits, opportunities, and challenges. *Energy Environ. Sci.* 11 (5), 1177–1196.
- Doshi, K., Mungray, A.A., 2020. Bio-route synthesis of carbon quantum dots from tulsi leaves and its application as a draw solution in forward osmosis. *J. Environ. Chem. Eng.* 8 (5), 104174.
- Dow, N., Gray, S., Li, J.-d., Zhang, J., Ostarcevic, E., Liubinas, A., Atherton, P., Roeszler, G., Gibbs, A., Duke, M., 2016. Pilot trial of membrane distillation driven by low grade waste heat: membrane fouling and energy assessment. *Desalination* 391, 30–42.
- Duong, H.C., Cooper, P., Nelemans, B., Cath, T.Y., Nghiem, L.D., 2015. Optimising thermal efficiency of direct contact membrane distillation by brine recycling for small-scale seawater desalination. *Desalination* 374, 1–9.
- Dutta, S., Dave, P., Nath, K., 2023. Progress and perspective for carbon quantum dots and analogous carbon-based nanomaterials in augmenting forward osmosis performance. *Sep. Purif. Rev.* 1–22.
- El-Bourawi, M.S., Ding, Z., Ma, R., Khayet, M., 2006. A framework for better understanding membrane distillation separation process. *J. Membr. Sci.* 285 (1), 4–29.
- Elimelech, M., Phillip, W.A., 2011. The future of seawater desalination: energy, technology, and the environment. *science* 333 (6043), 712–717.
- Fan, H., Zhang, M., Bhandari, B., Yang, C.-H., 2020. Food waste as a carbon source in carbon quantum dots technology and their applications in food safety detection. *Trends Food Sci. Technol.* 95, 86–96.
- Fane, A.G., Schofield, R.W., Fell, C.J.D., 1987. The efficient use of energy in membrane distillation. *Desalination* 64, 231–243.
- Figueira, M., Rodríguez-Jiménez, D., López, J., Reig, M., Cortina, J.L., Valderrama, C., 2023. Experimental and economic evaluation of nanofiltration as a pre-treatment for added-value elements recovery from seawater desalination brines. *Desalination* 549, 116321.
- Fowley, C., Nomikou, N., McHale, A.P., McCaughan, B., Callan, J.F., 2013. Extending the tissue penetration capability of conventional photosensitisers: a carbon quantum

- dot–protoporphyrin IX conjugate for use in two-photon excited photodynamic therapy. *Chem. Commun.* 49 (79), 8934–8936.
- Galiano, F., Santoro, S., Castro-Muñoz, R., Russo, F., Figoli, A., 2023. Smart and novel nanofiber membranes. In: Kargari, A., Matsuura, T., Shirazi, M.M.A. (Eds.), in *Electrospun and Nanofibrous Membranes*. Elsevier, pp. 603–623.
- Gao, A., 2016. Desalination of high-salinity water by membranes. University of Waterloo.
- Ge, Q., Wang, P., Wan, C., Chung, T.-S., 2012. Polyelectrolyte-Promoted Forward Osmosis-Membrane Distillation (FO-MD) Hybrid Process for Dye Wastewater Treatment. *Environ. Sci. Technol.* 46 (11), 6236–6243.
- Ge, Q., Han, G., Chung, T.-S., 2016. Effective As(III) removal by a multi-charged hydroacid complex draw solute facilitated forward osmosis-membrane distillation (FO-MD) processes. *Environ. Sci. Technol.* 50 (5), 2363–2370.
- Ghaffour, N., Soukane, S., Lee, J.G., Kim, Y., Alpatova, A., 2019. Membrane distillation hybrids for water production and energy efficiency enhancement: a critical review. *Appl. Energy* 254, 113698.
- Giagnorio, M., Casasso, A., Tiraferrri, A., 2021. Environmental sustainability of forward osmosis: the role of draw solute and its management. *Environ. Int.* 152, 106498.
- Gingerich, D.B., Mauter, M.S., 2015. Quantity, quality, and availability of waste heat from United States thermal power generation. *Environ. Sci. Technol.* 49 (14), 8297–8306.
- Gore, W.L., Gore, R.W., Gore, D.W., 1985. Desalination device and process, U. patent, Editor. Gore, W. L. & Associates, Inc.
- Gryta, M., 2007. Influence of polypropylene membrane surface porosity on the performance of membrane distillation process. *J. Membr. Sci.* 287 (1), 67–78.
- Gryta, M., 2017. The application of polypropylene membranes for production of fresh water from brines by membrane distillation. *Chem. Pap.* 71 (4), 775–784.
- Gryta, M., 2019. Studies of membrane scaling during water desalination by membrane distillation. *Chem. Pap.* 73 (3), 591–600.
- Guillén-Burrieza, E., Zaragoza, G., Miralles-Cuevas, S., Blanco, J., 2012. Experimental evaluation of two pilot-scale membrane distillation modules used for solar desalination. *J. Membr. Sci.* 409–410, 264–275.
- Guo, C.X., Dong, Y., Yang, H.B., Li, C.M., 2013. Graphene quantum dots as a green sensitizer to functionalize ZnO nanowire arrays on F-doped SnO<sub>2</sub> glass for enhanced photoelectrochemical water splitting. *Adv. Energy Mater.* 3 (8), 997–1003.
- Guo, C.X., Zhao, D., Zhao, Q., Wang, P., Lu, X., 2014. Na<sup>+</sup>-functionalized carbon quantum dots: a new draw solute in forward osmosis for seawater desalination. *Chem. Commun.* 50 (55), 7318–7321.
- Hancock, N.T., Cath, T.Y., 2009. Solute coupled diffusion in osmotically driven membrane processes. *Environ. Sci. Technol.* 43 (17), 6769–6775.
- Hanen, A., Fatma, K., Hibat, A., Khaoula, H., Bechir, C., Qusay, A., 2023. Novel composite membrane based on recycled low-density polyethylene-alumina used for vacuum membrane distillation. *Bull. Natl. Res. Cent.* 47 (1), 132.
- Hartanto, Y., Yun, S., Jin, B., Dai, S., 2015. Functionalized thermo-responsive microgels for high performance forward osmosis desalination. *Water Res.* 70, 385–393.
- Heinzl, W., Büttner, S., Lange, G., 2012. Industrialized modules for MED Desalination with polymer surfaces. *Desalin. Water Treat.* 42 (1–3), 177–180.
- Hoover, L.A., Phillip, W.A., Tiraferrri, A., Yip, N.Y., Elimelech, M., 2011. Forward with osmosis: emerging applications for greater sustainability. *Environ. Sci. Technol.* 45 (23), 9824–9830.
- Huang, L., Pei, J., Jiang, H., Hu, X., 2018. Water desalination under one sun using graphene-based material modified PTFE membrane. *Desalination* 442, 1–7.
- Husnain, T., Liu, Y., Riffat, R., Mi, B., 2015. Integration of forward osmosis and membrane distillation for sustainable wastewater reuse. *Sep. Purif. Technol.* 156, 424–431.
- Hussain, A., Janson, A., Matar, J.M., Adham, S., 2022. Membrane distillation: recent technological developments and advancements in membrane materials. *Emergent Mater.* 5 (2), 347–367.
- Ibraheem, B.M., Aani, S.A., Alsarayreh, A.A., Alsalhy, Q.F., Salih, I.K., 2023. Forward osmosis membrane: review of fabrication, modification, challenges and potential. *Membranes* 13 (4), 379.
- Ibrar, I., Naji, O., Sharif, A., Malekizadeh, A., Alhwari, A., Alanezi, A.A., Altaee, A., 2019. A review of fouling mechanisms, control strategies and real-time fouling monitoring techniques in forward osmosis. *Water* 11 (4), 695.
- Ibrar, I., Yadav, S., Naji, O., Alanezi, A.A., Ghaffour, N., Déon, S., Subbiah, S., Altaee, A., 2022. Development in forward Osmosis-Membrane distillation hybrid system for wastewater treatment. *Sep. Purif. Technol.* 286, 120498.
- Islam, M.S., Sultana, S., McCutcheon, J.R., Rahaman, M.S., 2019a. Treatment of fracking wastewaters via forward osmosis: evaluation of suitable organic draw solutions. *Desalination* 452, 149–158.
- Islam, M.S., Touati, K., Rahaman, M.S., 2019b. Feasibility of a hybrid membrane-based process (MF-FO-MD) for fracking wastewater treatment. *Sep. Purif. Technol.* 229, 115802.
- Jafarinejad, S., 2021. Forward osmosis membrane technology for nutrient removal/recovery from wastewater: Recent advances, proposed designs, and future directions. *Chemosphere* 263, 128116.
- Jalilah, P., 2019. Emerging Technologies for Sustainable Desalination Handbook. Current Science Association.
- Jiang, X., Qin, D., Mo, G., Feng, J., Yu, C., Mo, W., Deng, B., 2019. Ginkgo leaf-based synthesis of nitrogen-doped carbon quantum dots for highly sensitive detection of salazosulfapyridine in mouse plasma. *J. Pharm. Biomed. Anal.* 164, 514–519.
- Johnson, D.J., Suwaileh, W.A., Mohammed, A.W., Hilal, N., 2018. Osmotic's potential: an overview of draw solutes for forward osmosis. *Desalination* 434, 100–120.
- Johnson, R.A., Nguyen, M.H., 2017. Understanding membrane distillation and osmotic distillation. John Wiley & Sons.
- Joshi, P.N., Mathias, A., Mishra, A., 2018. Synthesis of ecofriendly fluorescent carbon dots and their biomedical and environmental applications. *Mater. Technol.* 33 (10), 672–680.
- Kalaiyaranan, G., Joseph, J., 2019. Cholesterol derived carbon quantum dots as fluorescence probe for the specific detection of hemoglobin in diluted human blood samples. *Mater. Sci. Eng.: C*. 94, 580–586.
- Kamel, A.H., 2022. Preparation and Characterization of a Novel Draw Solution for Water Desalination Using Forward Osmosis and Membrane Distillation, in *Chemical Engineering Department*. University of Technology-Iraq.
- Karanikola, V., Corral, A.F., Mette, P., Jiang, H., Arnoldand, R.G., Ela, W.P., 2014. Solar membrane distillation: desalination for the Navajo Nation. *Rev. Environ. Health* 29 (1–2), 67–70.
- Kayvani Fard, A., Rhadfi, T., Khraisheh, M., Atieh, M.A., Khraisheh, M., Hilal, N., 2016. Reducing flux decline and fouling of direct contact membrane distillation by utilizing thermal brine from MSF desalination plant. *Desalination* 379, 172–181.
- Klaysom, C., Cath, T.Y., Depuydt, T., Vankelecom, I.F., 2013. Forward and pressure retarded osmosis: potential solutions for global challenges in energy and water supply. *Chem. Soc. Rev.* 42 (16), 6959–6989.
- Koo, J.-W., Han, J.-H., Yun, T., Lee, S., Choi, J.-S., 2013. Integration of forward osmosis with membrane distillation: effect of operating conditions. *Desalin. Water Treat.* 51 (25–27), 5355–5361.
- Kullab, A., 2011. *Desalination using membrane distillation: experimental and numerical study*, in *School of Industrial Engineering and Management (ITM), Energy Technology, Heat and Power Technology*. KTH Royal Institute of Technology.
- Kumar, R., Al-Haddad, S., Al-Rughaib, M., Salman, M., 2016. Evaluation of hydrolyzed poly(isobutylene-alt-maleic anhydride) as a polyelectrolyte draw solution for forward osmosis desalination. *Desalination* 394, 148–154.
- Kwan, S.E., Bar-Zeev, E., Elimelech, M., 2015. Biofouling in forward osmosis and reverse osmosis: Measurements and mechanisms. *J. Membr. Sci.* 493, 703–708.
- Kwon, Y.-N., Kim, M.-J., Lee, Y.T., 2016. Application of a FO/MD-combined system for the desalination of saline solution. *Desalin. Water Treat.* 57 (31), 14347–14354.
- Lalia, B.S., Ahmed, F.E., Shah, T., Hilal, N., Hashaikeh, R., 2015. Electrically conductive membranes based on carbon nanostructures for self-cleaning of biofouling. *Desalination* 360, 8–12.
- Lay, W.C., Chong, T.H., Tang, C.Y., Fane, A.G., Zhang, J., Liu, Y., 2010. Fouling propensity of forward osmosis: investigation of the slower flux decline phenomenon. *Water Sci. Technol.* 61 (4), 927–936.
- Lee, K.L., Baker, R.W., Lonsdale, H.K., 1981. Membranes for power generation by pressure-retarded osmosis. *J. Membr. Sci.* 8 (2), 141–171.
- Lee, S., Cho, J., Elimelech, M., 2005. Combined influence of natural organic matter (NOM) and colloidal particles on nanofiltration membrane fouling. *J. Membr. Sci.* 262 (1), 27–41.
- Lee, S., Kim, Y., Hong, S., 2018. Treatment of industrial wastewater produced by desulfurization process in a coal-fired power plant via FO-MD hybrid process. *Chemosphere* 210, 44–51.
- Lee, S., Choi, J., Park, Y.-G., Shon, H., Ahn, C.H., Kim, S.-H., 2019. Hybrid desalination processes for beneficial use of reverse osmosis brine: Current status and future prospects. *Desalination* 454, 104–111.
- Lei, C.-W., Hsieh, M.-L., Liu, W.-R., 2019. A facile approach to synthesize carbon quantum dots with pH-dependent properties. *Dyes Pigments* 169, 73–80.
- León-Venegas, E., Vilches-Arenas, L.F., Fernández-Baco, C., Arroyo-Torralvo, F., 2023. Potential for water and metal recovery from acid mine drainage by combining hybrid membrane processes with selective metal precipitation. *Resour., Conserv. Recycl.* 188, 106629.
- Li, D., Zhang, X., Simon, G.P., Wang, H., 2013. Forward osmosis desalination using polymer hydrogels as a draw agent: Influence of draw agent, feed solution and membrane on process performance. *Water Res.* 47 (1), 209–215.
- Li, J., Hou, D., Li, K., Zhang, Y., Wang, J., Zhang, X., 2018. Domestic wastewater treatment by forward osmosis-membrane distillation (FO-MD) integrated system. *Water Sci. Technol.* 77 (6), 1514–1523.
- Li, M., Li, K., Wang, L., Zhang, X., 2020. Feasibility of concentrating textile wastewater using a hybrid forward osmosis-membrane distillation (FO-MD) process: performance and economic evaluation. *Water Res.* 172, 115488.
- Li, X.-M., Zhao, B., Wang, Z., Xie, M., Song, J., Nghiem, L.D., He, T., Yang, C., Li, C., Chen, G., 2014. Water reclamation from shale gas drilling flow-back fluid using a novel forward osmosis–vacuum membrane distillation hybrid system. *Water Sci. Technol.* 69 (5), 1036–1044.
- Lim, H., Liu, Y., Kim, H.Y., Son, D.I., 2018. Facile synthesis and characterization of carbon quantum dots and photovoltaic applications. *Thin Solid Films* 660, 672–677.
- Lim, S.Y., Shen, W., Gao, Z., 2015. Carbon quantum dots and their applications. *Chem. Soc. Rev.* 44 (1), 362–381.
- Liu, Q., Liu, C., Zhao, L., Ma, W., Liu, H., Ma, J., 2016. Integrated forward osmosis-membrane distillation process for human urine treatment. *Water Res.* 91, 45–54.
- Liu, Y., Mi, B., 2012. Combined fouling of forward osmosis membranes: synergistic foulant interaction and direct observation of fouling layer formation. *J. Membr. Sci.* 407–408, 136–144.
- Loeb, S., Titelman, L., Korngold, E., Freiman, J., 1997. Effect of porous support fabric on osmosis through a Loeb-Sourirajan type asymmetric membrane. *J. Membr. Sci.* 129 (2), 243–249.
- Lokare, O.R., Vidic, R.D., 2019. Impact of operating conditions on measured and predicted concentration polarization in membrane distillation. *Environ. Sci. Technol.* 53 (20), 11869–11876.
- Lokare, O.R., Tavakkoli, S., Wadekar, S., Khanna, V., Vidic, R.D., 2017a. Fouling in direct contact membrane distillation of produced water from unconventional gas extraction. *J. Membr. Sci.* 524, 493–501.

- Lokare, O.R., Tavakkoli, S., Rodriguez, G., Khanna, V., Vidic, R.D., 2017b. Integrating membrane distillation with waste heat from natural gas compressor stations for produced water treatment in Pennsylvania. Desalination 413, 144–153.
- Long, Q., Jia, Y., Li, J., Yang, J., Liu, F., Zheng, J., Yu, B., 2018. Recent advance on draw solutes development in forward osmosis. Processes 6 (9), 165.
- Lu, D., Liu, Q., Zhao, Y., Liu, H., Ma, J., 2018. Treatment and energy utilization of oily water via integrated ultrafiltration-forward osmosis-membrane distillation (UF-FO-MD) system. *J. Membr. Sci.* 548, 275–287.
- Lu, X., Arias Chavez, L.H., Romero-Vargas Castrillón, S., Ma, J., Elimelech, M., 2015. Influence of active layer and support layer surface structures on organic fouling propensity of thin-film composite forward osmosis membranes. *Environ. Sci. Technol.* 49 (3), 1436–1444.
- Lutchmiah, K., Verliefde, A.R.D., Roest, K., Rietveld, L.C., Cornelissen, E.R., 2014. Forward osmosis for application in wastewater treatment: a review. *Water Res.* 58, 179–197.
- Mahat, N.A., Shamsudin, S.A., Jullok, N., Ma'Radzi, A.H., 2020. Carbon quantum dots embedded polysulfone membranes for antibacterial performance in the process of forward osmosis. Desalination 493, 114618.
- McCUTCHEON, J.R., Elimelech, M., 2006. Influence of concentrative and dilutive internal concentration polarization on flux behavior in forward osmosis. *J. Membr. Sci.* 284 (1), 237–247.
- McCUTCHEON, J.R., Elimelech, M., 2007. Modeling water flux in forward osmosis: implications for improved membrane design. *AIChE J.* 53 (7), 1736–1744.
- McCUTCHEON, J.R., McGinnis, R.L., Elimelech, M., 2005. A novel ammonia–carbon dioxide forward (direct) osmosis desalination process. Desalination 174 (1), 1–11.
- Meindersma, G.W., Guijt, C.M., de Haan, A.B., 2006. Desalination and water recycling by air gap membrane distillation. Desalination 187 (1), 291–301.
- Mingming, L., 2012. Integration of nanoparticles as draw solute in forward osmosis. in: Department of Chemical and Biomolecular Engineering. National University of Singapore: National University of Singapore.
- Mohammad, A.W., Teow, Y.H., Ang, W.L., Chung, Y.T., Oatley-Radcliffe, D.L., Hilal, N., 2015. Nanofiltration membranes review: Recent advances and future prospects. Desalination 356, 226–254.
- Motsa, M.M., Mamba, B.B., D'Haese, A., Hoek, E.M.V., Verliefde, A.R.D., 2014. Organic fouling in forward osmosis membranes: the role of feed solution chemistry and membrane structural properties. *J. Membr. Sci.* 460, 99–109.
- Na, Y., Yang, S., Lee, S., 2014. Evaluation of citrate-coated magnetic nanoparticles as draw solute for forward osmosis. Desalination 347, 34–42.
- Nagy, E., 2014. A general, resistance-in-series, salt- and water flux models for forward osmosis and pressure-retarded osmosis for energy generation. *J. Membr. Sci.* 460, 71–81.
- Naidu, G., Tijing, L., Johir, M.A.H., Shon, H., Vigneswaran, S., 2020. Hybrid membrane distillation: Resource, nutrient and energy recovery. *J. Membr. Sci.* 599.
- Nasr, P., Sewilam, H., 2015. The potential of groundwater desalination using forward osmosis for irrigation in Egypt. *Clean. Technol. Environ. Policy* 17 (7), 1883–1895.
- Nawaz, M.S., Son, H.S., Jin, Y., Kim, Y., Soukane, S., Al-Hajji, M.A., Abu-Ghaib, M., Ghaffour, N., 2021. Investigation of flux stability and fouling mechanism during simultaneous treatment of different produced water streams using forward osmosis and membrane distillation. *Water Res.* 198, 117157.
- Nguyen, N.C., Chen, S.-S., Ho, S.-T., Nguyen, H.T., Ray, S.S., Nguyen, N.T., Hsu, H.-T., Le, N.C., Tran, T.T., 2018. Optimising the recovery of EDTA-2Na draw solution in forward osmosis through direct contact membrane distillation. *Sep. Purif. Technol.* 198, 108–112.
- Nguyen, N.C., Duong, H.C., Nguyen, H.T., Chen, S.-S., Le, H.Q., Ngo, H.H., Guo, W., Duong, C.C., Le, N.C., Bui, X.T., 2020. Forward osmosis–membrane distillation hybrid system for desalination using mixed trivalent draw solution. *J. Membr. Sci.* 603, 118029.
- Ni, T., Lin, J., Kong, L., Zhao, S., 2021. Omnipolymer membranes for distillation: opportunities and challenges. *Chin. Chem. Lett.* 32 (11), 3298–3306.
- Nicoll, P.G. Forward osmosis—A brief introduction. in: Proceedings of the international desalination association world congress on desalination and water reuse, Tianjin, China. 2013.
- Olatunji, S.O., Camacho, L.M., 2018. Heat and mass transport in modeling membrane distillation configurations: a review. *Front. Energy Res.* 6.
- Pan, S.-F., Dong, Y., Zheng, Y.-M., Zhong, L.-B., Yuan, Z.-H., 2017. Self-sustained hydrophilic nanofiber thin film composite forward osmosis membranes: Preparation, characterization and application for simulated antibiotic wastewater treatment. *J. Membr. Sci.* 523, 205–215.
- Pangarkar, B., Deshmukh, S., Sapkal, V., Sapkal, R., 2016. Review of membrane distillation process for water purification. *Desalin. Water Treat.* 57 (7), 2959–2981.
- Park, K., Kim, D.Y., Jang, Y.H., Kim, M.-G., Yang, D.R., Hong, S., 2020. Comprehensive analysis of a hybrid FO/crystallization/RO process for improving its economic feasibility to seawater desalination. *Water Res.* 171, 115426.
- Parthiban, V., Panda, S.K., Sahu, A.K., 2018. Highly fluorescent carbon quantum dots-Nafion as proton selective hybrid membrane for direct methanol fuel cells. *Electrochim. Acta* 292, 855–864.
- Parveen, F., 2018. Development of lab-scale forward osmosis membrane bioreactor (FO-MBR) with draw solute regeneration for wastewater treatment, in: Department of Engineering Science. University of Oxford.
- Pei, J., Gao, S., Sarp, S., Wang, H., Chen, X., Yu, J., Yue, T., Youravong, W., Li, Z., 2021. Emerging forward osmosis and membrane distillation for liquid food concentration: A review. *Compr. Rev. Food Sci. Food Saf.* 20 (2), 1910–1936.
- Phillip, W.A., Yong, J.S., Elimelech, M., 2010. Reverse draw solute permeation in forward osmosis: modeling and experiments. *Environ. Sci. Technol.* 44 (13), 5170–5176.
- Phunthsho, S., Shon, H.K., Hong, S., Lee, S., Vigneswaran, S., 2011. A novel low energy fertilizer driven forward osmosis desalination for direct fertigation: evaluating the performance of fertilizer draw solutions. *J. Membr. Sci.* 375 (1), 172–181.
- Phunthsho, S., Hong, S., Elimelech, M., Shon, H.K., 2013. Forward osmosis desalination of brackish groundwater: Meeting water quality requirements for fertigation by integrating nanofiltration. *J. Membr. Sci.* 436, 1–15.
- Piri, F., Shafee Afarani, M., Arabi, A.M., 2019. Synthesis of copper oxide quantum dots: effect of surface modifiers. *Mater. Res. Express* 6 (12), 125006.
- Qasim, M., Darwish, N.A., Sarp, S., Hilal, N., 2015. Water desalination by forward (direct) osmosis phenomenon: a comprehensive review. *Desalination* 374, 47–69.
- Ramon, G.Z., Hoek, E.M.V., 2013. Transport through composite membranes, part 2: Impacts of roughness on permeability and fouling. *J. Membr. Sci.* 425–426, 141–148.
- Ravi, J., Othman, M.H.D., Matsuura, T., Ro'il Bilad, M., El-badawy, T.H., Aziz, F., Ismail, A.F., Rahman, M.A., Jaafar, J., 2020. Polymeric membranes for desalination using membrane distillation: a review. *Desalination* 490, 114530.
- Ray, S.S., Chen, S.-S., Sangeetha, D., Chang, H.-M., Thanh, C.N.D., Le, Q.H., Ku, H.-M., 2018. Developments in forward osmosis and membrane distillation for desalination of waters. *Environ. Chem. Lett.* 16 (4), 1247–1265.
- Razmjou, A., Barati, M.R., Simon, G.P., Suzuki, K., Wang, H., 2013. Fast deswelling of nanocomposite polymer hydrogels via magnetic field-induced heating for emerging FO desalination. *Environ. Sci. Technol.* 47 (12), 6297–6305.
- Rezaei, M., Warsinger, D.M., Lienhard V, J.H., Duke, M.C., Matsuura, T., Samhaber, W. M., 2018. Wetting phenomena in membrane distillation: Mechanisms, reversals, and prevention. *Water Res.* 139, 329–352.
- Ricci, B.C., Skibinski, B., Koch, K., Mancel, C., Celestino, C.Q., Cunha, I.L.C., Silva, M.R., Alvim, C.B., Faria, C.V., Andrade, L.H., Lange, L.C., Amaral, M.C.S., 2019. Critical performance assessment of a submerged hybrid forward osmosis - membrane distillation system. *Desalination* 468, 114082.
- Sabet, M., Mahdavi, K., 2019. Green synthesis of high photoluminescence nitrogen-doped carbon quantum dots from grass via a simple hydrothermal method for removing organic and inorganic water pollutions. *Appl. Surf. Sci.* 463, 283–291.
- Sabzkar, M., Pourafshari Chenar, M., Maghsoud, Z., Mostaghisi, O., García-Payo, M.C., Khayet, M., 2021. Cyclic olefin polymer as a novel membrane material for membrane distillation applications. *J. Membr. Sci.* 621, 118845.
- Sanmartino, J.A., Khayet, M., García-Payo, M.C., 2016. Desalination by Membrane Distillation. In: Hankins, N.P., Singh, R. (Eds.), in: *Emerging Membrane Technology for Sustainable Water Treatment*. Elsevier: Boston, pp. 77–109.
- Sardari, K., Fyfe, P., Ranil Wickramasinghe, S., 2019. Integrated electrocoagulation – forward osmosis – membrane distillation for sustainable water recovery from hydraulic fracturing produced water. *J. Membr. Sci.* 574, 325–337.
- Sarkar, S., Banerjee, D., Ghorai, U.K., Das, N.S., Chattopadhyay, K.K., 2016. Size dependent photoluminescence property of hydrothermally synthesized crystalline carbon quantum dots. *J. Lumin.* 178, 314–323.
- Sarp, S., 2019. In Basile, A., Curcio, E., Inamuddin (Eds.), *Fundamentals of Pressure Retarded Osmosis, in Current Trends and Future Developments on (Bio-) Membranes*. Elsevier, pp. 271–283.
- Shaffer, D.L., Werber, J.R., Jaramillo, H., Lin, S., Elimelech, M., 2015. Forward osmosis: where are we now? *Desalination* 356, 271–284.
- Sharma, A., Das, J., 2019. Small molecules derived carbon dots: synthesis and applications in sensing, catalysis, imaging, and biomedicine. *J. Nanobiotechnology* 17 (1), 92.
- Sharqawy, M.H., Lienhard, J.H., Zubair, S.M., 2010. Thermophysical properties of seawater: a review of existing correlations and data. *Desalin. Water Treat.* 16 (1–3), 354–380.
- She, Q., Wang, R., Fane, A.G., Tang, C.Y., 2016. Membrane fouling in osmotically driven membrane processes: a review. *J. Membr. Sci.* 499, 201–233.
- Shi, Y., Liu, X., Wang, M., Huang, J., Jiang, X., Pang, J., Xu, F., Zhang, X., 2019. Synthesis of N-doped carbon quantum dots from bio-waste lignin for selective iron detection and cellular imaging. *Int. J. Biol. Macromol.* 128, 537–545.
- Shin, S., Kim, A.S., 2018. In: Hongbo, D., Audie, T., Wang, X. (Eds.), *Temperature effect on forward osmosis, in Osmotically Driven Membrane Processes—Approach, Development and Current Status*. InTech, London, UK, pp. 87–110 (InTech Rijeka, Croatia).
- Shirazi, S., Lin, C.-J., Chen, D., 2010. Inorganic fouling of pressure-driven membrane processes – a critical review. *Desalination* 250 (1), 236–248.
- Singh, A., Mohapatra, P.K., Kalyanasundaram, D., Kumar, S., 2019. Self-functionalized ultrastable water suspension of luminescent carbon quantum dots. *Mater. Chem. Phys.* 225, 23–27.
- Singh, S.K., Sharma, C., Maiti, A., 2021. A comprehensive review of standalone and hybrid forward osmosis for water treatment: membranes and recovery strategies of draw solutions. *J. Environ. Chem. Eng.* 9 (4), 105473.
- Singh, S.K., Sharma, C., Maiti, A., 2023. Modeling and experimental validation of forward osmosis process: parameters selection, permeate flux prediction, and process optimization. *J. Membr. Sci.* 672, 121439.
- Son, H.S., Soukane, S., Lee, J., Kim, Y., Kim, Y.-D., Ghaffour, N., 2021a. Towards sustainable circular brine reclamation using seawater reverse osmosis, membrane distillation and forward osmosis hybrids: an experimental investigation. *J. Environ. Manag.* 293, 112836.
- Son, H.S., Kim, Y., Nawaz, M.S., Al-Hajji, M.A., Abu-Ghaib, M., Soukane, S., Ghaffour, N., 2021b. Impact of osmotic and thermal isolation barrier on concentration and temperature polarization and energy efficiency in a novel FO-MD integrated module. *J. Membr. Sci.* 620, 118811.
- Song, H., Xie, F., Chen, W., Liu, J., 2018. FO/MD hybrid system for real dairy wastewater recycling. *Environ. Technol.* 39 (18), 2411–2421.

- Song, J., Yan, M., Ye, J., Zheng, S., Ee, L.Y., Wang, Z., Li, J., Huang, M., 2022. Research progress in external field intensification of forward osmosis process for water treatment: A critical review. *Water Res.* 222, 118943.
- Soukane, S., Elcik, H., Alpatova, A., Orfi, J., Ali, E., AlAnsary, H., Ghaffour, N., 2021. Scaling sets the limits of large scale membrane distillation modules for the treatment of high salinity feeds. *J. Clean. Prod.* 287, 125555.
- Sreedhar, I., Khatan, S., Gupta, R., Reddy, B.M., Venugopal, A., 2018. An odyssey of process and engineering trends in forward osmosis. *Environ. Sci.: Water Res. Technol.* 4 (2), 129–168.
- Stefani, M., Forward osmosis: influence of sucrose and sodium chloride as draw solutions on process performance, in: DIPARTIMENTO DI INGEGNERIA INDUSTRIALE. 2014, UNIVERSITÀ DEGLI STUDI DI PADOVA.
- Stone, M.L., Rae, C., Stewart, F.F., Wilson, A.D., 2013. Switchable polarity solvents as draw solutes for forward osmosis. *Desalination* 312, 124–129.
- Su, J., Yang, Q., Teo, J.F., Chung, T.-S., 2010. Cellulose acetate nanofiltration hollow fiber membranes for forward osmosis processes. *J. Membr. Sci.* 355 (1), 36–44.
- Su, J., Ong, R.C., Wang, P., Chung, T.S., Helmer, B.J., de Wit, J.S., 2013. Advanced FO membranes from newly synthesized CAP polymer for wastewater reclamation through an integrated FO-MD hybrid system. *AIChE J.* 59 (4), 1245–1254.
- Su, Z., Zhang, M., Xu, P., Zhao, Z., Wang, Z., Huang, H., Ouyang, T., 2021. Opportunities and strategies for multigrade waste heat utilization in various industries: A recent review. *Energy Convers. Manag.* 229, 113769.
- Suwaleh, W., Johnson, D., Jones, D., Hilal, N., 2019. An integrated fertilizer driven forward osmosis- renewables powered membrane distillation system for brackish water desalination: a combined experimental and theoretical approach. *Desalination* 471, 114126.
- Suwaleh, W., Pathak, N., Shon, H., Hilal, N., 2020. Forward osmosis membranes and processes: a comprehensive review of research trends and future outlook. *Desalination* 485, 114455.
- Suwaleh, W., Zargar, M., Abdala, A., Siddiqui, F.A., Khiadani, M., Abdel-Wahab, A., 2022. Concentration polarization control in stand-alone and hybrid forward osmosis systems: Recent technological advancements and future directions. *Chem. Eng. Res. Des.* 178, 199–223.
- Tajuddin, M.H., Yusof, N., Abdullah, N., Abidin, M.N.Z., Salleh, W.N.W., Ismail, A.F., Matsuura, T., Hairom, N.H.H., Misdan, N., 2019. Incorporation of layered double hydroxide nanofillers in polyamide nanofiltration membrane for high performance of salts rejections. *J. Taiwan Inst. Chem. Eng.* 97, 1–11.
- Tan, C.H., Ng, H.Y., 2008. Modified models to predict flux behavior in forward osmosis in consideration of external and internal concentration polarizations. *J. Membr. Sci.* 324 (1), 209–219.
- Tang, C.Y., She, Q., Lay, W.C., Wang, R., Fane, A.G., 2010. Coupled effects of internal concentration polarization and fouling on flux behavior of forward osmosis membranes during humic acid filtration. *J. Membr. Sci.* 354 (1–2), 123–133.
- Thomas, N., Mavukkandy, M.O., Louatadou, S., Arafat, H.A., 2017. Membrane distillation research & implementation: Lessons from the past five decades. *Sep. Purif. Technol.* 189, 108–127.
- Thorsen, T., Holt, T., 2009. The potential for power production from salinity gradients by pressure retarded osmosis. *J. Membr. Sci.* 335 (1), 103–110.
- Tirafiri, A., Kang, Y., Giannelis, E.P., Elimelech, M., 2012. Highly hydrophilic thin-film composite forward osmosis membranes functionalized with surface-tailored nanoparticles. *ACS Appl. Mater. Interfaces* 4 (9), 5044–5053.
- Ullah, R., Khraisheh, M., Esteves, R.J., McLeskey, J.T., AlGhouti, M., Gad-el-Hak, M., Vahedi Tafreshi, H., 2018. Energy efficiency of direct contact membrane distillation. *Desalination* 433, 56–67.
- Uragami, T., 2017. Science and technology of separation membranes. John Wiley & Sons.
- Valladares Linares, R., Yangali-Quintanilla, V., Li, Z., Amy, G., 2012. NOM and TEP fouling of a forward osmosis (FO) membrane: Fouulant identification and cleaning. *J. Membr. Sci.* 421–422, 217–224.
- Viader, G., Casal, O., Lefevre, B., de Arespochaga, N., Echevarría, C., López, J., Valderrama, C., Cortina, J.L., 2021. Integration of membrane distillation as volume reduction technology for in-land desalination brines management: pre-treatments and scaling limitations. *J. Environ. Manag.* 289, 112549.
- Wang, K.Y., Ong, R.C., Chung, T.-S., 2010. Double-skinned forward osmosis membranes for reducing internal concentration polarization within the porous sublayer. *Ind. Eng. Chem. Res.* 49 (10), 4824–4831.
- Wang, K.Y., Teoh, M.M., Nugroho, A., Chung, T.-S., 2011. Integrated forward osmosis-membrane distillation (FO-MD) hybrid system for the concentration of protein solutions. *Chem. Eng. Sci.* 66 (11), 2421–2430.
- Wang, P., Chung, T.-S., 2015. Recent advances in membrane distillation processes: membrane development, configuration design and application exploring. *J. Membr. Sci.* 474, 39–56.
- Wang, P., Cui, Y., Ge, Q., Fern Tew, T., Chung, T.-S., 2015. Evaluation of hydroacid complex in the forward osmosis-membrane distillation (FO-MD) system for desalination. *J. Membr. Sci.* 494, 1–7.
- Wang, Q., Wang, G., Liang, X., Dong, X., Zhang, X., 2019a. Supporting carbon quantum dots on NH2-MIL-125 for enhanced photocatalytic degradation of organic pollutants under a broad spectrum irradiation. *Appl. Surf. Sci.* 467–468, 320–327.
- Wang, Y., Hu, A., 2014. Carbon quantum dots: synthesis, properties and applications. *J. Mater. Chem. C* 2 (34), 6921–6939.
- Wang, Z., Horseman, T., Straub, A.P., Yip, N.Y., Li, D., Elimelech, M., Lin, S., 2019b. Pathways and challenges for efficient solar-thermal desalination. *Sci. Adv.* 5 (7).
- Warsinger, D.M., Swaminathan, J., Guillen-Burrieza, E., Arafat, H.A., Lienhard V, J.H., 2015. Scaling and fouling in membrane distillation for desalination applications: A review. *Desalination* 356, 294–313.
- Wei, J., Jian, X., Wu, C., Zhang, S., Yan, C., 2005. Influence of polymer structure on thermal stability of composite membranes. *J. Membr. Sci.* 256 (1), 116–121.
- Wilson, A.D., Stewart, F.F., 2013. Deriving osmotic pressures of draw solutes used in osmotically driven membrane processes. *J. Membr. Sci.* 431, 205–211.
- Winter, D., 2014. Membrane distillation: A thermodynamic, technological and economic analysis. University of Kaiserslautern, Germany.
- Winter, D., Koschikowski, J., Wieghaus, M., 2011. Desalination using membrane distillation: Experimental studies on full scale spiral wound modules. *J. Membr. Sci.* 375 (1), 104–112.
- Xie, M., Nghiem, L.D., Price, W.E., Elimelech, M., 2013. A forward osmosis–membrane distillation hybrid process for direct sewer mining: system performance and limitations. *Environ. Sci. Technol.* 47 (23), 13486–13493.
- Xie, M., Nghiem, L.D., Price, W.E., Elimelech, M., 2014. Toward resource recovery from wastewater: extraction of phosphorus from digested sludge using a hybrid forward osmosis-membrane distillation process. *Environ. Sci. Technol. Lett.* 1 (2), 191–195.
- Xie, M., Lee, J., Nghiem, L.D., Elimelech, M., 2015. Role of pressure in organic fouling in forward osmosis and reverse osmosis. *J. Membr. Sci.* 493, 748–754.
- Xie, Z., Nagaraja, N., Skillman, L., Li, D., Ho, G., 2017. Comparison of polysaccharide fouling in forward osmosis and reverse osmosis separations. *Desalination* 402, 174–184.
- Xu, X., Ray, R., Gu, Y., Ploehn, H.J., Gearheart, L., Raker, K., Scrivens, W.A., 2004. Electrophoretic analysis and purification of fluorescent single-walled carbon nanotube fragments. *J. Am. Chem. Soc.* 126 (40), 12736–12737.
- Xu, Y., Peng, X., Tang, C.Y., Fu, Q.S., Nie, S., 2010. Effect of draw solution concentration and operating conditions on forward osmosis and pressure retarded osmosis performance in a spiral wound module. *J. Membr. Sci.* 348 (1), 298–309.
- Yaeli, J., Method and apparatus for processing liquid solutions of suspensions particularly useful in the desalination of saline water, in: U.S. Patent and Trademark Office, U.S.P.A.T. Office, Editor. 1992: USA.
- Yang, S., Abdalkareem Jasim, S., Bokov, D., Chupradit, S., Nakhjiri, A.T., El-Shafay, A.S., 2022. Membrane distillation technology for molecular separation: a review on the fouling, wetting and transport phenomena. *J. Mol. Liq.* 349, 118115.
- Yen, S.K., Mehnas Haja N, F., Su, M., Wang, K.Y., Chung, T.-S., 2010. Study of draw solutes using 2-methylimidazole-based compounds in forward osmosis. *J. Membr. Sci.* 364 (1), 242–252.
- Yip, N.Y., Elimelech, M., 2012. Thermodynamic and energy efficiency analysis of power generation from natural salinity gradients by pressure retarded osmosis. *Environ. Sci. Technol.* 46 (9), 5230–5239.
- Yip, N.Y., Tirafiri, A., Phillip, W.A., Schiffman, J.D., Hoover, L.A., Kim, Y.C., Elimelech, M., 2011. Thin-film composite pressure retarded osmosis membranes for sustainable power generation from salinity gradients. *Environ. Sci. Technol.* 45 (10), 4360–4369.
- Yokozeki, A., 2006. Osmotic pressures studied using a simple equation-of-state and its applications. *Appl. Energy* 83 (1), 15–41.
- Yu, T., Wang, H., Guo, C., Zhai, Y., Yang, J., Yuan, J., 2018. A rapid microwave synthesis of green-emissive carbon dots with solid-state fluorescence and pH-sensitive properties. *R. Soc. Open Sci.* 5 (7), 180245.
- Yun, Y., Ma, R., Zhang, W., Fane, A.G., Li, J., 2006. Direct contact membrane distillation mechanism for high concentration NaCl solutions. *Desalination* 188 (1), 251–262.
- Zhang, J., Yu, S.-H., 2016. Carbon dots: large-scale synthesis, sensing and bioimaging. *Mater. Today* 19 (7), 382–393.
- Zhang, J., Zhang, N., Wang, D., Gao, B., Shon, H.K., Yang, X., Zhao, H., Wang, Z., 2023b. Polyamidoamine and carboxylated cellulose nanocrystal grafted antifouling forward osmosis membranes for efficient leachate treatment via integrated forward osmosis and membrane distillation process. *J. Membr. Sci.* 668, 121241.
- Zhang, R., Liu, Y., He, M., Su, Y., Zhao, X., Elimelech, M., Jiang, Z., 2016. Antifouling membranes for sustainable water purification: strategies and mechanisms. *Chem. Soc. Rev.* 45 (21), 5888–5924.
- Zhang, S., Wang, P., Fu, X., Chung, T.-S., 2014. Sustainable water recovery from oily wastewater via forward osmosis-membrane distillation (FO-MD). *Water Res.* 52, 112–121.
- Zhang, X., Jiang, M., Niu, N., Chen, Z., Li, S., Liu, S., Li, J., 2018. Natural-product-derived carbon dots: from natural products to functional materials. *ChemSusChem* 11 (1), 11–24.
- Zhang, X., Koirala, R., Pramanik, B., Fan, L., Date, A., Jegatheesan, V., 2023a. Challenges and advancements in membrane distillation crystallization for industrial applications. *Environ. Res.* 234, 116577.
- Zhao, D., Chen, S., Wang, P., Zhao, Q., Lu, X., 2014a. A dendrimer-based forward osmosis draw solute for seawater desalination. *Ind. Eng. Chem. Res.* 53 (42), 16170–16175.
- Zhao, D., Wang, P., Zhao, Q., Chen, N., Lu, X., 2014b. Thermoresponsive copolymer-based draw solution for seawater desalination in a combined process of forward osmosis and membrane distillation. *Desalination* 348, 26–32.
- Zhao, D.L., Chung, T.-S., 2018. Applications of carbon quantum dots (CQDs) in membrane technologies: a review. *Water Res.* 147, 43–49.
- Zhao, S., Zou, L., 2011a. Relating solution physicochemical properties to internal concentration polarization in forward osmosis. *J. Membr. Sci.* 379 (1), 459–467.
- Zhao, S., Zou, L., 2011b. Effects of working temperature on separation performance, membrane scaling and cleaning in forward osmosis desalination. *Desalination* 278 (1), 157–164.
- Zhao, S., Zou, L., Tang, C.Y., Mulcahy, D., 2012. Recent developments in forward osmosis: opportunities and challenges. *J. Membr. Sci.* 396, 1–21.

- Zhou, Y., Huang, M., Deng, Q., Cai, T., 2017. Combination and performance of forward osmosis and membrane distillation (FO-MD) for treatment of high salinity landfill leachate. *Desalination* 420, 99–105.
- Zohrabian, L., Hankins, N.P., Field, R.W., 2020. Hybrid forward osmosis-membrane distillation system: demonstration of technical feasibility. *J. Water Process Eng.* 33, 101042.
- Zou, S., Qin, M., He, Z., 2019. Tackle reverse solute flux in forward osmosis towards sustainable water recovery: reduction and perspectives. *Water Res.* 149, 362–374.